

**Dissertation zur Erlangung des Doktorgrades der  
Fakultät für Chemie und Pharmazie der  
Ludwig-Maximilians-Universität München**

**Direct Density Matrix Renormalization Group  
Approaches for Strong Correlation Effects in  
Quantum Chemistry**

Philipp Bertone Snajberk

aus

Starnberg, Deutschland

2017



Erklärung

Diese Dissertation wurde im Sinne von § 7 der Promotionsordnung vom 28. November 2011 von Herrn ..... Prof. Dr. Christian Ochsenfeld ..... betreut.

Eidesstattliche Versicherung

Diese Dissertation wurde eigenständig und ohne unerlaubte Hilfe erarbeitet.

München, .....

.....  
Philipp Bertone Snajberk

Dissertation eingereicht am ..... 03.02.2017 .....

1. Gutachter: ..... Prof. Dr. Christian Ochsenfeld .....

2. Gutachter: ..... Prof. Dr. Ulrich Schollwöck .....

Mündliche Prüfung am ..... 07.03.2017 .....



## **Acknowledgment**

I would like to thank my supervisor Prof. Dr. Christian Ochsenfeld for the great opportunity to conduct my research in his group. Furthermore, I want to thank all my colleagues for the great discussions and the great time we had. In the end, I also want to thank my whole family and especially my beloved wife Aviva Snajberk for her great support during my time as a PhD student.



## Abstract

An implementation of the single-site density matrix renormalization group (DMRG) approach for the quantum-chemical application to calculate approximate as well as exact electronic ground-state energies and wave functions of atoms and molecules is presented. The algorithm is formulated in terms of the variational and size-consistent class of wave functions, matrix product states, and their operator analogues, matrix product operators. A procedure to construct quantum-chemical Hamiltonian operators with long-range Coulomb interactions as matrix product operators is developed. The many-electron Hamiltonian operators are represented as sums and products of one-electron operators. For the efficient matrix product operator construction of quantum-chemical Hamiltonians, different basis spaces including discrete position and momentum space as well as molecular and atomic orbitals are investigated. Discrete position space yields the best matrix product operator size scaling, but introduces artificial long-range couplings in the kinetic energy term of the Hamiltonian which are a consequence of the DMRG algorithm in terms of matrix product states. The huge amount of discrete space points needed for an accurate description poses a problem because of the electron-electron interaction. Therefore, a momentum space or Fourier series expansion of the electron-electron interaction is shown which makes it possible to compress its matrix product operator representation. DMRG applied to quantum-chemical Hamiltonians in matrix product operator form can serve as means to directly (without mean-field treatment in advance) investigate quantum-chemical problems and find the analytically exact ground-state solution of small atoms and molecules. The next basis space analyzed in detail is the atomic orbital basis. The matrix product operator construction and the direct application of the DMRG method in this basis is examined. A physical compression scheme based on a singular value decomposition of the electron-electron interaction in the atomic orbital basis is demonstrated. Furthermore, DMRG calculations in the atomic orbital basis for certain systems where mean-field theory yields qualitatively wrong results and where higher-order approximative correction methods like truncated configuration interaction and coupled cluster cannot fully capture strong electron correlation effects are compared to results obtained in the molecular orbital basis. The comparison shows that atomic orbitals describe the physical situation well and thus lead to a tremendous reduction of the matrix product state dimension and the computational effort.





# Contents

<b>1</b>	<b>Introduction</b>	<b>1</b>
<b>2</b>	<b>Strongly correlated systems and numerical renormalization</b>	<b>5</b>
2.1	Strong correlation . . . . .	5
2.2	Quantum lattice models . . . . .	6
2.3	Brief introduction to the numerical renormalization group . . . . .	7
2.4	Key idea of the density matrix renormalization group . . . . .	7
2.5	Bridging quantum chemistry and physics . . . . .	9
<b>3</b>	<b>Theoretical framework</b>	<b>13</b>
3.1	Standard quantum mechanics or first quantization . . . . .	13
3.1.1	Single-particle operators and independent-particle states . . . . .	13
3.1.2	Two-particle operators and many-particle states . . . . .	15
3.2	The formalism of second quantization . . . . .	15
3.2.1	One-particle operators and anti-commutation relations . . . . .	15
3.2.2	Two-particle operators . . . . .	17
3.2.3	Change of basis . . . . .	17
3.2.4	Occupation number representation of many-particle states . . . . .	19
3.3	Quantum lattice models revisited . . . . .	19
<b>4</b>	<b>Calculus of matrix product states and operators</b>	<b>21</b>
4.1	Matrix product states . . . . .	21
4.1.1	Addition of matrix product states . . . . .	22
4.1.2	Scalar product of two matrix product states . . . . .	23
4.1.3	Invariance and normalization of matrix product states . . . . .	23
4.2	Matrix product operators . . . . .	24
4.2.1	Addition, multiplication, and norms of matrix product operators . . . . .	24
4.2.2	Construction of matrix product operators and simple examples . . . . .	25
4.3	Application of matrix product operators to matrix product states . . . . .	29
4.3.1	Expectation values . . . . .	30
4.3.2	Eigenvalue problems . . . . .	31
<b>5</b>	<b>Matrix product operator representations of the quantum-chemical Hamiltonian</b>	<b>37</b>
5.1	The choice of basis . . . . .	37
5.2	The quantum-chemical Hamiltonian in different basis types . . . . .	38
5.2.1	Hartree-Fock orbitals . . . . .	39
5.2.2	Atomic orbitals . . . . .	40
5.2.3	Discrete momentum space . . . . .	44
5.2.4	Discrete position space . . . . .	45
5.3	MPO-construction in the different basis types . . . . .	51

<b>6</b>	<b>Electronic structure studies with matrix product operators and states</b>	<b>53</b>
6.1	Ground-state search with the DMRG algorithm . . . . .	53
6.1.1	Minimizing the Lagrangian . . . . .	53
6.1.2	Implementational details on the single-site DMRG algorithm	55
6.1.3	Particle number conservation . . . . .	59
6.2	MPO compression schemes . . . . .	64
6.2.1	Reduction of the lattice size and momentum space expansion of the electron-electron interaction on a real-space lattice . . .	65
6.2.2	Singular value compression of the electron-electron interaction on an orbital lattice . . . . .	67
6.3	DMRG applications . . . . .	68
6.3.1	The He-atom and the H <sub>2</sub> -molecule on a real-space lattice . . .	68
6.3.2	Atomic orbital DMRG . . . . .	70
<b>7</b>	<b>Conclusion</b>	<b>79</b>
	<b>List of publications</b>	<b>83</b>
	<b>Bibliography</b>	<b>85</b>

# 1 Introduction

In non-relativistic quantum chemistry, atomic and molecular physics, effective one-electron theories such as mean-field theory have proven to be quite successful in describing the electronic structure of atoms or molecules around their equilibrium geometries. By its derivation, mean-field theory however is flawed by the fact that it can only capture a part of the electron correlation properly. One distinguishes weakly correlated or dynamically correlated and strongly or statically correlated electron systems. The latter cannot be described by mean-field theory since the description by one Slater-determinant—the simplest, physically correct quantum-mechanical many-body state of a non-interacting electron system fulfilling Pauli’s principle—is qualitatively wrong. The true many-electron state of a strongly correlated system must be a linear combination of all possible Slater-determinants. Such a physical situation can occur in chemistry when for instance bonds of a molecule are stretched. This results in a variety of equally possible Slater-determinantal states the electrons can adopt. In the field of quantum chemistry, this is called a multi-reference case because even the standard approximative quantum-chemical correlation methods such as the truncated configuration interaction (CI) or truncated coupled cluster (CC) method (single-reference methods) which are based on mean-field calculations cannot entirely correct the mean-field theory results (see Sherrill and Schaefer III. [1999] and Crawford and Schaefer [2000] for reviews on these methods). Higher-order approximations such as multi-reference configuration interaction and multi-reference coupled cluster methods or full-configuration interaction or infinite coupled cluster methods (as described in Szalay et al. [2011], Banerjee and Simons [1981], Sherrill [1995], and Čížek [1966]) have to be used. But, these approaches for including the full electron correlation are computationally highly expensive and only feasible for small quantum-chemical systems. To mention just a few applications, see the articles by, e.g., Bauschlicher Jr and Taylor [1986], Bauschlicher Jr et al. [1986], Bauschlicher Jr and Langhoff [1987], van Mourik and van Lenthe [1995], Werner et al. [2008] and Das et al. [2010]. Therefore, there is still the need for a numerical approach capable by design to describe the electronic structure of strongly correlated systems in quantum chemistry and reducing the computational effort.

Since its publication and its introduction to the field of quantum chemistry, the density matrix renormalization group (DMRG) method [White, 1992, 1993, White and Martin, 1999] has turned out to be a powerful numerical approach to diagonalize approximatively—and for certain small systems even exactly—quantum-mechanical Hamiltonians of strongly correlated systems not truncating physics and reducing the computational cost at the same time. The focus of this dissertation lies on the development and investigation of a quantum-chemically applicable DMRG method, in particular for strongly correlated molecules.

DMRG can be viewed as a mapping of the complicated many-body problem to a plethora of effective one-body problems which must be solved self-consistently. This mapping is achieved by a systematic approximation of the interacting many-electron

wave function bearing still the correct physics. This approximation is built upon a decomposition of the interacting many-body wave function expansion coefficients in terms of a product of matrices whose rank sets the extent of approximation. This wave function is called a matrix product state (MPS) (for a review, see Schollwöck [2011]). The operator analogues are called matrix product operators (MPO). These objects help to introduce the notion of locality to the Hamiltonian which otherwise contains long-ranged interaction terms and make the effective one-body mapping more efficient. This has led to the first research project of this dissertation since it has been unclear at the beginning of this dissertation how a Hamiltonian MPO can be constructed efficiently for quantum-chemical Hamiltonians in general. During the development of this work, several different procedures have been published [Keller et al., 2015, Keller and Reiher, 2016, Hubig et al., 2016], but the construction presented here for quantum-chemical Hamiltonians which have Coulombic long-range interactions is different. It is generally applicable and has good MPO-matrix size scaling as the MPO of the electron-electron interaction term can be systematically compressed from a size scaling of  $O(L^4)$  to  $O(L^2 N_{\text{trunc}})$ , where  $L$  is the number of single-particle states (orbitals) the electrons can possibly occupy and DMRG uses as local basis states called DMRG sites.  $N_{\text{trunc}}$  is the number of electron-electron interaction terms kept according to the used compression scheme. Two compression schemes are shown here: a physical compression scheme based on a singular value decomposition of the electron-electron interaction decomposing it into the product of interacting one-particle operators and one based on a momentum space or Fourier series expansion of the electron-electron interaction. Moreover, the presented MPO-construction procedure is parallelizable which allows to parallelize the DMRG algorithm at least locally. That means building the DMRG-typical effective one-body problems arising from the formulation of the DMRG algorithm in terms of matrix product states and matrix product operators can be done in parallel, which makes it possible to tackle larger problems.

Directly resulting from the matrix product operator construction of Hamiltonians with long-range electron interactions, the question and thus the second project arises: Which is the best basis to represent the Hamiltonian in? Inspired by Stoudenmire et al. [2012] for purely one-dimensional systems, a real three-dimensional quantum-field theoretical formulation of the quantum-chemical Hamiltonian and its matrix product operator construction on a three-dimensional discrete position space lattice is developed and analyzed. As it is shown, this makes DMRG directly applicable to quantum-chemical problems without any preceding mean-field calculation as opposed to common quantum-chemical DMRG implementations.

The idea of a direct DMRG method to solve quantum-chemical problems suffering strong electron correlation and situations where mean-field calculations are hard to converge has led to the next project of research in this dissertation. The quantum-chemical Gaussian basis sets (atomic orbitals) are investigated to form the local basis states for DMRG calculations, which makes mean-field calculations in advance unnecessary. Similar investigations have been done by Chan and Van Voorhis [2005] for non-orthogonal orbitals and a resulting non-Hermitian DMRG algorithm. They have used localized polarized atomic orbitals [Lee and Head-Gordon, 1997] and showed that these kind of orbitals outperform molecular orbitals regarding the energy convergence of DMRG. In this thesis, the Cholesky orthogonalized atomic orbital DMRG approach is developed, which is different with respect to the fact

that the DMRG algorithm is formulated here completely in terms of matrix product operators and matrix product states being the basis for a second-generation DMRG algorithm. It extends the approach by Chan and Van Voorhis [2005] regarding the use of generic Gaussian atomic orbital basis sets such as the STO-3G [Hehre et al., 1969] basis set as DMRG sites for linear molecules ranging from a hydrogen chain, elongated ethine  $C_2H_2$ , and small  $C_2$ -chains to simple cubic hydrogen. A natural ordering of these atomic orbitals with respect to the atom position and angular momentum of the orbitals is suggested and discussed compared to the use of molecular orbitals canonically sorted according to their orbital energies as suggested by White and Martin [1999]. Furthermore, the effect of using a larger Gaussian basis set such as the 6-31G [Hehre et al., 1972] or cc-pVDZ [Dunning Jr, 1989] basis sets is examined. As already mentioned, a small non-linear system, cubic hydrogen  $H_8$ , is studied to see if DMRG in terms of orthonormalized atomic orbitals does well even though the orbitals must be ordered in a chain-like fashion for DMRG using the matrix product state representation of the exact many-electron wave function. The use of atomic orbitals and their natural ordering for DMRG may become crucial for the simulation of non-linear systems in future projects when addressing the use of tensor network states [Murg et al., 2010, Marti et al., 2010, Nakatani and Chan, 2013]. Tensor network states (TNS) are the generalization of matrix product states. Using TNSs in combination with orthonormalized atomic orbitals could help to improve the performance of DMRG further since the actual electron correlation could better be represented. The atomic orbital ordering would be closer to the chemists' concept of how molecular bonds emerge (linear combination of atomic orbitals). Tensor network state techniques are not a subject of this dissertation.

This thesis is organized as follows: In chapters 2 and 3, the reader is introduced to the physical concepts and the theoretical framework of the present work. Chapter 4 is about the mathematical properties of matrix product states and matrix product operators. Chapter 5 shows how to construct Hamiltonians with long-range interaction terms as matrix product operators, in particular the quantum-chemical Hamiltonian in various basis spaces. In chapter 6, the DMRG algorithm implemented here for matrix product states and matrix product operators is presented. The two mentioned MPO-compression schemes are explained. Besides, practical calculations of atomic and molecular systems with the developed discrete real-space lattice and atomic orbital DMRG approaches are shown and discussed.



## 2 Strongly correlated systems and numerical renormalization

In the following, we first focus on the terms strong correlation and systems with exponentially large Hilbert space dimensions. In this context, the concepts of dynamic and static electron correlation are outlined. Therefore, we shortly introduce two numerical methods to tackle such systems: the numerical renormalization group and the density matrix renormalization group, which this thesis is mainly about. Moreover, since this text aims to be readable for both physicists and chemists, another numerical method named full-configuration interaction, which is well-known in quantum-chemistry, will shortly be introduced at the end of this chapter to highlight the similarities of the density matrix renormalization group to this quantum-chemical method and at the same time its differences.

The density matrix renormalization group (DMRG) was developed by White [1992, 1993] as an improvement of the numerical renormalization group (NRG) [Wilson, 1975]. The term “group” refers to a set of transformations to perform the “renormalization” during the algorithm. DMRG was originally tailored to investigate one-dimensional quantum lattice models.

In the following, the reader is provided with a short introduction to the above named numerical methods for strongly correlated systems.

### 2.1 Strong correlation

Before we continue, one should clarify the notion of strong correlation. As strongly correlated, one normally defines systems which can no longer be described as an effective single-particle system. In quantum chemistry, this normally goes under the name non-dynamic or static electron correlation. One of the most prominent and successful approaches where one tries to map a system of interacting particles to such an effective one-particle problem is the mean-field or Hartree-Fock approximation. The Hartree-Fock approximation can capture the part of correlation which is known as dynamic electron correlation. As a good reference for the Hartree-Fock approach, see Szabo and Ostlund [1996], but it will not be subject of this thesis.

Good chemical and physical examples of systems where the applicability of mean-field approaches breaks down are manifold. On the one hand, there are transition metal compounds or, on the other hand, systems close to their critical point of a phase transition of the second kind. These phase transitions are for instance the transitions from ferromagnetic to paramagnetic or metallic to insulating behavior. All of these critical phenomena have in common that the characteristic length scale—the correlation length—diverges. Due to the absence of a characteristic length scale, Wilson [1975] came up with the idea of real-space renormalization.

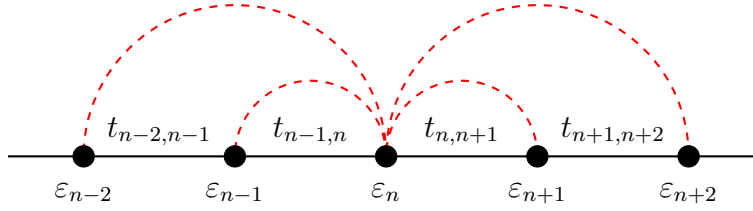


Figure 2.1: A visualization of a one-dimensional quantum lattice model consisting of a chain of sites (filled circles). A particle on site  $n$  has a kinetic energy or on-site energy of  $\varepsilon_n$  and can hop to its neighboring sites, which is governed by the hopping terms  $t_{n,n+1}$  and  $t_{n-1,n}$  (black lines). Each lattice site is here coupled to all the other lattice sites via a so far undetermined interaction term (red dashed lines).

## 2.2 Quantum lattice models

To get a better understanding of how NRG and DMRG work, one should also briefly commit oneself to the notion of quantum lattice models. In physics, such models are for instance to describe bulk effects in solids like the influence of impurities on the conductivity. They are also suitable to describe phase transitions like ferromagnetic materials turning to paramagnetic materials or metals becoming insulators [Vojta, 2003, Imada et al., 1998]. The range of applications is huge. Quantum lattice models can moreover be used to analyze the electronic structure of small molecules [Wilson, 1990, White and Martin, 1999, Chan and Sharma, 2011, Wouters and Van Neck, 2014, Stoudenmire et al., 2012].

What is characteristic for quantum lattice models is the fact that the Hilbert space dimension of the many-particle wave function to be determined increases exponentially the more lattice sites one considers. Therefore, it is mostly not feasible to obtain the exact solution of a quantum lattice model, especially if the number of lattice sites is infinite. Lattice sites can have several meanings: either they characterize—in a tight-binding picture—real atomic sites in a crystal, i.e., for example the positively charged ions in a metal which form the crystal lattice, or they just represent a mathematical grid or mesh of points which can have many origins. One of them could be the discretization of a continuous theory like when dealing with electrons as quantum fields.

Fig. 2.1 shows a pictorial example of a quantum lattice model where  $L$  lattice sites—whatever meaning they have—are coupled by so-called hopping terms and every lattice site interacts in a certain way (e.g., Coulomb interaction) with all the other sites. As already pointed out, the sites of a lattice model need not be real points in space. They can also be an abstract quantum-mechanical state like an atomic or a molecular orbital in the field of quantum chemistry. Basically, it can be any quantum-mechanical state one can think of.

The most famous quantum lattice models are the Hubbard model and the Ising model, which both have greatly contributed to understand quantum-mechanical phenomena in condensed matter physics and even to build new methods on top of them [Hubbard, 1963, Ising, 1925].



## 2.3 Brief introduction to the numerical renormalization group

The numerical renormalization group by Wilson [1975] is a non-perturbative method and was developed with the goal to find solutions to quantum impurity models, which are lattice models, such as the Kondo problem. The Kondo model is a model to describe the physical situation where electrons in metals can scatter at magnetic impurities (e.g., iron in copper), which results in an increase of resistivity when the temperature goes to absolute zero [Kondo, 1964].

NRG is a method to investigate so-called quantum impurity models. These are systems where a small, exactly solvable system—named impurity—is coupled to a “bath” of continuous states [Bulla et al., 2008]. The key steps during the NRG procedure are as follows: First of all, the model of an impurity interacting with a continuous bath is discretized and mapped onto a semi-infinite chain, where the impurity system represents the first site. Now in an iterative manner, one diagonalizes the system step by step starting with the impurity site. In each step, one new site is added to the system Hamiltonian  $\hat{H}_L$  ( $L$  is the number of sites)

$$\hat{H}_L \longrightarrow \hat{H}_{L+1}, \quad |i_L\rangle \longrightarrow |i_L\rangle \otimes |s\rangle, \quad (2.1)$$

which is then again diagonalized. Here,  $|i_L\rangle$  are the many-particle eigenstates of  $\hat{H}_L$  and  $|s\rangle$  represents the states in the Hilbert space at the site  $L + 1$ . To avoid an exponential growth of the Hilbert space dimension when adding new sites to the system, a truncation or renormalization scheme is introduced such that only the many-particle eigenstates  $|i_L\rangle$  with the lowest-lying eigenvalues are kept after the diagonalization of  $\hat{H}_L$ .

It turned out that, even if this approach was quite successful, it was flawed by its criterion to truncate the many-particle Hilbert space.

## 2.4 Key idea of the density matrix renormalization group

Instead of taking the eigenstates with the corresponding lowest-lying many-particle eigenvalues, DMRG improved on the criterion to truncate the Hilbert space of the system to investigate by turning to the eigenbasis of the density matrix.

Considering its basic idea, DMRG is quite similar to the above mentioned numerical renormalization group approach and it can handle almost any one-dimensional quantum lattice model such as the famous Hubbard model or any lattice model which originates from discretizing continuous space. What the mathematical structure of a quantum lattice model looks like will be explained in detail later in this thesis.

The DMRG algorithm published by White [1992] is based on a blocking procedure (see Fig. 2.2) where all the one-particle states or—in terms of a lattice—sites of the underlying system are grouped in two blocks and a single site in the middle (single-site algorithm). Now, one can assume that the total ground-state wave function has

## 2 Strongly correlated systems and numerical renormalization

the form

$$|\psi\rangle = \sum_{lnr} \Psi_{ln,r} |ln\rangle |r\rangle, \quad (2.2)$$

where  $|ln\rangle$  and  $|r\rangle$  are the many-particle basis states of the left block plus the local basis  $|n\rangle$  of the single site in the middle of the chain and the right block, respectively. In general, the basis  $|lnr\rangle$  is exponentially large. Therefore, one has to truncate or renormalize the basis. As truncation, DMRG uses the reduced density operator or matrix of one of the blocks. The reduced density operator for one of the blocks (for example for the left block) can be obtained from the quantum-mechanical density operator

$$\hat{\rho} = |\psi\rangle \langle\psi| \quad (2.3)$$

$$= \sum_{lnr,l'n'r'} \Psi_{ln,r} \Psi_{l'n',r'}^* |lnr\rangle \langle l'n'r'| \quad (2.4)$$

by tracing out or summing up all the many-particle degrees of freedom of the other block (the right block in this example)

$$\hat{\rho}^{\text{left}} = \sum_{lnr,l'n'r',r''} \Psi_{ln,r} \Psi_{l'n',r'}^* |ln\rangle \langle r''|r\rangle \langle l'n'| \langle r'|r''\rangle. \quad (2.5)$$

Assuming that the block basis states are orthonormal, one can write

$$\hat{\rho}^{\text{left}} = \sum_{ln,l'n',r} \Psi_{ln,r} \Psi_{l'n',r}^* |ln\rangle \langle l'n'| \quad (2.6)$$

and the reduced density matrix of the left block together with the central site reads

$$\hat{\rho}_{ln,l'n'}^{\text{left}} = \sum_r \Psi_{ln,r} \Psi_{l'n',r}^*. \quad (2.7)$$

This reduced density matrix is now diagonalized, but one only keeps the eigenstates with—up to a given threshold—largest eigenvalues of the reduced density matrix. The truncated eigenbasis of the reduced density matrix serves as the renormalization transformation because the ground-state wave function is now projected into this truncated eigenbasis, which makes sure that the Hilbert space dimension of the wave function does not grow exponentially with increasing number of sites. In this way, it is possible to determine the ground-state wave function of a system iteratively.

This section is not meant to describe the DMRG algorithm in full detail as there are excellent reviews by Schollwöck [2005] and Hallberg [2006]. In this thesis, we focus on the state-of-the-art formulation of the DMRG approach in terms of new mathematical objects known as matrix product states and corresponding matrix product operators [Schollwöck, 2011, McCulloch, 2007, Verstraete and Cirac, 2006]. These objects make it possible to map the seek for a solution of the stationary many-particle Schrödinger equation [Schrödinger, 1926] in operator-state notation (Dirac notation)

$$\hat{H} |\psi\rangle = E |\psi\rangle \quad (2.8)$$

to a set of effective one-particle Schrödinger equations which are to be solved instead. In Eq. (2.8), the operator  $\hat{H}$  is the Hamiltonian—the operator of total energy of a

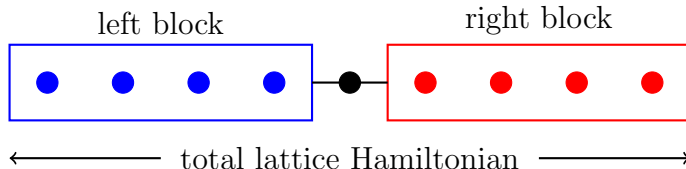


Figure 2.2: Single-site DMRG blocking. The filled circles represent the single-particle states or sites on which the ground-state wave function of a system is expanded. The single-particle states are mapped onto a chain and grouped into a left block (blue) and a right block (red) plus one single-particle state (black circle) in between. All the single-particle states can also be seen as sites in the formulation of a quantum lattice Hamiltonian.

quantum system—and  $|\psi\rangle$  is the state with energy  $E$  a quantum system is in.

We are going to give a thorough introduction to these new classes of wave functions and operators and how the DMRG algorithm is implemented in terms of these objects later in this thesis.

## 2.5 Bridging quantum chemistry and physics

Since this thesis is supposed to be readable for physicists as chemists alike, we should briefly explain some of the differences and similarities in handling theoretical problems. In quantum chemistry, basically every calculation is based on a mean-field or Hartree-Fock calculation which gives a first starting point for further calculations to solve electronic structure problems.

The Hartree-Fock approach (HF) [Hartree, 1928, Fock, 1930, Hartree and Hartree, 1935] is the attempt to take electron interactions into account but, at the same time, looking for the simplest possible many-body solution which fulfills every physical requirements like anti-symmetry of the electronic wave function. Such a wave function refers to the so-called Slater determinant [Slater, 1929] which has the form for a system of  $N$  electrons

$$\psi_{\text{HF}}(\mathbf{x}_1, \mathbf{x}_2, \dots, \mathbf{x}_N) = \frac{1}{\sqrt{N!}} \det \begin{pmatrix} \varphi_1(\mathbf{x}_1) & \varphi_2(\mathbf{x}_1) & \cdots & \varphi_N(\mathbf{x}_1) \\ \varphi_1(\mathbf{x}_2) & \varphi_2(\mathbf{x}_2) & & \\ \vdots & & \ddots & \\ \varphi_1(\mathbf{x}_N) & & & \varphi_N(\mathbf{x}_N) \end{pmatrix} \quad (2.9)$$

or in short in bra-ket notation.

$$|\psi_{\text{HF}}\rangle = |\varphi_1\varphi_2\cdots\varphi_N\rangle. \quad (2.10)$$

The  $\varphi_i(\mathbf{x}_j)$  denote the  $i$ th single-particle state or orbital which is occupied by the  $j$ th electron at position  $\mathbf{x}_j$ . Although this wave function bears all physical properties, it does not describe the physical reality properly. Therefore, so-called post-HF or correlation methods which are to improve the results from mean-field calculations and describe physics correctly were developed. One specific method in the

field of quantum chemistry is the so-called full-configuration interaction method, which will be now introduced shortly (for introductions on the method, see amongst others Knowles and Handy [1984], Sherrill [1995], and Sherrill and Schaefer III. [1999]). Assume the  $|\varphi_i\rangle$  form a complete basis set of orthonormal basis states  $\mathcal{B} = \{|\varphi_i\rangle \mid \|\varphi_i\| = 1, \langle\varphi_i|\varphi_j\rangle = \delta_{ij}, i, j = 1, 2, \dots\}$ , then it is clear that the Hartree-Fock state is just one combination of an infinite large set of possible many-body states the superposition of which yields the correct exact wave function of a  $N$ -electron system. In quantum-chemical literature, it is commonly written as

$$|\psi\rangle = \Psi_0 |\psi_{\text{HF}}\rangle + \sum_{ia} \Psi_i^a |\psi_i^a\rangle + \sum_{ij,ab} \Psi_{ij}^{ab} |\psi_{ij}^{ab}\rangle + \dots, \quad (2.11)$$

where  $\Psi_0, \Psi_i^a, \Psi_{ij}^{ab}$ , etc. are the expansion coefficients of the configuration interaction expansion. One obtains the exact wave function by mathematically exciting electrons from the HF-state orbitals to other in the HF-state unoccupied orbitals  $|\varphi_i\rangle \rightarrow |\varphi_a\rangle$  (for a pictorial example see Fig. 2.3). Thus, a hierarchy of zero-, one-, two-particle and so on excitations or configurations emerges. Assuming a complete basis set of size  $L \gg N$ , Eq. (2.11) can most generally and compactly be written in the form

$$|\psi\rangle = \sum_{n_1 n_2 \dots n_L} \Psi_{n_1 n_2 \dots n_L} |\varphi_1^{n_1} \varphi_2^{n_2} \dots \varphi_L^{n_L}\rangle \quad \left( \sum_{i=1}^L n_i = N \right) \quad (2.12)$$

with the constrained that the sum over all  $n_i$  must equal the particle number  $N$ . The  $n_i \in \{0; 1\}$  measure if the orbital  $i$  is unoccupied (0) or occupied (1) and thus contributes to the expansion of the wave function or not. Eq. (2.12) shows the most striking difference of standard quantum-chemical approaches to find a numerically exact solution to direct methods like DMRG. In contrast to Eq. (2.11), Eq. (2.12) does not have any reference state except the empty vacuum state. At the beginning, every many-particle basis state in Eq. (2.12) is assumed to contribute to the expansion and the numerical method at hand—in the case of this thesis—DMRG finds the correct expansion coefficients or weights of the exact many-body wave function.

Eventually, it must be pointed out, even though the density matrix renormalization group ansatz is said to be equivalent to the method of full-configuration interaction (exact diagonalization of a problem) [Chan and Sharma, 2011, White and Martin, 1999, Daul et al., 1999], it can be used to diagonalize quantum-mechanical problems where a full-CI or an exact diagonalization treatment is computationally too expensive. To illustrate that will be a main part of this thesis.

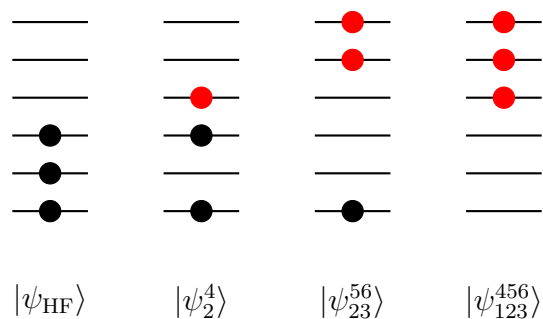


Figure 2.3: Visualization of the full-configuration interaction method which serves as a means in quantum-chemistry to get numerically exact results. One needs a reference state, normally the HF-state, and constructs all possible many-body basis states by “exciting” electrons from orbitals which are occupied in the HF-state (black circles) to unoccupied states (red circles). The picture shows a hierarchy of zero-, one-, two- and three-particle excitations.



# 3 Theoretical framework

The reader of this chapter is provided with an overview of the theoretical framework needed to understand the following chapters. This chapter is mainly about the formalism of second quantization as it can be found in the books by Bruus and Flensberg [2004], Giuliani and Vignale [2005], or Helgaker et al. [2014]. It is a theoretical formalism to deal with many-particle systems which is based on whether a single-particle state is occupied or not. Hence, it also has the name “occupation number representation”. Second quantization is an operator-based formulation of quantum mechanics. That means that the physical properties of indistinguishable particles like Pauli’s principle are encoded in operators instead of the many-body wave function. In the following, the focus merely lies on the second-quantization formulation of electronic systems.

## 3.1 Standard quantum mechanics or first quantization

### 3.1.1 Single-particle operators and independent-particle states

Consider a generic Hamiltonian describing an electron in a potential  $V(\mathbf{x})$  in atomic units

$$\hat{H} = -\frac{1}{2}\Delta + V(\mathbf{x}) \quad (3.1)$$

where  $\Delta = \frac{d^2}{dx^2} + \frac{d^2}{dy^2} + \frac{d^2}{dz^2}$  is the Laplace operator. Assume that one is able to find a solution to the associated Schrödinger equation

$$\hat{H} |\varphi_n\rangle = E_n |\varphi_n\rangle \quad (3.2)$$

with  $|\varphi_n\rangle$  and  $E_n$  being the  $n$ th eigenstate and eigenvalue of  $\hat{H}$ . The  $|\varphi_n\rangle$  form a complete set of basis states

$$\sum_n |\varphi_n\rangle \langle \varphi_n| = \hat{1} \quad (3.3)$$

$$\int d^3x \varphi_m^*(\mathbf{x}) \varphi_n(\mathbf{x}) = \delta_{mn}. \quad (3.4)$$

$\hat{1}$  is the identity operator and  $\delta_{mn}$  is the Kronecker-delta symbol. Then, it is clear that a matrix element of a generic operator in this basis reads

$$O_{mn} = \langle \varphi_m | \hat{O} | \varphi_n \rangle \quad (3.5)$$

$$= \langle \varphi_m | \hat{1} \hat{O} | \varphi_n \rangle \quad (3.6)$$

### 3 Theoretical framework

$$= \langle \varphi_m | \int d^3x |\mathbf{x}\rangle \langle \mathbf{x}| \hat{O} | \varphi_n \rangle \quad (3.7)$$

$$= \int d^3x \varphi_m^*(\mathbf{x}) \left( \hat{O} \varphi_n \right) (\mathbf{x}). \quad (3.8)$$

It was used that the position space is a complete basis as well and that one gets the wave function by projection onto position space

$$\int d^3x |\mathbf{x}\rangle \langle \mathbf{x}| = \hat{1} \quad (3.9)$$

$$\varphi_n(\mathbf{x}) = \langle \mathbf{x} | \varphi_n \rangle. \quad (3.10)$$

Consequently, an operator can be expressed in terms of its matrix elements

$$\hat{O} = \hat{1} \hat{O} \hat{1} \quad (3.11)$$

$$= \sum_{mn} |\varphi_m\rangle \langle \varphi_m| \hat{O} |\varphi_n\rangle \langle \varphi_n| \quad (3.12)$$

$$= \sum_{mn} O_{mn} |\varphi_m\rangle \langle \varphi_n|. \quad (3.13)$$

The last equation is the so-called first-quantization representation of quantum-mechanical operators.

Now, consider a system of  $N$  independent electrons. The Hamiltonian then becomes

$$\hat{H}^N = \sum_{i=1}^N \left( -\frac{1}{2} \Delta_i + V(\mathbf{x}_i) \right). \quad (3.14)$$

It can be shown that a simple product ansatz  $|\psi_{n_1 n_2 \dots n_N}^N\rangle = |\varphi_{n_1}\rangle \cdot |\varphi_{n_2}\rangle \cdots |\varphi_{n_N}\rangle$  is a solution of the Schrödinger equation

$$\hat{H}^N |\psi_{n_1 n_2 \dots n_N}^N\rangle = E_{n_1 n_2 \dots n_N}^N |\psi_{n_1 n_2 \dots n_N}^N\rangle \quad (3.15)$$

with

$$E_{n_1 n_2 \dots n_N}^N = E_{n_1} + E_{n_2} + \cdots + E_{n_N}. \quad (3.16)$$

The solution states  $|\psi_{n_1 n_2 \dots n_N}^N\rangle$  lack some important physical property, namely anti-symmetry. Therefore, one can use the fact that any linear combination of these states is a solution of the  $N$ -particle Schrödinger equation and thus incorporates the correct physics

$$|\phi\rangle = \sum_{n_1 n_2 \dots n_N} C_{n_1 n_2 \dots n_N} |\psi_{n_1 n_2 \dots n_N}^N\rangle. \quad (3.17)$$

Anti-symmetry is included in the expansion coefficients  $C_{n_1 n_2 \dots n_N}$ . This leads to the sort of states called Slater determinants [Slater, 1929] written here briefly as

$$|\phi\rangle = |\varphi_1 \varphi_2 \cdots \varphi_N\rangle. \quad (3.18)$$



### 3.1.2 Two-particle operators and many-particle states

Let us now modify Eq. (3.14) by adding a term which couples two electrons

$$\hat{H}^N = \sum_{i=1}^N \left( -\frac{1}{2} \Delta_i + V(\mathbf{x}_i) \right) + \frac{1}{2} \sum_{i \neq j} U(\mathbf{x}_i, \mathbf{x}_j). \quad (3.19)$$

$U(\mathbf{x}_i, \mathbf{x}_j)$  is what one calls a two-particle operator. It can readily be expanded in a set of complete single-particle basis states

$$\hat{U}_{ij} = \sum_{mnpq} u_{mnpq} |\varphi_m\rangle |\varphi_n\rangle \langle \varphi_p| \langle \varphi_q| \quad (3.20)$$

where

$$u_{mnpq} = \int d^3x_i d^3x_j \varphi_m^*(\mathbf{x}_i) \varphi_n^*(\mathbf{x}_j) U(\mathbf{x}_i, \mathbf{x}_j) \varphi_p(\mathbf{x}_i) \varphi_q(\mathbf{x}_j). \quad (3.21)$$

It is not any longer possible to write the solution state of Eq. (3.19) as a linear combination of products of the single-particle states  $|\varphi\rangle$ . The two-particle operator introduces correlation between electrons in different orbitals. Since the Slater determinants also form a complete basis set, the most general ansatz is a superposition of N-particle Slater determinants

$$|\psi\rangle = \sum_k \Psi_k |\phi_k\rangle \quad (3.22)$$

or, when we assume that we have a complete set of  $L \gg N$  orbitals, one can also write

$$|\psi\rangle = \sum_{n_1 n_2 \dots n_L} \Psi_{n_1 n_2 \dots n_L} \delta_{\sum_i n_i, N} |\varphi_1^{n_1} \varphi_2^{n_2} \dots \varphi_L^{n_L}\rangle. \quad (3.23)$$

The  $n_i$  indicate whether the orbital  $|\varphi_i\rangle$  has been taken into the expansion or not, so whether the orbital is occupied by an electron or not. In the following, the reader is provided with a short introduction to a many-particle formalism called second quantization which is wholly built on the electron-orbital occupation.

## 3.2 The formalism of second quantization

As opposed to most books on the subject of second quantization [Bruus and Flensberg, 2004, Giuliani and Vignale, 2005, Helgaker et al., 2014], we take a more heuristic way inspired by quantum field theory [Altland and Simons, 2010]. Electrons are considered as field excitations in the vacuum and all the physical properties of identical particles are expressed by operator actions instead of encoded in the many-particle wave function.

### 3.2.1 One-particle operators and anti-commutation relations

If one knew the exact electronic density  $\rho(\mathbf{x})$  of a system in advance, any one-particle quantity could be calculated easily. Classically, for a continuously defined observable  $O(\mathbf{x})$  like for instance the electrostatic potential of a point charge, summing up all

### 3 Theoretical framework

particle contributions yields

$$O = \int d^3x O(\mathbf{x})\rho(\mathbf{x}) \quad (3.24)$$

which is analogous to the quantum-mechanical expectation value of the observable  $\hat{O}$

$$\langle \hat{O} \rangle = \int d^3x \psi^*(\mathbf{x})O(\mathbf{x})\psi(\mathbf{x}). \quad (3.25)$$

Bearing in mind that any physical observable in quantum mechanics is mathematically represented by a Hermitian operator, one must recognize that the electronic density at a point in space needs to be an operator as well and Eq. (3.24) becomes

$$\langle \hat{O} \rangle = \int d^3x O(\mathbf{x})\hat{\rho}(\mathbf{x}) \quad (3.26)$$

$$= \int d^3x \hat{\psi}^\dagger(\mathbf{x})O(\mathbf{x})\hat{\psi}(\mathbf{x}). \quad (3.27)$$

The last equation shows the second quantization formulation of quantum mechanics in position or real space. The name ‘‘second quantization’’ is derived from the fact that, superficially speaking, not only operator spectra are quantized but also wave function excitations considering the wave function as an operator itself. It holds

$$\hat{\rho}(\mathbf{x}) = \hat{\psi}^\dagger(\mathbf{x})\hat{\psi}(\mathbf{x}) \quad (3.28)$$

$$\hat{N} = \int d^3x \hat{\rho}(\mathbf{x}). \quad (3.29)$$

$\hat{N}$  is the particle number operator counting the number of particles in a N-particle state  $|\psi^N\rangle$

$$\hat{N}|\psi^N\rangle = N|\psi^N\rangle. \quad (3.30)$$

The operators  $\hat{\psi}^\dagger(\mathbf{x})$  and  $\hat{\psi}(\mathbf{x})$  are termed field operators and can be viewed as creators and destructors of particles in a superposition of single-particle states at the position  $\mathbf{x}$  in space.

In order to obey Pauli’s exclusion principle, one must require that these operators fulfill the so-called anti-commutation relations

$$\{\hat{\psi}(\mathbf{x}), \hat{\psi}(\mathbf{x}')\} = 0 \quad (3.31)$$

$$\{\hat{\psi}^\dagger(\mathbf{x}), \hat{\psi}^\dagger(\mathbf{x}')\} = 0 \quad (3.32)$$

$$\{\hat{\psi}(\mathbf{x}), \hat{\psi}^\dagger(\mathbf{x}')\} = \delta(\mathbf{x} - \mathbf{x}') \quad (\forall \mathbf{x}, \mathbf{x}' \in \mathbb{R}^3). \quad (3.33)$$

The curly brackets mean that

$$\{\hat{A}, \hat{B}\} = \hat{A}\hat{B} + \hat{B}\hat{A} \quad (3.34)$$

and  $\delta(\mathbf{x} - \mathbf{x}')$  is the Dirac- $\delta$  function. These relations make sure that it is impossible to create two electrons at the same position in space

$$\hat{\psi}^\dagger(\mathbf{x})\hat{\psi}^\dagger(\mathbf{x}) = 0. \quad (3.35)$$

### 3.2.2 Two-particle operators

As an example for a two-particle operator, the reader may be referred to the electron-electron interaction in atomic units

$$U(\mathbf{x}, \mathbf{x}') = \frac{1}{|\mathbf{x} - \mathbf{x}'|}. \quad (3.36)$$

Classically, the electrostatic interaction energy of two charge distributions is calculated as follows

$$U = \frac{1}{2} \int d^3x d^3x' U(\mathbf{x}, \mathbf{x}') \rho(\mathbf{x}) \rho(\mathbf{x}'). \quad (3.37)$$

The second-quantized analogue is thus

$$\hat{U} = \frac{1}{2} \int d^3x d^3x' U(\mathbf{x}, \mathbf{x}') \hat{\rho}(\mathbf{x}) \hat{\rho}(\mathbf{x}'). \quad (3.38)$$

However, the last equation is not fully correct because it includes a nonphysical term where  $\mathbf{x}$  equals  $\mathbf{x}'$ . That is why one must subtract this term to have a valid description of physics

$$\hat{U} = \frac{1}{2} \int d^3x d^3x' U(\mathbf{x}, \mathbf{x}') \left( \hat{\rho}(\mathbf{x}) \hat{\rho}(\mathbf{x}') - \delta(\mathbf{x} - \mathbf{x}') \hat{\psi}^\dagger(\mathbf{x}) \hat{\psi}(\mathbf{x}') \right). \quad (3.39)$$

Using the anti-commutation relations for electrons, the last expression can be brought into the form

$$\hat{U} = \frac{1}{2} \int d^3x d^3x' U(\mathbf{x}, \mathbf{x}') \left( \hat{\psi}^\dagger(\mathbf{x}) \hat{\psi}(\mathbf{x}) \hat{\psi}^\dagger(\mathbf{x}') \hat{\psi}(\mathbf{x}') - \delta(\mathbf{x} - \mathbf{x}') \hat{\psi}^\dagger(\mathbf{x}) \hat{\psi}(\mathbf{x}') \right) \quad (3.40)$$

$$= \frac{1}{2} \int d^3x d^3x' U(\mathbf{x}, \mathbf{x}') \hat{\psi}^\dagger(\mathbf{x}) \left( \hat{\psi}(\mathbf{x}) \hat{\psi}^\dagger(\mathbf{x}') - \delta(\mathbf{x} - \mathbf{x}') \right) \hat{\psi}(\mathbf{x}') \quad (3.41)$$

$$= -\frac{1}{2} \int d^3x d^3x' U(\mathbf{x}, \mathbf{x}') \hat{\psi}^\dagger(\mathbf{x}) \hat{\psi}^\dagger(\mathbf{x}') \hat{\psi}(\mathbf{x}) \hat{\psi}(\mathbf{x}') \quad (3.42)$$

$$= \frac{1}{2} \int d^3x d^3x' U(\mathbf{x}, \mathbf{x}') \hat{\psi}^\dagger(\mathbf{x}) \hat{\psi}^\dagger(\mathbf{x}') \hat{\psi}(\mathbf{x}') \hat{\psi}(\mathbf{x}). \quad (3.43)$$

Therefore, a generic Hamiltonian with electron-electron interaction can be written in second-quantized form in real space as

$$\begin{aligned} \hat{H} = & \int d^3x \hat{\psi}^\dagger(\mathbf{x}) (T(\mathbf{x}) + V(\mathbf{x})) \hat{\psi}(\mathbf{x}) \\ & + \frac{1}{2} \int d^3x d^3x' U(\mathbf{x}, \mathbf{x}') \hat{\psi}^\dagger(\mathbf{x}) \hat{\psi}^\dagger(\mathbf{x}') \hat{\psi}(\mathbf{x}') \hat{\psi}(\mathbf{x}) \end{aligned} \quad (3.44)$$

with  $T(\mathbf{x})$ ,  $V(\mathbf{x})$  and  $U(\mathbf{x}, \mathbf{x}')$  being the kinetic energy, external potential, and the electron-electron interaction.

### 3.2.3 Change of basis

In some cases, it may be better to work in another basis. Assume the  $|\varphi_i\rangle$  form a complete orthonormal basis set. Then the field operators can be expanded in a set

### 3 Theoretical framework

of new creation and annihilation operators  $\hat{c}_i^\dagger$  and  $\hat{c}_i$

$$\hat{\psi}^\dagger(\mathbf{x}) = \sum_i \varphi_i^*(\mathbf{x}) \hat{c}_i^\dagger \quad (3.45)$$

$$\hat{\psi}(\mathbf{x}) = \sum_i \varphi_i(\mathbf{x}) \hat{c}_i \quad (3.46)$$

which fulfill the same anti-commutation relations

$$\{\hat{c}_i, \hat{c}_j\} = 0 \quad (3.47)$$

$$\{\hat{c}_i^\dagger, \hat{c}_j^\dagger\} = 0 \quad (3.48)$$

$$\{\hat{c}_i, \hat{c}_j^\dagger\} = \delta_{ij}. \quad (3.49)$$

$\delta_{ij}$  is the Kronecker- $\delta$  symbol. In this new generic basis, the Hamiltonian in Eq. (3.44) attains the shape

$$\hat{H} = \sum_{ij} h_{ij} \hat{c}_i^\dagger \hat{c}_j + \frac{1}{2} \sum_{ijkl} u_{ijkl} \hat{c}_i^\dagger \hat{c}_j^\dagger \hat{c}_l \hat{c}_k \quad (3.50)$$

where it has been defined

$$h_{ij} = \int d^3x \varphi_i^*(\mathbf{x}) (T(\mathbf{x}) + V(\mathbf{x})) \varphi_j(\mathbf{x}) \quad (3.51)$$

$$u_{ijkl} = \int d^3x d^3x' \varphi_i^*(\mathbf{x}) \varphi_k(\mathbf{x}) U(\mathbf{x}, \mathbf{x}') \varphi_j^*(\mathbf{x}') \varphi_l(\mathbf{x}'). \quad (3.52)$$

Besides, the particle number operator turns to

$$\hat{N} = \int d^3x \hat{\psi}^\dagger(\mathbf{x}) \hat{\psi}(\mathbf{x}) \quad (3.53)$$

$$= \sum_{ij} \int d^3x \varphi_i^*(\mathbf{x}) \varphi_j(\mathbf{x}) \hat{c}_i^\dagger \hat{c}_j \quad (3.54)$$

$$= \sum_{ij} \delta_{ij} \hat{c}_i^\dagger \hat{c}_j \quad (3.55)$$

$$= \sum_i \hat{c}_i^\dagger \hat{c}_i \quad (3.56)$$

where the operator  $\hat{c}_i^\dagger \hat{c}_i$  measures the occupancy  $n_i \in \{0; 1\}$  (0: unoccupied, 1: occupied) of the orbital  $|\varphi_i\rangle$ . That is why this operator is shortly written as

$$\hat{n}_i = \hat{c}_i^\dagger \hat{c}_i. \quad (3.57)$$

The orbitals  $|\varphi_i\rangle$  are eigenstates of  $\hat{n}_i$  obeying the eigenvalue equation

$$\hat{n}_i |\varphi_i\rangle = n_i |\varphi_i\rangle \quad (3.58)$$

with eigenvalues  $n_i$ .

### 3.2.4 Occupation number representation of many-particle states

A key concept of second quantization is that it is not important to know how the explicit form of the single-particle states looks like—except for the matrix elements. What matters is if the state  $|\varphi_i\rangle$  is occupied by an electron or not. By this means, it is possible to expand a many-particle state in the so-called occupation number or Fock space. Consider we have a space of  $L$  single-particle states  $|\varphi_i\rangle$ , then a many-particle state can be written in terms of occupation numbers  $n_i$  as

$$|\psi\rangle = \sum_{n_1 n_2 \dots n_L} \Psi_{n_1 n_2 \dots n_L} |n_1 n_2 \dots n_L\rangle . \quad (3.59)$$

$|n_1 n_2 \dots n_L\rangle$  is termed occupation number or Fock state and indicates which of the single-particle states  $|\varphi_i\rangle$  are occupied by electrons. For instance, in the state  $|01100\rangle$  the second and third orbital is occupied and the rest is empty. An occupation number state is a many-particle state and is completely similar to a Slater determinant because

$$|01100\rangle = \hat{c}_2^\dagger \hat{c}_3^\dagger |0\rangle \quad (3.60)$$

$$= -\hat{c}_3^\dagger \hat{c}_2^\dagger |0\rangle . \quad (3.61)$$

A particular occupation number state can be obtained by creating particles and putting them into the completely empty or vacuum state  $|0\rangle$

$$|n_1 n_2 \dots n_L\rangle = \hat{c}_1^{\dagger n_1} \hat{c}_2^{\dagger n_2} \dots \hat{c}_L^{\dagger n_L} |0\rangle . \quad (3.62)$$

One can see that an occupation number state fulfills the requirement of anti-symmetry which an electronic many-body state must fulfill due to the anti-commutation relations of the creation and annihilation operators.

To conclude, the great advantage and biggest difference of second quantization or the occupation number representation compared to first quantization is that the crucial physics of many-electron systems is mathematically encoded in a canonical operator algebra of anti-commuting creation and annihilation operators all emerging operators and states can be reduced to.

## 3.3 Quantum lattice models revisited

In principle, every quantum-mechanical problem formulated in second quantization can be seen as a quantum lattice model. Take for example the Hamiltonian of a simple molecule like  $\text{H}_2$

$$\hat{H} = \sum_{ij,\sigma} h_{ij} \hat{c}_{i\sigma}^\dagger \hat{c}_{j\sigma} + \frac{1}{2} \sum_{ijkl,\sigma\sigma'} u_{ijkl} \hat{c}_{i\sigma}^\dagger \hat{c}_{j\sigma'}^\dagger \hat{c}_{l\sigma'} \hat{c}_{k\sigma} \quad (3.63)$$

in the basis of Hartree-Fock orbitals  $|\varphi_i\rangle$ . The  $z$ -component of the electron-spin had to be introduced in the last equation ( $\sigma \in \{\uparrow; \downarrow\}$ ). The  $h_{ij}$  are the matrix elements of the one-electron part (kinetic energy plus potential of the nuclei) and  $u_{ijkl}$  is the electron-electron interaction. Eq. (3.63) can be considered as the Hamiltonian of an abstract quantum lattice model when the single-particle basis states or orbitals are

### 3 Theoretical framework

thought of as lattice sites in an abstract one-dimensional lattice which are occupied by the electrons of the system. This is how all the quantum-chemical implementations of the density matrix renormalization group look like. One starts with a Hartree-Fock calculation and takes the resulting orbitals as lattice sites. So, DMRG becomes a pure post-Hartree-Fock method.

Yet, there is another way to obtain a lattice model. Take the real-space representation of Eq. (3.63)

$$\begin{aligned} \hat{H} = & \sum_{\sigma} \int d^3x \hat{\psi}_{\sigma}^{\dagger}(\mathbf{x}) \frac{-1}{2} \Delta \hat{\psi}_{\sigma}(\mathbf{x}) + \sum_{\sigma} \int d^3x V(\mathbf{x}) \hat{\psi}_{\sigma}^{\dagger}(\mathbf{x}) \hat{\psi}_{\sigma}(\mathbf{x}) \\ & + \frac{1}{2} \sum_{\sigma\sigma'} \int d^3x d^3x' U(\mathbf{x}, \mathbf{x}') \hat{\psi}_{\sigma}^{\dagger}(\mathbf{x}) \hat{\psi}_{\sigma'}^{\dagger}(\mathbf{x}') \hat{\psi}_{\sigma'}(\mathbf{x}') \hat{\psi}_{\sigma}(\mathbf{x}) \end{aligned} \quad (3.64)$$

and discretize it as shown in the reference by Stoudenmire et al. [2012] for a purely one-dimensional chain of hydrogen atoms where the electrons are only allowed to move along the chain and not perpendicular to it. That means one introduces a characteristic length  $\delta$ —and at the same time accuracy measure—the electrons cannot go below. This length becomes the lattice spacing of an artificial lattice emerging from discretizing the continuum and changing from integration to summation. In the limit  $\delta \rightarrow 0$ , it is valid to cast the last equation of a continuous model into a lattice model of the shape

$$\hat{H} = \sum_{\mathbf{i}, \sigma} t_{\mathbf{i}, \mathbf{j}} \hat{c}_{\mathbf{i}\sigma}^{\dagger} \hat{c}_{\mathbf{j}\sigma} + \sum_{\mathbf{i}, \sigma} v_{\mathbf{i}} \hat{n}_{\mathbf{i}\sigma} + \frac{1}{2} \sum_{\mathbf{i}, \mathbf{j}, \sigma\sigma'} u_{\mathbf{i}, \mathbf{j}} \hat{c}_{\mathbf{i}\sigma}^{\dagger} \hat{c}_{\mathbf{j}\sigma'}^{\dagger} \hat{c}_{\mathbf{j}\sigma'} \hat{c}_{\mathbf{i}\sigma}. \quad (3.65)$$

$t_{\mathbf{i}, \mathbf{j}}$ ,  $v_{\mathbf{i}}$  and  $u_{\mathbf{i}, \mathbf{j}}$  are the discrete versions of the kinetic energy, potential of the nuclei with charges  $Z_A$  and positions  $\mathbf{R}_A$ , and the electron-electron interaction

$$t_{\mathbf{i}, \mathbf{j}} = \begin{cases} -\frac{1}{2\delta^2} \delta_{|\mathbf{i}-\mathbf{j}|, 1}, & \mathbf{i} \neq \mathbf{j} \\ \frac{3}{\delta^2}, & \mathbf{i} = \mathbf{j} \end{cases} \quad (3.66)$$

$$v_{\mathbf{i}} = \sum_A \frac{-Z_A}{|\delta\mathbf{i} - \mathbf{R}_A|} \quad (3.67)$$

$$u_{\mathbf{i}, \mathbf{j}} = \frac{1}{\delta|\mathbf{i} - \mathbf{j}|}. \quad (3.68)$$

The bold-type indices  $\mathbf{i}, \mathbf{j} \in \mathbb{Z}^3$  are the discrete lattice vectors

$$\mathbf{x} = \delta\mathbf{i}, \quad (3.69)$$

which holds in the limit of an infinitesimal lattice spacing and infinitely many lattice sites. The exact details how to discretize a three-dimensional continuous model will be given later in this thesis. However, the latter ansatz is a good starting point for numerical simulations because it does not need a pre-Hartree-Fock calculation. It can be used immediately for a DMRG calculation and contains all the correct physics but only on a lattice or grid of artificial points.

# 4 Calculus of matrix product states and operators

This chapter is meant to give an overview of the relatively new field of quantum-mechanical state classes called matrix product states (MPS) as used in [Östlund and Rommer, 1995, Rommer and Östlund, 1997] and corresponding operators known as matrix product operators (MPO) which more and more occur in simulations of quantum-many-body systems. MPSs and MPOs are normally used to reduce the amount of computer resources needed for a quantum-mechanical simulation. They make it possible to break the many-body Schrödinger equation down to a system of effective, easily diagonalizable one-particle Schrödinger equations. So, exponentially demanding numerical calculations can be facilitated tremendously. For an excellent review, see Schollwöck [2011].

## 4.1 Matrix product states

Consider the most general ansatz for a many-particle wave function formulated in second quantization

$$|\psi\rangle = \sum_{\mathbf{n}} \Psi_{\mathbf{n}} |\mathbf{n}\rangle, \quad (4.1)$$

where  $|\mathbf{n}\rangle = |n_1 n_2 \dots n_L\rangle$  is an occupation number vector or Fock state of length  $L$ . For a given occupation  $n_1, n_2$ , etc.  $\Psi_{\mathbf{n}}$  is a scalar quantity. Now assume we can find a way to write  $\Psi_{\mathbf{n}}$  as a product of matrices

$$\Psi_{\mathbf{n}} = \Psi_{n_1 n_2 \dots n_L} \quad (4.2)$$

$$= \Psi^{n_1} \Psi^{n_2} \dots \Psi^{n_L}. \quad (4.3)$$

$\Psi^{n_1}$  and  $\Psi^{n_L}$  are row and column vectors respectively. This matrix product factorization may for example be achieved by a consecutive singular value (SVD) or QR decomposition [Gentle, 2012]:

$$\Psi_{n_1 n_2 \dots n_L} = \sum_{i_1} U_{i_1}^{n_1} S_{i_1 j_1} V_{j_1, n_2 \dots n_L} = \sum_{i_1} \Psi_{i_1}^{n_1} \Psi'_{i_1, n_2 \dots n_L} \quad (\text{SVD}) \quad (4.4)$$

$$\Psi_{n_1 n_2 \dots n_L} = \sum_{i_1} Q_{i_1}^{n_1} R_{i_1, n_2 \dots n_L} = \sum_{i_1} \Psi_{i_1}^{n_1} \Psi'_{i_1, n_2 \dots n_L} \quad (\text{QR}) \quad (4.5)$$

In the next step,  $\Psi'$  is decomposed and so on. In the end, one obtains

$$\Psi_{n_1 n_2 \dots n_L} = \sum_{i_1 i_2 \dots i_{L-1}} \Psi_{i_1}^{n_1} \Psi_{i_1 i_2}^{n_2} \dots \Psi_{i_{L-1}}^{n_L} \quad (4.6)$$

and Eq. (4.1) can be rewritten as

$$|\psi\rangle = \sum_{n_1 n_2 \dots n_L} \Psi^{n_1} \Psi^{n_2} \dots \Psi^{n_L} |n_1 n_2 \dots n_L\rangle. \quad (4.7)$$

Eq. (4.7) is called matrix product state due to its matrix product structure. Eq. (4.7) can in principle always be obtained from Eq. (4.1) by a consecutive matrix factorization technique as shown above and is thus exact but in practice, it is unfeasible because the number of expansion coefficients  $\Psi_{n_1 n_2 \dots n_L}$  increases exponentially with the number of included single-particle states  $L$ . Assuming that the occupation numbers  $n_1, n_2, \dots$  up to  $n_L$  can take the values 0 or 1, the Hilbert space dimension  $D = \dim(\mathcal{H})$  of the wave function grows like

$$D(L) = 2^L. \quad (4.8)$$

Eq. (4.7) will only serve as an approximation of Eq. (4.1) in practical cases. Even though it serves as an approximation, a MPS has two nice features: First, one can tune the variational freedom of a MPS by adjusting the size of the matrices  $\Psi^n$  which form the MPS. Secondly, let us assume that for a given  $n \in \{0, 1\}$ , all  $\Psi^n$  are matrices of size  $M \times M$  (except for the first and last one which are  $1 \times M$  and  $M \times 1$ ), then it is possible to truncate the Hilbert space such that

$$D(L) = 2^L \xrightarrow{\text{MPS}} 2M^2L - 4M(M - 1). \quad (4.9)$$

### 4.1.1 Addition of matrix product states

Assume now we have two states  $|\psi\rangle$  and  $|\phi\rangle$  in MPS form. They can be added and yield a new MPS

$$|\tilde{\psi}\rangle = a|\psi\rangle + b|\phi\rangle \quad (a, b \in \mathbb{C}) \quad (4.10)$$

$$= \sum_{n_1 n_2 \dots n_L} (a\Psi^{n_1} \Psi^{n_2} \dots \Psi^{n_L} + b\Phi^{n_1} \Phi^{n_2} \dots \Phi^{n_L}) |n_1 n_2 \dots n_L\rangle \quad (4.11)$$

$$= \sum_{n_1 n_2 \dots n_L} (a\Psi^{n_1} \oplus b\Phi^{n_1}) (\Psi^{n_2} \oplus \Phi^{n_2}) \dots (\Psi^{n_L} \oplus \Phi^{n_L}) |n_1 n_2 \dots n_L\rangle \quad (4.12)$$

$$= \sum_{n_1 n_2 \dots n_L} \tilde{\Psi}^{n_1} \tilde{\Psi}^{n_2} \dots \tilde{\Psi}^{n_L} |n_1 n_2 \dots n_L\rangle, \quad (4.13)$$

where  $\oplus$  denotes the direct sum or Kronecker sum. The Kronecker sum of two  $M \times M'$  matrices  $\mathbf{A}$  and  $\mathbf{B}$  is defined as

$$\mathbf{A} \oplus \mathbf{B} = \begin{pmatrix} \mathbf{A} & \mathbf{0} \\ \mathbf{0} & \mathbf{B} \end{pmatrix}. \quad (4.14)$$

For two  $M$ -dimensional column vectors  $\mathbf{u}$  and  $\mathbf{v}$ , it is defined as

$$\mathbf{u} \oplus \mathbf{v} = \begin{pmatrix} \mathbf{u} \\ \mathbf{v} \end{pmatrix}. \quad (4.15)$$



### 4.1.2 Scalar product of two matrix product states

Consider two states  $|\psi\rangle$  and  $|\phi\rangle$  in MPS form, then one can of course also calculate the scalar product or overlap of these two states, which can be done fairly efficiently due to the matrix product structure

$$\langle\psi|\phi\rangle = \sum_{\substack{m_1 m_2 \dots m_L \\ n_1 n_2 \dots n_L}} (\Psi^{m_1} \Psi^{m_2} \dots \Psi^{m_L})^* (\Phi^{n_1} \Phi^{n_2} \dots \Phi^{n_L}) \langle \mathbf{m} | \mathbf{n} \rangle \quad (4.16)$$

$$= \underbrace{\left( \sum_{n_1} \Psi^{n_1 \dagger} \Phi^{n_1} \right)}_{=M^{(1)}} \left( \sum_{n_2} \Psi^{n_2 \dagger} \Phi^{n_2} \right) \dots \left( \sum_{n_L} \Psi^{n_L \dagger} \Phi^{n_L} \right) \quad (4.17)$$

$$= \underbrace{\left( \sum_{n_2} \Psi^{n_2 \dagger} M^{(1)} \Phi^{n_2} \right)}_{=M^{(2)}} \dots \left( \sum_{n_L} \Psi^{n_L \dagger} \Phi^{n_L} \right) \quad (4.18)$$

$$\vdots \\ = \sum_{n_L} \Psi^{n_L \dagger} M^{(L-1)} \Phi^{n_L} . \quad (4.19)$$

In this way, one can for instance calculate norms of wave functions in MPS form.

### 4.1.3 Invariance and normalization of matrix product states

It is often useful to work with normalized matrix product states. A MPS is normalized by orthogonalization of its constituent matrices, which can always be done at any time due to the fact that a general MPS is invariant under transformations of the kind

$$|\psi\{\mathbf{X}\}\rangle = \sum_{n_1 n_2 \dots n_L} \Psi^{n_1} \mathbf{X}_1 \mathbf{X}_1^{-1} \Psi^{n_2} \mathbf{X}_2 \dots \mathbf{X}_{L-1}^{-1} \Psi^{n_L} |n_1 n_2 \dots n_L\rangle \quad (4.20)$$

$$= \sum_{n_1 n_2 \dots n_L} \Psi^{n_1} \Psi^{n_2} \dots \Psi^{n_L} |n_1 n_2 \dots n_L\rangle \quad (4.21)$$

$$= |\psi\rangle . \quad (4.22)$$

As sketched above, a MPS can thus be normalized by a consecutive QR decomposition for example

$$|\psi\rangle = \sum_{n_1 n_2 \dots n_L} \mathbf{Q}^{n_1} \mathbf{Q}^{n_2} \dots \Psi^{n_L} . \quad (4.23)$$

The squared norm of  $|\psi\rangle$  can now be calculated with what was shown in the last section

$$\|\psi\|^2 = \langle\psi|\psi\rangle \quad (4.24)$$

$$= \sum_{n_L} \Psi^{n_L \dagger} \Psi^{n_L} \quad (4.25)$$

Eq. (4.25) results from the fact that

$$\sum_n Q^{n\dagger} Q^n = \mathbf{1}. \quad (4.26)$$

The normalized MPS then reads

$$|\psi\rangle = \sum_{n_1 n_2 \dots n_L} \frac{Q^{n_1} Q^{n_2} \dots \Psi^{n_L}}{\sqrt{\sum_{m_L} \Psi^{m_L\dagger} \Psi^{m_L}}} |n_1 n_2 \dots n_L\rangle. \quad (4.27)$$

Everything shown here can equivalently be obtained when orthogonalizing and normalizing  $|\psi\rangle$  via a RQ decomposition from the right instead of a QR decomposition from the left.

## 4.2 Matrix product operators

The following sections are meant to extend and explain in more detail the concept of matrix product operators also partly described in Snajberk and Ochsenfeld [2017a,b] (see the publication list).

The operator analogues of matrix product states are matrix product operators (MPO). These objects are the key to efficient quantum-mechanical many-body simulations like the search for the ground-state of a system. The MPO form of an operator can theoretically be obtained by a consecutive matrix factorization like for a MPS

$$\hat{O} = \sum_{mn} O_{mn} |m\rangle \langle n| \quad (4.28)$$

$$= \sum_{mn} O^{m_1 n_1} O^{m_2 n_2} \dots O^{m_L n_L} |m\rangle \langle n|. \quad (4.29)$$

The only difference is that a MPO matrix bears two basis indices  $m$  and  $n$  instead of one. This is also not manageable in practical applications because one must know the whole matrix representation of  $\hat{O}$  in an exponentially large basis in advance. In quantum-mechanical calculations, it is important to find a compact and efficient representation of the Hamiltonian as a matrix product operator.

### 4.2.1 Addition, multiplication, and norms of matrix product operators

As well as matrix product states, MPOs can be added. Consider two operators  $\hat{A}$  and  $\hat{B}$  in MPO form, then

$$\hat{O} = \hat{A} + \hat{B} \quad (4.30)$$

$$= \sum_{mn} (A^{m_1 n_1} \oplus B^{m_1 n_1}) (A^{m_2 n_2} \oplus B^{m_2 n_2}) \dots (A^{m_L n_L} \oplus B^{m_L n_L}) |m\rangle \langle n| \quad (4.31)$$

$$= \sum_{mn} O^{m_1 n_1} O^{m_2 n_2} \dots O^{m_L n_L} |m\rangle \langle n|. \quad (4.32)$$

MPOs can also be multiplied

$$\hat{O} = \hat{A}\hat{B} \quad (4.33)$$

$$= \sum_{mnn'} \left( \mathbf{A}^{m_1 n'_1} \otimes \mathbf{B}^{n'_1 n_1} \right) \left( \mathbf{A}^{m_2 n'_2} \otimes \mathbf{B}^{n'_2 n_2} \right) \dots \left( \mathbf{A}^{m_L n'_L} \otimes \mathbf{B}^{n'_L n_L} \right) |\mathbf{m}\rangle \langle \mathbf{n}| \quad (4.34)$$

$$= \sum_{mn} \mathbf{O}^{m_1 n_1} \mathbf{O}^{m_2 n_2} \dots \mathbf{O}^{m_L n_L} |\mathbf{m}\rangle \langle \mathbf{n}|. \quad (4.35)$$

The symbol  $\otimes$  denotes the Kronecker product which is defined for two  $M \times N$  matrices  $\mathbf{A}$  and  $\mathbf{B}$  such that

$$\mathbf{A} \otimes \mathbf{B} = \begin{pmatrix} a_{11}\mathbf{B} & a_{12}\mathbf{B} & \dots & a_{1N}\mathbf{B} \\ a_{21}\mathbf{B} & a_{22}\mathbf{B} & & \\ \vdots & & \ddots & \\ a_{M1}\mathbf{B} & & & a_{MN}\mathbf{B} \end{pmatrix}. \quad (4.36)$$

The multiplication of two MPOs hence yields a MPO. The problem for this operation is that it increases the dimension of the resulting MPO  $\hat{O}$ . The size of the operator matrices increases

$$\mathbf{O}^{mn} = \sum_{n'} \left( \mathbf{A}^{mn'} \otimes \mathbf{B}^{n'n} \right), \quad (4.37)$$

where  $\mathbf{O}^{mn}$  is a  $M^2 \times N^2$  matrix when  $\mathbf{A}$  and  $\mathbf{B}$  are of size  $M \times N$ . This size increase is important when it comes to calculating quadratic operators like the variance of an observable  $\hat{O}$

$$\text{var}(\hat{O}) = \langle \hat{O}^2 \rangle - \langle \hat{O} \rangle^2. \quad (4.38)$$

Norms of matrix product operators can be calculated as straightforwardly as for MPS using the norm equivalent for operators

$$\|\hat{O}\| = \sqrt{\text{Tr}(\hat{O}^\dagger \hat{O})} \quad (\text{Frobenius norm}). \quad (4.39)$$

### 4.2.2 Construction of matrix product operators and simple examples

Consider a general, diagonal one-particle operator  $\hat{O}$  in second quantization formulation

$$\hat{O} = \sum_k \varepsilon_k \hat{n}_k, \quad (4.40)$$

where the index  $k$  runs over all single-particle states.  $\hat{n}_k$  represents the occupation number operator for the state  $k$  and the  $\varepsilon_k$  are the eigenvalues of  $\hat{O}$ . The goal is now to bring the operator  $\hat{O}$  to MPO form Eq. (4.29). This can best be done by looking at the matrix elements of  $\hat{O}$

$$\langle m_1 m_2 \dots m_L | \hat{O} | n_1 n_2 \dots n_L \rangle = \sum_k \varepsilon_k \langle m_1 m_2 \dots m_L | \hat{n}_k | n_1 n_2 \dots n_L \rangle \quad (4.41)$$

$$= \sum_k \delta_{m_1 n_1} \delta_{m_2 n_2} \dots \varepsilon_k n_k \delta_{m_k n_k} \dots \delta_{m_L n_L}. \quad (4.42)$$

#### 4 Calculus of matrix product states and operators

This shows that one can write the matrix of  $\hat{O}$  in the occupation number basis as

$$\mathbf{O} = \sum_k \mathbf{1}_1 \otimes \mathbf{1}_2 \otimes \cdots \otimes \varepsilon_k \boldsymbol{\eta}_k \otimes \cdots \otimes \mathbf{1}_L \quad (4.43)$$

or as operator

$$\hat{O} = \sum_k \hat{\mathbf{1}}_1 \otimes \hat{\mathbf{1}}_2 \otimes \cdots \otimes \varepsilon_k \hat{\boldsymbol{\eta}}_k \otimes \cdots \otimes \hat{\mathbf{1}}_L. \quad (4.44)$$

The occupation number operator  $\hat{n}$  has been redefined ( $\hat{n} \rightarrow \hat{\eta}$ ) such that it now acts on a particular single-particle state instead of a whole occupation number or Fock state

$$\hat{n}_k |n_1 n_2 \cdots n_L\rangle = |n_1\rangle \otimes |n_2\rangle \otimes \cdots \otimes \hat{\eta}_k |n_k\rangle \otimes \cdots \otimes |n_L\rangle \quad (4.45)$$

$$= |n_1\rangle \otimes |n_2\rangle \otimes \cdots \otimes n_k |n_k\rangle \otimes \cdots \otimes |n_L\rangle. \quad (4.46)$$

The new redefined local occupation number operator  $\hat{\eta}$  is defined by its matrix action. For spin orbitals, this action is

$$\boldsymbol{\eta} = \begin{pmatrix} 0 & 0 \\ 0 & 1 \end{pmatrix} \quad (4.47)$$

and for spatial orbitals where one assumes four different possible occupation states  $|0\rangle, |\uparrow\rangle, |\downarrow\rangle$  or  $|\uparrow\downarrow\rangle$

$$\boldsymbol{\eta} = \begin{pmatrix} 0 & 0 & 0 & 0 \\ 0 & 1 & 0 & 0 \\ 0 & 0 & 1 & 0 \\ 0 & 0 & 0 & 2 \end{pmatrix}. \quad (4.48)$$

Eq. (4.44) can now be brought into MPO shape

$$\hat{O} = (\hat{\mathbf{1}}_1 \quad \varepsilon_1 \hat{\boldsymbol{\eta}}_1) \odot \begin{pmatrix} \hat{\mathbf{1}}_2 & \varepsilon_2 \hat{\boldsymbol{\eta}}_2 \\ 0 & \hat{\mathbf{1}}_2 \end{pmatrix} \odot \cdots \odot \begin{pmatrix} \varepsilon_L \hat{\boldsymbol{\eta}}_L \\ \hat{\mathbf{1}}_L \end{pmatrix} \quad (4.49)$$

$$= \hat{\mathbf{O}}_1 \odot \hat{\mathbf{O}}_2 \odot \cdots \odot \hat{\mathbf{O}}_L. \quad (4.50)$$

The  $\hat{\mathbf{O}}_k$  are here operator-valued matrices. We have also introduced a new symbol  $\odot$  for clarity of notation. This operation symbol is meant to unite the features of both the standard matrix product and the tensor product  $\otimes$ . Eq. (4.50) is an equivalent representation of a MPO because

$$\hat{O} = \hat{\mathbf{O}}_1 \odot \hat{\mathbf{O}}_2 \odot \cdots \odot \hat{\mathbf{O}}_L \quad (4.51)$$

$$= \sum_{\mathbf{m}\mathbf{n}} \langle \mathbf{m} | \hat{\mathbf{O}}_1 \odot \hat{\mathbf{O}}_2 \odot \cdots \odot \hat{\mathbf{O}}_L | \mathbf{n} \rangle | \mathbf{m} \rangle \langle \mathbf{n} | \quad (4.52)$$

$$= \sum_{\mathbf{m}\mathbf{n}} \langle m_1 | \hat{\mathbf{O}}_1 | n_1 \rangle \langle m_2 | \hat{\mathbf{O}}_2 | n_2 \rangle \cdots \langle m_L | \hat{\mathbf{O}}_L | n_L \rangle | \mathbf{m} \rangle \langle \mathbf{n} | \quad (4.53)$$

$$= \sum_{\mathbf{m}\mathbf{n}} \mathbf{O}^{m_1 n_1} \mathbf{O}^{m_2 n_2} \cdots \mathbf{O}^{m_L n_L} | \mathbf{m} \rangle \langle \mathbf{n} |. \quad (4.54)$$

The last equations show the features of the  $\odot$  symbol.

Now, let us turn to a more complicated example

$$\hat{T} = \sum_{kl} t_{kl} \hat{c}_k^\dagger \hat{c}_l \quad (4.55)$$

which can for instance describe the kinetic energy of an electron moving on a real-space grid. This example is more complicated because one now has to include the anti-commutativity of electrons into the matrix product operator framework. However, first of all, one must sort and order the single-particle states or lattice sites here

$$\hat{T} = \sum_k t_k \hat{n}_k + \sum_{k < l} \left( t_{kl} \hat{c}_k^\dagger \hat{c}_l + t_{kl}^* \hat{c}_l^\dagger \hat{c}_k \right). \quad (4.56)$$

One can see that the first sum will lead to a MPO of the form Eq. (4.49) and the second sum to a MPO which will be discussed in the following. The procedure is almost the same as sketched above and one has first to look at the matrix elements of the creation and annihilation operators to see how to construct the MPO representation. Assume  $k < l$ , then

$$\langle \mathbf{m} | \hat{c}_k^\dagger \hat{c}_l | \mathbf{n} \rangle = (-1)^{n_k + \dots + n_{l-1}} \langle \dots m_k \dots m_l \dots | \dots n_k + 1 \dots n_l - 1 \dots \rangle \quad (4.57)$$

$$\begin{aligned} &= \delta_{m_1 n_1} \dots (-1)^{n_k} \delta_{m_k n_{k+1}} (-1)^{n_{k+1}} \delta_{m_{k+1} n_{k+1}} \\ &\quad \dots \delta_{m_l n_{l-1}} \dots \delta_{m_L n_L}. \end{aligned} \quad (4.58)$$

Thus, we conclude that the operator can be written as

$$\hat{c}_k^\dagger \hat{c}_l = \hat{1}_1 \otimes \dots \otimes \hat{\zeta}_k^{L\dagger} \otimes \hat{f}_{k+1} \otimes \dots \otimes \hat{\zeta}_l^L \otimes \dots \otimes \hat{1}_L. \quad (4.59)$$

By redefining the operators' action, we have to introduce operators which we call fermionic anti-commutation operators and which are defined by their matrix action

$$\mathbf{f} = \begin{pmatrix} 1 & 0 \\ 0 & -1 \end{pmatrix}. \quad (4.60)$$

The now locally acting creation and annihilation operators  $\hat{\zeta}^\dagger$  and  $\hat{\zeta}$  have the form (for all  $k$ )

$$\zeta^{L\dagger} = \begin{pmatrix} 0 & 0 \\ 1 & 0 \end{pmatrix}, \quad \zeta^L = \begin{pmatrix} 0 & 1 \\ 0 & 0 \end{pmatrix}. \quad (4.61)$$

The superscript  $L$  suggests that  $\hat{\zeta}^{L\dagger}$  and  $\hat{\zeta}^L$  annihilate and create from the right to the left on a chain of points (It is important not to confuse them with the number of single-particle states or points in the chain  $L$ ). Basically, the same holds for the other creation and annihilation operator combination

$$\langle \mathbf{m} | \hat{c}_l^\dagger \hat{c}_k | \mathbf{n} \rangle = (-1)^{1+n_k + \dots + n_{l-1}} \langle \dots m_k \dots m_l \dots | \dots n_k - 1 \dots n_l + 1 \dots \rangle \quad (4.62)$$

$$\begin{aligned} &= \delta_{m_1 n_1} \dots (-1)^{1+n_k} \delta_{m_k n_{k-1}} (-1)^{n_{k+1}} \delta_{m_{k+1} n_{k+1}} \\ &\quad \dots \delta_{m_l n_{l+1}} \dots \delta_{m_L n_L}. \end{aligned} \quad (4.63)$$

The slight difference is the additional factor of  $-1$  which leads to another set of creation and annihilation operators which annihilate and create from the left to the

right (superscript  $R$ )

$$\zeta^{R\dagger} = \begin{pmatrix} 0 & 0 \\ 1 & 0 \end{pmatrix}, \quad \zeta^R = \begin{pmatrix} 0 & 1 \\ 0 & 0 \end{pmatrix}. \quad (4.64)$$

It can be recognized that the  $L$ - and  $R$ -operators are identical for spin orbitals as single-particle states, however, for spatial orbitals, one must distinguish between different spin orientations ( $\uparrow$  or  $\downarrow$ ) and  $L$  and  $R$ . The operators must then have the form

$$\zeta_{\uparrow}^{L\dagger} = \begin{pmatrix} 0 & 0 & 0 & 0 \\ 1 & 0 & 0 & 0 \\ 0 & 0 & 0 & 0 \\ 0 & 0 & -1 & 0 \end{pmatrix}, \quad \zeta_{\uparrow}^L = \begin{pmatrix} 0 & 1 & 0 & 0 \\ 0 & 0 & 0 & 0 \\ 0 & 0 & 0 & 1 \\ 0 & 0 & 0 & 0 \end{pmatrix} \quad (4.65)$$

$$\zeta_{\uparrow}^{R\dagger} = \begin{pmatrix} 0 & 0 & 0 & 0 \\ 1 & 0 & 0 & 0 \\ 0 & 0 & 0 & 0 \\ 0 & 0 & 1 & 0 \end{pmatrix}, \quad \zeta_{\uparrow}^R = \begin{pmatrix} 0 & 1 & 0 & 0 \\ 0 & 0 & 0 & 0 \\ 0 & 0 & 0 & -1 \\ 0 & 0 & 0 & 0 \end{pmatrix} \quad (4.66)$$

$$\zeta_{\downarrow}^{L\dagger} = \begin{pmatrix} 0 & 0 & 0 & 0 \\ 0 & 0 & 0 & 0 \\ 1 & 0 & 0 & 0 \\ 0 & 1 & 0 & 0 \end{pmatrix}, \quad \zeta_{\downarrow}^L = \begin{pmatrix} 0 & 0 & 1 & 0 \\ 0 & 0 & 0 & -1 \\ 0 & 0 & 0 & 0 \\ 0 & 0 & 0 & 0 \end{pmatrix} \quad (4.67)$$

$$\zeta_{\downarrow}^{R\dagger} = \begin{pmatrix} 0 & 0 & 0 & 0 \\ 0 & 0 & 0 & 0 \\ 1 & 0 & 0 & 0 \\ 0 & -1 & 0 & 0 \end{pmatrix}, \quad \zeta_{\downarrow}^R = \begin{pmatrix} 0 & 0 & 1 & 0 \\ 0 & 0 & 0 & 1 \\ 0 & 0 & 0 & 0 \\ 0 & 0 & 0 & 0 \end{pmatrix}. \quad (4.68)$$

The fermionic anti-commutation operator reads as matrix

$$\mathbf{f} = \begin{pmatrix} 1 & 0 & 0 & 0 \\ 0 & -1 & 0 & 0 \\ 0 & 0 & -1 & 0 \\ 0 & 0 & 0 & 1 \end{pmatrix}. \quad (4.69)$$

The entry of  $-1$  in the spin dependent creation and annihilation operator matrices results from the anti-symmetry principle of fermionic wave functions or anti-commutativity of fermionic creation and annihilation operators for electrons with spin. The  $4 \times 4$  operators will especially be important in this thesis for the implementation of the Hamiltonian for quantum-chemical systems.

Now, we nearly have everything to cast Eq. (4.56) into MPO form. However, one problem remains. It is the term  $t_{kl}$  and its conjugate which couple two sites or single-particle states  $k$  and  $l$  (The notions “site” and “single-particle state” are used interchangeably here). Therefore, one must find a way to “decouple” somehow these states in order to obtain a site-by-site picture of a matrix product operator. This can be achieved by a matrix factorization like the QR decomposition

$$t_{kl} = \sum_i q_{ki} r_{il}. \quad (4.70)$$

Thus, one can write

$$\sum_{k<l} t_{kl} \hat{c}_k^\dagger \hat{c}_l = \sum_{i,k<l} q_{ki} r_{il} \hat{c}_k^\dagger \hat{c}_l \quad (4.71)$$

$$= \sum_{i,k<l} \left( q_{ki} \hat{c}_k^\dagger \right) (r_{il} \hat{c}_l) \quad (4.72)$$

$$= \sum_{i,k<l} \hat{q}_k^{(i)} \hat{r}_l^{(i)} \quad (4.73)$$

$$= \sum_i \hat{t}_{\text{MPO}}^{(i)} \quad (4.74)$$

which leads to a sum of operators which can be represented as matrix product operators

$$\hat{t}_{\text{MPO}}^{(i)} = \left( \hat{1}_1 \quad q_{1i} \hat{\zeta}_1^{L\dagger} \quad 0 \right) \odot \begin{pmatrix} \hat{1}_2 & q_{2i} \hat{\zeta}_2^{L\dagger} & 0 \\ 0 & \hat{f}_2 & r_{i2} \hat{\zeta}_2^L \\ 0 & 0 & \hat{1}_2 \end{pmatrix} \odot \cdots \odot \begin{pmatrix} 0 \\ r_{iL} \hat{\zeta}_L^L \\ \hat{1}_L \end{pmatrix} \quad (4.75)$$

$$= \hat{t}_1^{(i)} \odot \hat{t}_2^{(i)} \odot \cdots \odot \hat{t}_L^{(i)}. \quad (4.76)$$

This of course holds for the conjugated part of Eq. (4.56) as well. We conclude that Eq. (4.56) can be written as a sum of MPOs

$$\hat{T} = \sum_{i=0}^L \hat{t}_{\text{MPO}}^{(i)}, \quad (4.77)$$

where the  $i = 0$  MPO refers to the operator containing the sum of occupation number operators  $\sum_k t_k \hat{n}_k$ . We will come back to the construction of MPOs when it comes to how to construct and implement quantum-chemical Hamiltonians.

### 4.3 Application of matrix product operators to matrix product states

With what has been shown so far, one is also able to apply a MPO to a MPS which again yields a MPS. Consider we have a MPO  $\hat{O}$  of length  $L$

$$\hat{O} = \hat{O}_1 \odot \hat{O}_2 \odot \cdots \odot \hat{O}_L \quad (4.78)$$

$$= \sum_{\mathbf{m}\mathbf{n}} \mathcal{O}^{m_1 n_1} \mathcal{O}^{m_2 n_2} \cdots \mathcal{O}^{m_L n_L} |\mathbf{m}\rangle \langle \mathbf{n}| \quad (4.79)$$

and a MPS  $|\psi\rangle$

$$|\psi\rangle = |\Psi_1\rangle \odot |\Psi_2\rangle \odot \cdots \odot |\Psi_L\rangle \quad (4.80)$$

$$= \sum_{\mathbf{n}} \Psi^{n_1} \Psi^{n_2} \cdots \Psi^{n_L} |\mathbf{n}\rangle. \quad (4.81)$$

Here, a similar shorthand notation for MPSs as for MPOs was introduced

$$|\Psi\rangle = \sum_n \Psi^n |n\rangle . \quad (4.82)$$

When we apply  $\hat{O}$  to  $|\psi\rangle$ , one obtains a new MPS  $|\phi\rangle$

$$\hat{O}|\psi\rangle = \hat{O}_1|\Psi_1\rangle \odot \hat{O}_2|\Psi_2\rangle \odot \cdots \odot \hat{O}_L|\Psi_L\rangle \quad (4.83)$$

$$= \sum_{mn} (\mathbf{O}^{m_1 n_1} \otimes \Psi^{n_1}) (\mathbf{O}^{m_2 n_2} \otimes \Psi^{n_2}) \cdots (\mathbf{O}^{m_L n_L} \otimes \Psi^{n_L}) |\mathbf{m}\rangle \quad (4.84)$$

$$= \sum_{\mathbf{m}} \Phi^{m_1} \Phi^{m_2} \cdots \Phi^{m_L} |\mathbf{m}\rangle \quad (4.85)$$

$$= |\Phi_1\rangle \odot |\Phi_2\rangle \odot \cdots \odot |\Phi_L\rangle \quad (4.86)$$

$$= |\phi\rangle . \quad (4.87)$$

Applying MPOs to MPSs bears the same problem as multiplying two MPOs together. The size of the resulting state matrices increase by the Kronecker product of the operator and the old state matrices.

### 4.3.1 Expectation values

Expectation values of quantum-mechanical observables can readily be calculated in the MPO-MPS framework since calculating expectation values is nothing but evaluating the scalar product or overlap of two matrix product states where one of them is just the product of the observable representing operator  $\hat{O}$  and the state  $|\psi\rangle$ . Assume that  $|\psi\rangle$  is normalized, then the expectation value of  $\hat{O}$  reads [Griffiths, 2013, Messiah, 2014]

$$\langle O \rangle = \langle \psi | \hat{O} | \psi \rangle . \quad (4.88)$$

As an example, consider the particle number operator defined in second quantization as

$$\hat{N} = \sum_{k=1}^L \hat{n}_k , \quad (4.89)$$

where the sum runs over all  $L$  single-particle states. It has the following MPO representation

$$\hat{N} = \begin{pmatrix} \hat{1}_1 & \hat{\eta}_1 \end{pmatrix} \odot \begin{pmatrix} \hat{1}_2 & \hat{\eta}_2 \\ 0 & \hat{1}_2 \end{pmatrix} \odot \cdots \odot \begin{pmatrix} \hat{\eta}_L \\ \hat{1}_L \end{pmatrix} \quad (4.90)$$

$$= \hat{N}_1 \odot \hat{N}_2 \odot \cdots \odot \hat{N}_L . \quad (4.91)$$

The expectation value of this operator can be calculated easily since its operator matrix size is just  $2 \times 2$  except for the first and last one

$$\langle \hat{N} \rangle = \langle \psi | \hat{N} | \psi \rangle \quad (4.92)$$



$$\begin{aligned}
 &= \sum_{m_L n_L} \Psi^{m_L^\dagger} \dots \left( \sum_{m_2 n_2} \Psi^{m_2^\dagger} \left( \sum_{m_1 n_1} \Psi^{m_1^\dagger} (\mathbf{N}^{m_1 n_1} \otimes \Psi^{n_1}) \right) (\mathbf{N}^{m_2 n_2} \otimes \Psi^{n_2}) \right) \\
 &\quad \dots (\mathbf{N}^{m_L n_L} \otimes \Psi^{n_L}) .
 \end{aligned} \tag{4.93}$$

The last equation exactly corresponds to the efficient evaluation of MPS scalar products.

### 4.3.2 Eigenvalue problems

The real strength of working with MPOs and MPSs lies at reducing the formal degrees of freedom or renormalizing the basis. In quantum-mechanics, it is often the case that one is interested in finding solutions of eigenvalue problems. The numerical solution of these problems highly depends on the degrees of freedom a particular problem consists of. With degrees of freedom, one normally refers to the Hilbert space or basis a wave function must be expanded in for instance. Consider again an operator  $\hat{O}$  and a state  $|\psi\rangle$  which fulfill the eigenvalue equation

$$\hat{O} |\psi\rangle = \omega |\psi\rangle , \tag{4.94}$$

where  $\omega$  is the eigenvalue.  $\hat{O}$  and  $|\psi\rangle$  have MPO and MPS form, respectively. A great feature of MPSs and MPOs is that one is able to trace out or sum up degrees of freedom whose exact determination and representation do not matter currently

$$|\psi\rangle = |\Psi_1\rangle \odot |\Psi_2\rangle \odot \dots \odot |\Psi_L\rangle \tag{4.95}$$

$$= |\mathcal{L}\rangle \odot |\Psi_k\rangle \odot |\mathcal{R}\rangle \tag{4.96}$$

$$\hat{O} = \hat{O}_1 \odot \hat{O}_2 \odot \dots \odot \hat{O}_L \tag{4.97}$$

$$= \hat{\mathcal{P}} \odot \hat{O}_k \odot \hat{\mathcal{Q}} . \tag{4.98}$$

$|\mathcal{L}\rangle$ ,  $|\mathcal{R}\rangle$  and  $\hat{\mathcal{P}}$  and  $\hat{\mathcal{Q}}$  are sets of states and operators which are obtained when one sums over all local basis states  $|n\rangle$  and performs the matrix multiplication up to the  $k$ th position

$$|\mathcal{L}\rangle = \sum_{n_1 n_2 \dots n_{k-1}} \Psi^{n_1} \Psi^{n_2} \dots \Psi^{n_{k-1}} |n_1 n_2 \dots n_{k-1}\rangle \tag{4.99}$$

$$|l\rangle = \sum_{\substack{n_1 n_2 \dots n_{k-1} \\ l_1 l_2 \dots l_{k-2}}} \Psi_{l_1}^{n_1} \Psi_{l_1 l_2}^{n_2} \dots \Psi_{l_{k-2} l}^{n_{k-1}} |n_1 n_2 \dots n_{k-1}\rangle \tag{4.100}$$

$$|\mathcal{R}\rangle = \sum_{n_{k+1} \dots n_{L-1} n_L} \Psi^{n_{k+1}} \dots \Psi^{n_{L-1}} \Psi^{n_L} |n_{k+1} \dots n_{L-1} n_L\rangle \tag{4.101}$$

$$|r\rangle = \sum_{\substack{n_{k+1} \dots n_{L-1} n_L \\ r_{k+1} \dots r_{L-2} r_{L-1}}} \Psi_{r_{k+1}}^{n_{k+1}} \dots \Psi_{r_{L-2} r_{L-1}}^{n_{L-1}} \Psi_{r_{L-1}}^{n_L} |n_{k+1} \dots n_{L-1} n_L\rangle \tag{4.102}$$

$$\hat{\mathcal{P}} = \sum_{\substack{m_1 m_2 \dots m_{k-1} \\ n_1 n_2 \dots n_{k-1}}} \mathbf{O}^{m_1 n_1} \mathbf{O}^{m_2 n_2} \dots \mathbf{O}^{m_{k-1} n_{k-1}} |m_1 m_2 \dots m_{k-1}\rangle \langle n_1 n_2 \dots n_{k-1}| \tag{4.103}$$

#### 4 Calculus of matrix product states and operators

$$\hat{\mathcal{P}}_\alpha = \sum_{\substack{m_1 m_2 \cdots m_{k-1} \\ n_1 n_2 \cdots n_{k-1} \\ \alpha_1 \alpha_2 \cdots \alpha_{k-2}}} O_{\alpha_1}^{m_1 n_1} O_{\alpha_1 \alpha_2}^{m_2 n_2} \cdots O_{\alpha_{k-2} \alpha}^{m_{k-1} n_{k-1}} |m_1 m_2 \cdots m_{k-1}\rangle \langle n_1 n_2 \cdots n_{k-1}| \quad (4.104)$$

$$\begin{aligned} \hat{\mathcal{Q}} &= \sum_{\substack{m_{k+1} \cdots m_{L-1} m_L \\ n_{k+1} \cdots n_{L-1} n_L}} \mathbf{O}^{m_{k+1} n_{k+1}} \cdots \mathbf{O}^{m_{L-1} n_{L-1}} \mathbf{O}^{m_L n_L} |m_{k+1} \cdots m_{L-1} m_L\rangle \\ &\quad \times \langle n_{k+1} \cdots n_{L-1} n_L| \end{aligned} \quad (4.105)$$

$$\begin{aligned} \hat{\mathcal{Q}}_{\alpha'} &= \sum_{\substack{m_{k+1} \cdots m_{L-1} m_L \\ n_{k+1} \cdots n_{L-1} n_L \\ \alpha_{k+1} \cdots \alpha_{L-2} \alpha_{L-1}}} O_{\alpha' \alpha_{k+1}}^{m_{k+1} n_{k+1}} \cdots O_{\alpha_{L-2} \alpha_{L-1}}^{m_{L-1} n_{L-1}} O_{\alpha_{L-1}}^{m_L n_L} |m_{k+1} \cdots m_{L-1} m_L\rangle \\ &\quad \times \langle n_{k+1} \cdots n_{L-1} n_L| \end{aligned} \quad (4.106)$$

( $|l\rangle \in |\mathcal{L}\rangle$ ,  $|r\rangle \in |\mathcal{R}\rangle$ ,  $\hat{\mathcal{P}}_\alpha \in \hat{\mathcal{P}}$ ,  $\hat{\mathcal{Q}}_{\alpha'} \in \hat{\mathcal{Q}}$ ). In the last equations, we changed from bold type matrix notation to index notation, for instance

$$\Psi^n \longrightarrow \Psi_{l'l}^n \quad (4.107)$$

$$\mathbf{O}^{mn} \longrightarrow O_{\beta\alpha}^{mn}. \quad (4.108)$$

Eq. (4.94) can thus be transformed into an effective eigenvalue equation for the site  $k$ . This is achieved by projecting Eq. (4.94) onto the set of states  $\langle \mathcal{L}' m_k \mathcal{R}' |$

$$\langle \mathcal{L}' m_k \mathcal{R}' | \hat{\mathcal{O}} | \psi \rangle = \langle \mathcal{L}' m_k \mathcal{R}' | \psi \rangle \quad (4.109)$$

$$\langle \mathcal{L}' | \hat{\mathcal{P}} | \mathcal{L} \rangle \langle m_k | \hat{\mathcal{O}}_k | \Psi_k \rangle \langle \mathcal{R}' | \hat{\mathcal{Q}} | \mathcal{R} \rangle = \omega \langle \mathcal{L}' | \mathcal{L} \rangle \langle m_k | \Psi_k \rangle \langle \mathcal{R}' | \mathcal{R} \rangle \quad (4.110)$$

$$\mathcal{P}_{\mathcal{L}} \langle m_k | \hat{\mathcal{O}}_k | \Psi_k \rangle \mathcal{Q}_{\mathcal{R}} = \omega \mathcal{S}_{\mathcal{L}} \langle m_k | \Psi_k \rangle \mathcal{S}_{\mathcal{R}}. \quad (4.111)$$

All the expressions in the last equation are tensorial quantities. But it is not immediately obvious how the terms have to be contracted. Fig. 4.1 and Fig. 4.2 make clear how the tensors above are to be contracted in a pictured way. It also becomes clear when we change to index notation

$$\sum_{n_k l r \alpha \alpha'} \mathcal{P}_{\mathcal{L}' \alpha l} O_{\alpha \alpha'}^{m_k n_k} \Psi_{l r}^{n_k} \mathcal{Q}_{\mathcal{R}' \alpha' r} = \omega \sum_{l r} \mathcal{S}_{\mathcal{L}' l} \Psi_{l r}^{m_k} \mathcal{S}_{\mathcal{R}' r} \quad (4.112)$$

$$\sum_{n_k l r \alpha \alpha'} \langle l' | \hat{\mathcal{P}}_\alpha | l \rangle O_{\alpha \alpha'}^{m_k n_k} \Psi_{l r}^{n_k} \langle r' | \hat{\mathcal{Q}}_{\alpha'} | r \rangle = \omega \sum_{l r} \langle l' | l \rangle \langle r' | r \rangle \Psi_{l r}^{m_k} \quad (4.113)$$

$$\sum_{n_k l r} O_{l' r', l r}^{m_k n_k} \Psi_{l r}^{n_k} = \omega \sum_{l r} \mathcal{S}_{l' r', l r} \Psi_{l r}^{m_k}. \quad (4.114)$$

The last equation turns out to be quite similar to a generalized eigenvalue equation of the form

$$\mathbf{A} \vec{v} = \omega \mathbf{B} \vec{v}. \quad (4.115)$$

It can be transformed to a standard eigenvalue problem by normalizing the MPS state as previously shown by a QR decomposition. Then, we get

$$\mathcal{S}_{l' r', l r} = \langle l' | l \rangle \langle r' | r \rangle \quad (4.116)$$

$$= \delta_{l'l} \delta_{r'r} \quad (4.117)$$

$$= 1_{l' r', l r}. \quad (4.118)$$

### 4.3 Application of matrix product operators to matrix product states

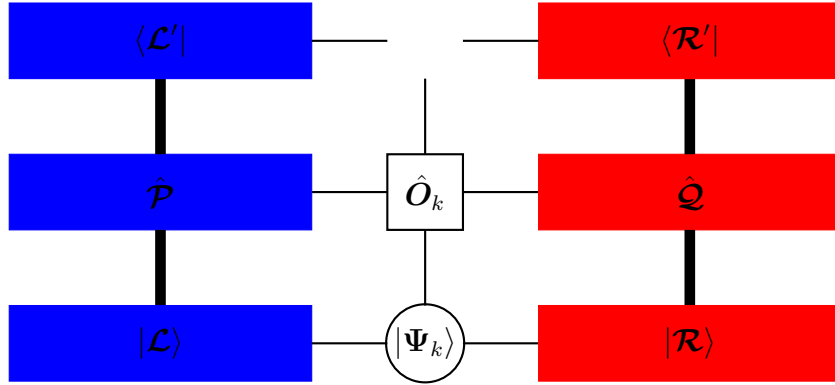
In this way, we obtain

$$\sum_{n_k l r} \mathcal{O}_{l' r', l r}^{m_k n_k} \Psi_{l r}^{n_k} = \omega \Psi_{l' r'}^{m_k} \quad (4.119)$$

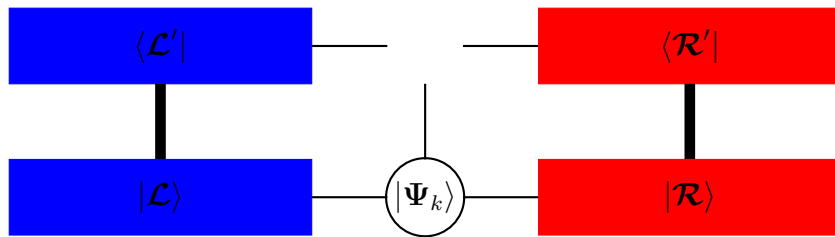
or reshaped into matrices and vectors

$$\mathcal{O}_k \vec{\Psi}_k = \omega \vec{\Psi}_k. \quad (4.120)$$

It was shown here how MPSs and MPOs make it possible to break complicated many-body eigenvalue problems down to a set of effective one-body problems which can be solved by diagonalization since the degrees of freedom have been reduced by projection onto a smaller effective, renormalized basis set. This is crucial for the DMRG algorithm as it will be pointed out later.

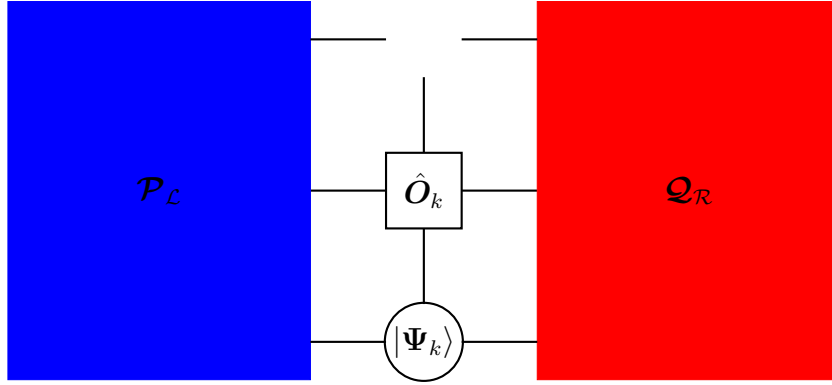


(a) Left hand side of Eq. (4.111).

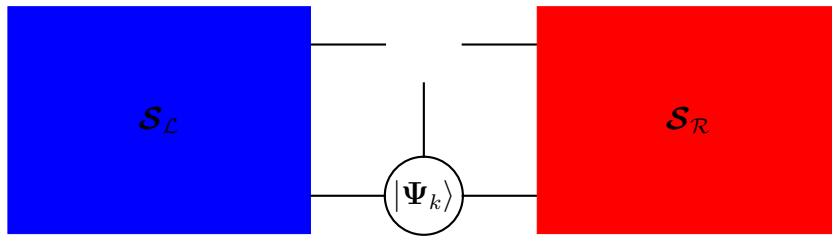


(b) Right hand side of Eq. (4.111).

Figure 4.1: Visualization of the contraction scheme in Eq. (4.111). Vertical lines refer to the contraction over the local single-particle basis states  $|n\rangle$ . The thick vertical lines are supposed to illustrate that all the single-particle states up to the site  $k$  have to be contracted. Horizontal lines denote the indices of the operator and state matrices in the MPO and MPS, respectively. The blue and red rectangles indicate that all the operator and state matrices have been multiplied out up to the site  $k$  to form new effective block operators and states. The open spot where the horizontal and the vertical lines are not connected to anything points out that the resulting quantity is a tensor of rank three.



(a) Left hand side of Eq. (4.111).



(b) Right hand side of Eq. (4.111).

Figure 4.2: Visualization of the contraction scheme in Eq. (4.111). Vertical lines refer to the contraction over the local single-particle basis states  $|n\rangle$ . Horizontal lines denote the indices of the operator and state matrices in the MPO and MPS, respectively. The large blue and red rectangles indicate that all the operator and state matrices have been multiplied out up to the site  $k$  and all the single-particle basis states have been contracted. The open spot where the horizontal and the vertical lines are open indicates that the resulting quantity is a tensor of rank three.



# 5 Matrix product operator representations of the quantum-chemical Hamiltonian

While the previous chapters have been mainly about the background known from literature, the following chapter shows the first main research part of this thesis. The quantum-chemical Hamiltonian is presented and expressed in various sets of orbitals. Its matrix product operator representation is discussed with respect to good computational scaling. For this purpose, the right choice of single-particle basis states is vital. The problem of finding a suitable matrix product operator representation is due to the repulsive long-range nature of the electron-electron interaction which is an intrinsic problem of correlation methods. Moreover, the scaling of the MPO-representation of the electron-electron interaction with “lattice” size is discussed. All that can also be found in Snajberk and Ochsenfeld [2017a,b] (see the list of publications) in a compact form.

## 5.1 The choice of basis

It is a common fact that the proper choice of basis states is crucial to describe the correct physics and for the efficient simulation of quantum-many-electron systems. It is often useful to have a basis which diagonalizes at least a part of the many-electron problem but this is hard to find in practice. In quantum-chemical simulations, one mostly relies on orbitals as a starting point which are obtained during a Hartree-Fock or mean-field calculation  $|\varphi_i\rangle$ . These orbitals can also be expanded in a set of basis states, which leads to the so-called linear combination of atomic orbitals (LCAO)

$$|\varphi_i\rangle = \sum_{\nu} c_{\nu i} |\chi_{\nu}\rangle . \quad (5.1)$$

These states are termed “atomic” because the  $|\chi_{\nu}\rangle$  are states which are considered to be centered around an atom like the eigenstates of a single hydrogen atom in the description of molecular hydrogen. Taking atomic orbitals as basis states has led to atomic-orbital-based methods (see, e.g., Kussmann et al. [2013] for a recent review). These orbitals are typically superpositions of Gaussian functions. In physics, the most fundamental basis types are the position or real space and momentum space, i.e., one tries to describe quantum-mechanical processes on a discrete real-space or momentum-space grid. Discrete states in real and momentum space form a complete set of basis states themselves.

In the following, it is demonstrated how quantum-chemical Hamiltonians of an atom or a molecule formulated in second quantization look like for different basis representations and which of these representations is the most suitable for the

construction of a matrix product operator form of the Hamiltonian.

## 5.2 The quantum-chemical Hamiltonian in different basis types

The stationary Schrödinger equation (in atomic units) of a quantum-chemical system normally consists of three parts: the kinetic and interaction potential energy of the involved nuclei and electrons. Additionally, there is an interaction potential between the nuclei and the electrons

$$\left( \sum_A -\frac{1}{2M} \Delta_{\mathbf{R}_A} + \frac{1}{2} \sum_{A \neq A'} \frac{Z_A Z_{A'}}{|\mathbf{R}_A - \mathbf{R}_{A'}|} + \sum_i -\frac{1}{2} \Delta_{\mathbf{x}_i} + \frac{1}{2} \sum_{i \neq i'} \frac{1}{|\mathbf{x}_i - \mathbf{x}_{i'}|} + \sum_{iA} \frac{-Z_A}{|\mathbf{x}_i - \mathbf{R}_A|} \right) \psi(\mathbf{x}_1, \mathbf{x}_2, \dots; \mathbf{R}_1, \mathbf{R}_2, \dots) = \mathcal{E} \psi(\mathbf{x}_1, \mathbf{x}_2, \dots; \mathbf{R}_1, \mathbf{R}_2, \dots). \quad (5.2)$$

$Z_A$  and  $\mathbf{R}_A$  represent the charges and positions of the nuclei whereas  $\mathbf{x}_i$  are the space coordinates of the electrons.  $\mathcal{E}$  is the total nuclear and electronic energy.  $\psi(\mathbf{x}_1, \mathbf{x}_2, \dots; \mathbf{R}_1, \mathbf{R}_2, \dots)$  denotes the wave function of the system. Therefore, the quantum-chemical Hamiltonian can in general be written as

$$\hat{H} = \hat{H}_{\text{nuc}} + \hat{H}_e + \hat{H}_{\text{nuc-e}}. \quad (5.3)$$

This problem is hardly solvable, but due to the inertia of the atomic nuclei originating from their high mass ratio compared to the electron mass, the atomic nuclei in the above Schrödinger equation can be treated semi-classically as point-charges whose movement has been frozen (Born-Oppenheimer approximation [Born and Oppenheimer, 1927]). This results in a set of purely electronic Schrödinger equations for every position of the nuclei  $\{\mathbf{R}\}$

$$\left( \sum_i -\frac{1}{2} \Delta_{\mathbf{x}_i} + \sum_{iA} \frac{-Z_A}{|\mathbf{x}_i - \mathbf{R}_A|} + \frac{1}{2} \sum_{i \neq i'} \frac{1}{|\mathbf{x}_i - \mathbf{x}_{i'}|} \right) \psi_{\{\mathbf{R}\}}(\mathbf{x}_1, \mathbf{x}_2, \dots) = E \psi_{\{\mathbf{R}\}}(\mathbf{x}_1, \mathbf{x}_2, \dots). \quad (5.4)$$

The nucleus-nucleus interaction energy term has been dropped in the upper equation because it is just a constant which can simply be added to the total electronic energy  $E$ . The second quantization formulation of the Hamiltonian of Eq. (5.4) reads

$$\hat{H} = \sum_{\sigma} \int d^3x \hat{\psi}_{\sigma}^{\dagger}(\mathbf{x}) \frac{-1}{2} \Delta \hat{\psi}_{\sigma}(\mathbf{x}) + \sum_{\sigma} \int d^3x \sum_A \frac{-Z_A}{|\mathbf{x} - \mathbf{R}_A|} \hat{\psi}_{\sigma}^{\dagger}(\mathbf{x}) \hat{\psi}_{\sigma}(\mathbf{x}) + \frac{1}{2} \sum_{\sigma\sigma'} \int d^3x d^3x' \frac{1}{|\mathbf{x} - \mathbf{x}'|} \hat{\psi}_{\sigma}^{\dagger}(\mathbf{x}) \hat{\psi}_{\sigma'}^{\dagger}(\mathbf{x}') \hat{\psi}_{\sigma'}(\mathbf{x}') \hat{\psi}_{\sigma}(\mathbf{x}), \quad (5.5)$$



where  $\sigma$  and  $\sigma'$  denote the  $z$ -component of the electron-spin. Here, the continuous real space forms a complete orthonormal basis

$$\hat{1} = \int d^3x |\mathbf{x}\rangle \langle \mathbf{x}| \quad (5.6)$$

$$\langle \mathbf{x} | \mathbf{x}' \rangle = \delta(\mathbf{x} - \mathbf{x}'). \quad (5.7)$$

In the next subsections, different basis spaces which may be appropriate for the MPO-construction of the above Hamiltonian are presented.

### 5.2.1 Hartree-Fock orbitals

The probably most common basis in the field of quantum chemistry is spanned by the Hartree-Fock orbitals. So, assume that one has performed a mean-field or Hartree-Fock calculation which yields a set of states  $|\varphi_i\rangle$  with the properties

$$\hat{1} = \sum_i |\varphi_i\rangle \langle \varphi_i| \quad (5.8)$$

$$\langle \varphi_i | \varphi_j \rangle = \delta_{ij}. \quad (5.9)$$

These states are the eigenstates of the Fock operator—an effective one-particle Hamilton operator. The Fock operator is an operator obtained by extremizing the energy expectation value with respect to the wave function requiring that the wave function is a Slater determinant (cf. the textbook by Szabo and Ostlund [1996]). Eq. (5.5) can be transformed into the Hartree-Fock-orbital basis by the operator transformation

$$\hat{\psi}_\sigma^\dagger(\mathbf{x}) = \sum_i \varphi_i^*(\mathbf{x}) \hat{c}_{i\sigma}^\dagger \quad (5.10)$$

$$\hat{\psi}_\sigma(\mathbf{x}) = \sum_i \varphi_i(\mathbf{x}) \hat{c}_{i\sigma}. \quad (5.11)$$

Since the Hartree-Fock orbitals are orthonormal and complete, the new creation and annihilation operators  $\hat{c}_{i\sigma}^\dagger$  and  $\hat{c}_{i\sigma}$  fulfill the fundamental anti-commutation relations for electrons. After inserting this transformation into the Hamiltonian, one arrives at the equation

$$\begin{aligned} \hat{H} &= \sum_{ij,\sigma} \int d^3x \varphi_i^*(\mathbf{x}) \frac{-1}{2} \Delta \varphi_j(\mathbf{x}) \hat{c}_{i\sigma}^\dagger \hat{c}_{j\sigma} \\ &\quad + \sum_{ij,\sigma} \int d^3x \varphi_i^*(\mathbf{x}) \sum_A \frac{-Z_A}{|\mathbf{x} - \mathbf{R}_A|} \varphi_j(\mathbf{x}) \hat{c}_{i\sigma}^\dagger \hat{c}_{j\sigma} \end{aligned} \quad (5.12)$$

$$\begin{aligned} &\quad + \frac{1}{2} \sum_{ijkl,\sigma\sigma'} \int d^3x d^3x' \frac{\varphi_i^*(\mathbf{x}) \varphi_j^*(\mathbf{x}') \varphi_k(\mathbf{x}) \varphi_l(\mathbf{x}')}{|\mathbf{x} - \mathbf{x}'|} \hat{c}_{i\sigma}^\dagger \hat{c}_{j\sigma'}^\dagger \hat{c}_{l\sigma'} \hat{c}_{k\sigma} \\ &= \sum_{ij,\sigma} h_{ij} \hat{c}_{i\sigma}^\dagger \hat{c}_{j\sigma} + \frac{1}{2} \sum_{ijkl,\sigma\sigma'} u_{ijkl} \hat{c}_{i\sigma}^\dagger \hat{c}_{j\sigma'}^\dagger \hat{c}_{l\sigma'} \hat{c}_{k\sigma}, \end{aligned} \quad (5.13)$$

with

$$h_{ij} = \int d^3x \varphi_i^*(\mathbf{x}) \left( \frac{-1}{2} \Delta + \sum_A \frac{-Z_A}{|\mathbf{x} - \mathbf{R}_A|} \right) \varphi_j(\mathbf{x}) \quad (5.14)$$

$$u_{ijkl} = \int d^3x d^3x' \frac{\varphi_i^*(\mathbf{x}) \varphi_j^*(\mathbf{x}') \varphi_k(\mathbf{x}) \varphi_l(\mathbf{x}')}{|\mathbf{x} - \mathbf{x}'|}. \quad (5.15)$$

The first sum in Eq. (5.13) can now easily be brought into MPO-shape as shown in chapter 4. We need to decouple the states  $i$  and  $j$ —or, in a quantum lattice model picture, sites—by a matrix factorization such as QR

$$h_{ij} = \sum_a q_{ia} r_{aj}. \quad (5.16)$$

With that, one can write the first sum as

$$\sum_{ij,\sigma} h_{ij} \hat{c}_{i\sigma}^\dagger \hat{c}_{j\sigma} = \sum_{i\sigma} h_{ii} \hat{n}_{i\sigma} + \sum_{a,i < j,\sigma} \left( q_{ia} r_{aj} \hat{c}_{i\sigma}^\dagger \hat{c}_{j\sigma} + \text{h. c.} \right) \quad (5.17)$$

$$\begin{aligned} &= (\hat{1}_1 \quad h_{11} \hat{\eta}_1) \odot \begin{pmatrix} \hat{1}_2 & h_{22} \hat{\eta}_2 \\ 0 & \hat{1}_2 \end{pmatrix} \odot \cdots \odot \begin{pmatrix} h_{LL} \hat{\eta}_L \\ \hat{1}_L \end{pmatrix} \\ &\quad + \sum_{a\sigma} (\hat{1}_1 \quad q_{1a} \hat{\zeta}_{1\sigma}^{L\dagger} \quad 0) \odot \begin{pmatrix} \hat{1}_2 & q_{2a} \hat{\zeta}_{2\sigma}^{L\dagger} & 0 \\ 0 & \hat{f}_2 & r_{a2} \hat{\zeta}_{2\sigma}^L \\ 0 & & \hat{1}_2 \end{pmatrix} \odot \cdots \odot \begin{pmatrix} 0 \\ r_{aL} \hat{\zeta}_{L\sigma}^L \\ \hat{1}_L \end{pmatrix} \\ &\quad + \text{h. c.} \end{aligned} \quad (5.18)$$

$$= \hat{\mathbf{h}}_1 \odot \hat{\mathbf{h}}_2 \odot \cdots \odot \hat{\mathbf{h}}_L \quad (5.19)$$

$$= \hat{h}_{\text{MPO}}, \quad (5.20)$$

where it was assumed to have in total  $L$  orbitals. “h. c.” denotes the Hermitian-conjugated part of the sum. The size of the operator matrices of  $\hat{h}_{\text{MPO}}$  is  $12L + 2$  and thus scales linearly with the number of basis orbitals taken into account. This is never a problem concerning the computational cost.

The MPO-construction of the electron-electron interaction is more tricky and the central problem of quantum chemistry. That is why the discussion of its construction is shifted to the next subsection.

## 5.2.2 Atomic orbitals

We can basically change to any orbital basis we like. In quantum chemistry, one usually expresses the Hartree-Fock orbitals (usually denoted as molecular orbitals, MOs) in terms of atomic orbitals. These are atom-centered states which need not be either normalized or orthogonal. The completeness and orthogonality relations of a non-orthogonal basis set  $|\chi_\mu\rangle$  reads

$$\hat{1} = \sum_{\mu\mu'} S_{\mu\mu'}^{-1} |\chi_\mu\rangle \langle\chi_{\mu'}| \quad (5.21)$$

$$\langle\chi_\mu|\chi_{\mu'}\rangle = S_{\mu\mu'}, \quad (5.22)$$

## 5.2 The quantum-chemical Hamiltonian in different basis types

where  $S_{\mu\mu'}$  denotes the overlap of the basis states

$$S_{\mu\mu'} = \int d^3x \chi_{\mu}^*(\mathbf{x}) \chi_{\mu'}(\mathbf{x}). \quad (5.23)$$

One can thus expand the Hartree-Fock orbitals in these atomic orbitals using the relations above

$$|\varphi_i\rangle = \sum_{\mu\mu'} S_{\mu\mu'}^{-1} \langle \chi_{\mu'} | \varphi_i \rangle |\chi_{\mu}\rangle \quad (5.24)$$

or, speaking in second quantization language, the creation and annihilation operators of the Hartree-Fock states

$$\hat{c}_{i\sigma}^{\dagger} = \sum_{\mu\mu'} S_{\mu\mu'}^{-1} \langle \chi_{\mu'} | \varphi_i \rangle \hat{c}_{\mu\sigma}^{\dagger} \quad (5.25)$$

$$\hat{c}_{i\sigma} = \sum_{\mu\mu'} S_{\mu\mu'}^{-1*} \langle \varphi_i | \chi_{\mu'} \rangle \hat{c}_{\mu\sigma}. \quad (5.26)$$

The anti-commutation relations in a non-orthogonal basis then are

$$\{\hat{c}_{\mu\sigma}, \hat{c}_{\mu'\sigma'}\} = 0 \quad (5.27)$$

$$\{\hat{c}_{\mu\sigma}^{\dagger}, \hat{c}_{\mu'\sigma'}^{\dagger}\} = 0 \quad (5.28)$$

$$\{\hat{c}_{\mu\sigma}, \hat{c}_{\mu'\sigma'}^{\dagger}\} = S_{\mu\mu'} \delta_{\sigma\sigma'}. \quad (5.29)$$

One then obtains for the quantum-chemical electronic Hamiltonian in an atomic orbital (non-orthogonal) basis

$$\hat{H} = \sum_{ij,\sigma} h_{ij} \hat{c}_{i\sigma}^{\dagger} \hat{c}_{j\sigma} + \frac{1}{2} \sum_{ijkl,\sigma\sigma'} u_{ijkl} \hat{c}_{i\sigma}^{\dagger} \hat{c}_{j\sigma'}^{\dagger} \hat{c}_{l\sigma'} \hat{c}_{k\sigma} \quad (5.30)$$

$$\begin{aligned} &= \sum_{ij,\sigma,\mu\mu',\nu\nu'} S_{\mu\mu'}^{-1} \langle \chi_{\mu'} | \varphi_i \rangle \langle \varphi_i | \hat{h} | \varphi_j \rangle S_{\nu\nu'}^{-1*} \langle \varphi_j | \chi_{\nu'} \rangle \hat{c}_{\mu\sigma}^{\dagger} \hat{c}_{\nu\sigma} \\ &\quad + \frac{1}{2} \sum_{\substack{ijkl,\sigma\sigma' \\ \mu\mu',\nu\nu',\kappa\kappa',\lambda\lambda'}} S_{\mu\mu'}^{-1} S_{\nu\nu'}^{-1} \langle \chi_{\mu'} | \varphi_i \rangle \langle \chi_{\nu'} | \varphi_j \rangle \langle \varphi_i; \varphi_j | \hat{U} | \varphi_k; \varphi_l \rangle S_{\kappa\kappa'}^{-1*} S_{\lambda\lambda'}^{-1*} \quad (5.31) \\ &\quad \times \langle \varphi_k | \chi_{\kappa'} \rangle \langle \varphi_l | \chi_{\lambda'} \rangle \hat{c}_{\mu\sigma}^{\dagger} \hat{c}_{\nu\sigma'}^{\dagger} \hat{c}_{\lambda\sigma'} \hat{c}_{\kappa\sigma} \end{aligned}$$

$$\begin{aligned} &= \sum_{\mu\mu',\nu\nu',\sigma} S_{\mu\mu'}^{-1} \langle \chi_{\mu'} | \hat{h} | \chi_{\nu'} \rangle S_{\nu'\nu}^{-1} \hat{c}_{\mu\sigma}^{\dagger} \hat{c}_{\nu\sigma} \\ &\quad + \frac{1}{2} \sum_{\substack{\mu\mu',\nu\nu',\kappa\kappa',\lambda\lambda' \\ \sigma\sigma'}} S_{\mu\mu'}^{-1} S_{\nu\nu'}^{-1} \langle \chi_{\mu'}; \chi_{\nu'} | \hat{U} | \chi_{\kappa'}; \chi_{\lambda'} \rangle S_{\kappa'\kappa}^{-1} S_{\lambda'\lambda}^{-1} \hat{c}_{\mu\sigma}^{\dagger} \hat{c}_{\nu\sigma'}^{\dagger} \hat{c}_{\lambda\sigma'} \hat{c}_{\kappa\sigma} \quad (5.32) \end{aligned}$$

$$= \sum_{\mu\nu,\sigma} \tilde{h}_{\mu\nu} \hat{c}_{\mu\sigma}^{\dagger} \hat{c}_{\nu\sigma} + \frac{1}{2} \sum_{\mu\nu\kappa\lambda,\sigma\sigma'} \tilde{u}_{\mu\nu\kappa\lambda} \hat{c}_{\mu\sigma}^{\dagger} \hat{c}_{\nu\sigma'}^{\dagger} \hat{c}_{\lambda\sigma'} \hat{c}_{\kappa\sigma}. \quad (5.33)$$

The elements of the one-electron term  $\tilde{h}_{\mu\nu}$  and of the electron-electron interaction  $\tilde{u}_{\mu\nu\kappa\lambda}$  have been defined as follows

$$\tilde{h}_{\mu\nu} = \sum_{\mu'\nu'} S_{\mu\mu'}^{-1} \langle \chi_{\mu'} | \hat{h} | \chi_{\nu'} \rangle S_{\nu'\nu}^{-1} \quad (5.34)$$

$$= \sum_{\mu'\nu'} S_{\mu\mu'}^{-1} \left( \int d^3x \chi_{\mu'}^*(\mathbf{x}) \left( \frac{-1}{2} \Delta + \sum_A \frac{-Z_A}{|\mathbf{x} - \mathbf{R}_A|} \right) \chi_{\nu'}(\mathbf{x}) \right) S_{\nu'\nu}^{-1} \quad (5.35)$$

$$\tilde{u}_{\mu\nu\kappa\lambda} = \sum_{\mu'\nu'\kappa'\lambda'} S_{\mu\mu'}^{-1} S_{\nu\nu'}^{-1} \langle \chi_{\mu'}; \chi_{\nu'} | \hat{U} | \chi_{\kappa'}; \chi_{\lambda'} \rangle S_{\kappa'\kappa}^{-1} S_{\lambda'\lambda}^{-1} \quad (5.36)$$

$$= \sum_{\mu'\nu'\kappa'\lambda'} S_{\mu\mu'}^{-1} S_{\nu\nu'}^{-1} \left( \int d^3x d^3x' \frac{\chi_{\mu'}^*(\mathbf{x}) \chi_{\nu'}^*(\mathbf{x}') \chi_{\kappa'}(\mathbf{x}) \chi_{\lambda'}(\mathbf{x}')}{|\mathbf{x} - \mathbf{x}'|} \right) S_{\kappa'\kappa}^{-1} S_{\lambda'\lambda}^{-1}. \quad (5.37)$$

Now, let us turn to the construction of the matrix product operator of the two-electron part  $\hat{U}$ .

First of all, it is convenient to group operators with the same spin-variable

$$\hat{U} = \frac{1}{2} \sum_{\mu\nu\kappa\lambda, \sigma\sigma'} \tilde{u}_{\mu\nu\kappa\lambda} \hat{c}_{\mu\sigma}^\dagger \hat{c}_{\nu\sigma'}^\dagger \hat{c}_{\lambda\sigma'} \hat{c}_{\kappa\sigma} \quad (5.38)$$

$$= \frac{1}{2} \sum_{\mu\nu\kappa\lambda, \sigma\sigma'} \tilde{u}_{\mu\nu\kappa\lambda} \left( \hat{c}_{\mu\sigma}^\dagger \hat{c}_{\kappa\sigma} \hat{c}_{\nu\sigma'}^\dagger \hat{c}_{\lambda\sigma'} - \delta_{\sigma\sigma'} S_{\kappa\nu} \hat{c}_{\mu\sigma}^\dagger \hat{c}_{\lambda\sigma'} \right) \quad (5.39)$$

$$= \frac{1}{2} \sum_{\mu\nu\kappa\lambda, \sigma\sigma'} \tilde{u}_{\mu\nu\kappa\lambda} \hat{c}_{\mu\sigma}^\dagger \hat{c}_{\kappa\sigma} \hat{c}_{\nu\sigma'}^\dagger \hat{c}_{\lambda\sigma'} - \frac{1}{2} \sum_{\mu\nu\kappa\lambda, \sigma} \tilde{u}_{\mu\nu\kappa\lambda} S_{\kappa\nu} \hat{c}_{\mu\sigma}^\dagger \hat{c}_{\lambda\sigma}. \quad (5.40)$$

It can immediately be seen that the 4-rank tensorial quantity  $\tilde{u}_{\mu\nu\kappa\lambda}$  is the major problem in the MPO-construction process. Again, one must find a clever way to decouple the orbitals  $\mu$ ,  $\nu$ ,  $\kappa$  and  $\lambda$ . This can be achieved by a matrix decomposition technique as for the one-electron term

$$\sum_{\mu\nu\kappa\lambda} \tilde{u}_{\mu\nu\kappa\lambda} = \sum_{\alpha\mu\nu\kappa\lambda} q_{\mu\kappa, \alpha} r_{\alpha, \nu\lambda}. \quad (5.41)$$

Thus, the electron-electron part can be rewritten as sum of products of one-body operators

$$\hat{U} = \frac{1}{2} \sum_{\mu\nu\kappa\lambda, \sigma\sigma'} \tilde{u}_{\mu\nu\kappa\lambda} \hat{c}_{\mu\sigma}^\dagger \hat{c}_{\kappa\sigma} \hat{c}_{\nu\sigma'}^\dagger \hat{c}_{\lambda\sigma'} - \frac{1}{2} \sum_{\mu\nu\kappa\lambda, \sigma} \tilde{u}_{\mu\nu\kappa\lambda} S_{\kappa\nu} \hat{c}_{\mu\sigma}^\dagger \hat{c}_{\lambda\sigma} \quad (5.42)$$

$$= \frac{1}{2} \sum_{\alpha} \left( \sum_{\mu\kappa, \sigma} q_{\mu\kappa, \alpha} \hat{c}_{\mu\sigma}^\dagger \hat{c}_{\kappa\sigma} \right) \left( \sum_{\nu\lambda, \sigma'} r_{\alpha, \nu\lambda} \hat{c}_{\nu\sigma'}^\dagger \hat{c}_{\lambda\sigma'} \right) - \frac{1}{2} \sum_{\alpha} \sum_{\mu\nu\kappa\lambda, \sigma} q_{\mu\kappa, \alpha} S_{\kappa\nu} r_{\alpha, \nu\lambda} \hat{c}_{\mu\sigma}^\dagger \hat{c}_{\lambda\sigma} \quad (5.43)$$

$$= \frac{1}{2} \sum_{\alpha} \left( \sum_{\mu\kappa, \sigma} q_{\mu\kappa, \alpha} \hat{c}_{\mu\sigma}^\dagger \hat{c}_{\kappa\sigma} \right) \left( \sum_{\nu\lambda, \sigma'} r_{\alpha, \nu\lambda} \hat{c}_{\nu\sigma'}^\dagger \hat{c}_{\lambda\sigma'} \right) - \frac{1}{2} \sum_{\alpha} \left( \sum_{\mu\lambda, \sigma} u_{\mu\lambda}^{(\alpha)} \hat{c}_{\mu\sigma}^\dagger \hat{c}_{\lambda\sigma} \right). \quad (5.44)$$

All the one-body operators can be brought into MPO-form as already shown and the MPO-representation of  $\hat{U}$  can be written as

$$\hat{U} = \sum_{\alpha} \left( \hat{q}_{\text{MPO}}^{(\alpha)} \hat{r}_{\text{MPO}}^{(\alpha)} - \hat{u}_{\text{MPO}}^{(\alpha)} \right) \quad (5.45)$$

$$= \sum_{\alpha} \hat{U}_{\text{MPO}}^{(\alpha)}. \quad (5.46)$$

## 5.2 The quantum-chemical Hamiltonian in different basis types

It must be mentioned here that it is convenient to work with orthonormalized atomic orbitals instead of non-orthogonalized ones to retrieve the canonical anti-commutation relations. This can for example be done by a Cholesky decomposition [Gentle, 2012] of the overlap matrix

$$\mathbf{S} = \mathbf{L}\mathbf{L}^\dagger, \quad (5.47)$$

where  $\mathbf{L}$  is a lower triangular matrix. The inverse of the Cholesky matrix  $\mathbf{L}$  serves as transformation from a non-orthogonal to an orthogonal and normalized atomic orbital basis

$$\hat{a}_{\mu\sigma}^\dagger = \sum_{\mu'} L_{\mu\mu'}^{-1*} \hat{c}_{\mu'\sigma}^\dagger \quad (5.48)$$

$$\hat{a}_{\mu\sigma} = \sum_{\mu'} L_{\mu\mu'}^{-1} \hat{c}_{\mu'\sigma} \quad (5.49)$$

$$S_{\mu\mu'} \longrightarrow \delta_{\mu\mu'}, \quad (5.50)$$

where the transformed creation and annihilation operators fulfill the canonical anti-commutation relations

$$\{\hat{a}_{\mu\sigma}, \hat{a}_{\nu\sigma'}\} = 0 \quad (5.51)$$

$$\{\hat{a}_{\mu\sigma}^\dagger, \hat{a}_{\nu\sigma'}^\dagger\} = 0 \quad (5.52)$$

$$\{\hat{a}_{\mu\sigma}, \hat{a}_{\nu\sigma'}^\dagger\} = \delta_{\sigma\sigma'} \delta_{\mu\nu}. \quad (5.53)$$

The Hamiltonian in the now orthonormalized atomic orbital basis reads

$$\hat{H} = \sum_{\mu\nu,\sigma} h_{\mu\nu}^{\text{ON}} \hat{a}_{\mu\sigma}^\dagger \hat{a}_{\nu\sigma} + \frac{1}{2} \sum_{\mu\nu\kappa\lambda,\sigma\sigma'} u_{\mu\nu\kappa\lambda}^{\text{ON}} \hat{a}_{\mu\sigma}^\dagger \hat{a}_{\nu\sigma'}^\dagger \hat{a}_{\lambda\sigma'} \hat{a}_{\kappa\sigma} \quad (5.54)$$

with

$$h_{\mu\nu}^{\text{ON}} = \sum_{\mu'\nu'} L_{\mu\mu'}^{-1} \tilde{h}_{\mu'\nu'} L_{\nu'\nu}^{\dagger-1} \quad (5.55)$$

$$u_{\mu\nu\kappa\lambda}^{\text{ON}} = \sum_{\mu'\nu'\kappa'\lambda'} L_{\mu\mu'}^{-1} L_{\nu\nu'}^{-1} \tilde{u}_{\mu'\nu'\kappa'\lambda'} L_{\kappa'\kappa}^{\dagger-1} L_{\lambda'\lambda}^{\dagger-1}. \quad (5.56)$$

The ‘‘ON’’ stands for ‘‘orthonormalized’’.

The conversion of  $\hat{U}$  to a MPO is exact, so it requires no approximation. But, it unfortunately involves the product of two MPOs. Suppose the size of every one-body MPO scales with the number of orbitals  $L$  as  $12L + 2$ , then the size of the product of two such one-body MPOs scales as  $(12L + 2)^2 = 144L^2 + 48L + 4$ . Additionally, one has to sum the resulting MPOs  $L^2$  times. Therefore, a scaling of  $O(L^4)$  for the size of the two-electron operator as MPO results. The advantage of using orthonormalized atomic orbitals compared to HF-orbitals is that Eq. (5.54) can directly be treated with the density matrix renormalization group without a pre-HF calculation. The only input needed is the one- and two-electron integrals  $h_{\mu\nu}^{\text{ON}}$  and  $u_{\mu\nu\kappa\lambda}^{\text{ON}}$ .

### 5.2.3 Discrete momentum space

Another basis widely used in condensed matter physics is the momentum space representation. Here, the basis states or orbitals are plane wave states which can be seen as performing a Fourier transform of the field operators

$$\hat{\psi}_\sigma^\dagger(\mathbf{x}) = \frac{1}{\sqrt{\mathcal{V}}} \sum_{\mathbf{k}} e^{i\mathbf{k}\mathbf{x}} \hat{c}_{\mathbf{k}\sigma}^\dagger \quad (5.57)$$

$$\hat{\psi}_\sigma(\mathbf{x}) = \frac{1}{\sqrt{\mathcal{V}}} \sum_{\mathbf{k}} e^{-i\mathbf{k}\mathbf{x}} \hat{c}_{\mathbf{k}\sigma}, \quad (5.58)$$

where  $\mathcal{V}$  is the system volume and  $\mathbf{k}$  are discrete or quantized momentum vectors because its components are taken to be integer multiples of  $\frac{2\pi}{\ell}$

$$k_{x,y,z} = \frac{2\pi}{\ell} n_{x,y,z}, \quad n_{x,y,z} \in \mathbb{Z}. \quad (5.59)$$

$\ell$  is the volume along one coordinate axis or the edge length of a box the system is embedded in ( $\mathcal{V} = \ell^3$ ).  $\frac{1}{\sqrt{\mathcal{V}}}$  is the normalization factor to ensure that the momentum space creation and annihilation operators fulfill the canonical anti-commutation relations

$$\{\hat{c}_{\mathbf{k}\sigma}, \hat{c}_{\mathbf{k}'\sigma'}^\dagger\} = \frac{1}{\mathcal{V}} \int d^3x d^3x' e^{i\mathbf{k}\mathbf{x}} e^{-i\mathbf{k}'\mathbf{x}'} \{\hat{\psi}_\sigma(\mathbf{x}), \hat{\psi}_{\sigma'}^\dagger(\mathbf{x}')\} \quad (5.60)$$

$$= \frac{1}{\mathcal{V}} \int d^3x d^3x' e^{i\mathbf{k}\mathbf{x}} e^{-i\mathbf{k}'\mathbf{x}'} \delta(\mathbf{x} - \mathbf{x}') \quad (5.61)$$

$$= \frac{1}{\mathcal{V}} \int d^3x e^{i(\mathbf{k}-\mathbf{k}')\mathbf{x}} \quad (5.62)$$

$$= \delta_{\mathbf{k}\mathbf{k}'} \delta_{\sigma\sigma'}. \quad (5.63)$$

Inserting the momentum space basis, one obtains for the Hamiltonian

$$\hat{H} = \sum_{\mathbf{k}_1\mathbf{k}_2,\sigma} h_{\mathbf{k}_1\mathbf{k}_2} \hat{c}_{\mathbf{k}_1\sigma}^\dagger \hat{c}_{\mathbf{k}_2\sigma} + \frac{1}{2} \sum_{\mathbf{k}_1\mathbf{k}_2\mathbf{k}_3\mathbf{k}_4,\sigma\sigma'} u_{\mathbf{k}_1\mathbf{k}_2\mathbf{k}_3\mathbf{k}_4} \hat{c}_{\mathbf{k}_1\sigma}^\dagger \hat{c}_{\mathbf{k}_2\sigma'}^\dagger \hat{c}_{\mathbf{k}_4\sigma'} \hat{c}_{\mathbf{k}_3\sigma}. \quad (5.64)$$

At first sight, the overall form of  $\hat{H}$  is the same as for every single-particle basis one can think of. But, let us take a closer look at the one- and two-electron integral expressions:

$$h_{\mathbf{k}_1\mathbf{k}_2} = \int \frac{d^3x}{\mathcal{V}} \left( e^{i\mathbf{k}_1\mathbf{x}} \frac{-1}{2} \Delta e^{-i\mathbf{k}_2\mathbf{x}} + \sum_A \frac{-Z_A}{|\mathbf{x} - \mathbf{R}_A|} e^{i(\mathbf{k}_1 - \mathbf{k}_2)\mathbf{x}} \right) \quad (5.65)$$

$$= \frac{\mathbf{k}_2^2}{2} \delta_{\mathbf{k}_1\mathbf{k}_2} + \sum_A \frac{-4\pi Z_A e^{i\mathbf{R}_A(\mathbf{k}_1 - \mathbf{k}_2)}}{\mathcal{V}(\mathbf{k}_1 - \mathbf{k}_2)^2} \quad (5.66)$$

$$u_{\mathbf{k}_1\mathbf{k}_2\mathbf{k}_3\mathbf{k}_4} = \int \frac{d^3x d^3x'}{\mathcal{V}^2} \frac{e^{i(\mathbf{k}_1 - \mathbf{k}_3)\mathbf{x}} e^{i(\mathbf{k}_2 - \mathbf{k}_4)\mathbf{x}'}}{|\mathbf{x} - \mathbf{x}'|} \quad (5.67)$$

$$= \int \frac{d^3x d^3x'}{\mathcal{V}^2} \frac{e^{i(\mathbf{k}_1 - \mathbf{k}_3)\mathbf{x}} e^{i(\mathbf{k}_2 - \mathbf{k}_4)\mathbf{x}'}}{|\mathbf{x}|} e^{i(\mathbf{k}_1 - \mathbf{k}_3)\mathbf{x}'} \quad (5.68)$$

$$= \int \frac{d^3x}{\mathcal{V}} \frac{e^{i(\mathbf{k}_1 - \mathbf{k}_3)\mathbf{x}}}{|\mathbf{x}|} \delta_{\mathbf{k}_2 - \mathbf{k}_4, \mathbf{k}_3 - \mathbf{k}_1} \quad (5.69)$$

$$= \frac{4\pi}{\mathcal{V}(\mathbf{k}_2 - \mathbf{k}_4)^2} \delta_{\mathbf{k}_2 - \mathbf{k}_4, \mathbf{k}_3 - \mathbf{k}_1}. \quad (5.70)$$

The advantage of the momentum space representation is that the Hamiltonian in this basis can be viewed as describing a quantum lattice model. Such a problem can be tackled directly by a numerical diagonalization alternative like the density matrix renormalization group method without having to carry out a preliminary mean-field calculation. A further advantage of turning to momentum space is that the electrostatic Coulomb potential is not as long-ranged as in real space. A major drawback, however, is the MPO-construction of the electron-electron term. All four momentum states  $\mathbf{k}_1$ ,  $\mathbf{k}_2$ ,  $\mathbf{k}_3$  and  $\mathbf{k}_4$  are coupled because of momentum conservation reflected by the Kronecker- $\delta$  symbol  $\delta_{\mathbf{k}_2 - \mathbf{k}_4, \mathbf{k}_3 - \mathbf{k}_1}$ . This leads to the same size scaling of  $O(L^4)$  for the MPO matrices of the electron-electron operator.

### 5.2.4 Discrete position space

The next prominent basis in physics is real or position space. The quantum-chemical Hamiltonian in continuous real space formulation reads

$$\hat{H} = \sum_{\sigma} \int d^3x \hat{\psi}_{\sigma}^{\dagger}(\mathbf{x}) \frac{-1}{2} \Delta \hat{\psi}_{\sigma}(\mathbf{x}) + \sum_{\sigma} \int d^3x \sum_A \frac{-Z_A}{|\mathbf{x} - \mathbf{R}_A|} \hat{\rho}_{\sigma}(\mathbf{x}) + \frac{1}{2} \sum_{\sigma\sigma'} \int d^3x d^3x' \frac{\hat{\psi}_{\sigma}^{\dagger}(\mathbf{x}) \hat{\psi}_{\sigma'}^{\dagger}(\mathbf{x}') \hat{\psi}_{\sigma'}(\mathbf{x}') \hat{\psi}_{\sigma}(\mathbf{x})}{|\mathbf{x} - \mathbf{x}'|} \quad (5.71)$$

$$= \sum_{\sigma} \int d^3x \hat{\psi}_{\sigma}^{\dagger}(\mathbf{x}) \frac{-1}{2} \Delta \hat{\psi}_{\sigma}(\mathbf{x}) + \sum_{\sigma} \int d^3x \sum_A \frac{-Z_A}{|\mathbf{x} - \mathbf{R}_A|} \hat{\rho}_{\sigma}(\mathbf{x}) + \frac{1}{2} \sum_{\sigma\sigma'} \int d^3x d^3x' \frac{1}{|\mathbf{x} - \mathbf{x}'|} \left( \hat{\rho}_{\sigma}(\mathbf{x}) \hat{\rho}_{\sigma'}(\mathbf{x}') - \delta_{\sigma\sigma'} \delta(\mathbf{x} - \mathbf{x}') \hat{\psi}_{\sigma}^{\dagger}(\mathbf{x}) \hat{\psi}_{\sigma'}(\mathbf{x}') \right). \quad (5.72)$$

Such a continuous model is numerically hard to treat. Therefore, one often introduces a grid and divides the continuum into a set of discrete lattice points with lattice spacing  $\delta$  (see Fig. 5.1). Always assuming infinitely many lattice sites and a vanishing lattice spacing  $\delta$ , one can rewrite the Hamiltonian of the continuous model in terms of discrete lattice sites producing a quantum-mechanical lattice model. In the following, it is shown how the mapping from the three-dimensional continuum to a three-dimensional lattice is achieved for the kinetic, external and electron-electron energy terms as it has been done for a one-dimensional continuous real-space system by Stoudenmire et al. [2012].

#### Kinetic energy

To discretize the kinetic energy part, one must discretize the Laplacian  $\Delta = \frac{\partial^2}{\partial x^2} + \frac{\partial^2}{\partial y^2} + \frac{\partial^2}{\partial z^2}$ . In the limit  $\delta \rightarrow 0$ , one can substitute the derivative of a function—or

here of the field annihilation operator—by its differential quotient

$$\frac{\partial}{\partial x} \hat{\psi}(x, y, z) = \frac{\hat{\psi}(x + \frac{\delta}{2}, y, z) - \hat{\psi}(x - \frac{\delta}{2}, y, z)}{\delta} \quad (5.73)$$

$$\frac{\partial^2}{\partial x^2} \hat{\psi}(x, y, z) = \frac{\hat{\psi}(x + \delta, y, z) + \hat{\psi}(x - \delta, y, z) - 2\hat{\psi}(x, y, z)}{\delta^2}. \quad (5.74)$$

The same holds for the derivatives with respect to all the other coordinates. Thus, the discretized Laplacian reads

$$\begin{aligned} \Delta \hat{\psi}(x, y, z) = \frac{1}{\delta^2} \left( \hat{\psi}(x + \delta, y, z) + \hat{\psi}(x - \delta, y, z) + \hat{\psi}(x, y + \delta, z) + \hat{\psi}(x, y - \delta, z) \right. \\ \left. + \hat{\psi}(x, y, z + \delta) + \hat{\psi}(x, y, z - \delta) - 6\hat{\psi}(x, y, z) \right). \end{aligned} \quad (5.75)$$

Now, one can change from integration to summation using the fact that the electron density is nothing but electron number per unit volume ( $d^3x = \delta^3$ ), which leads to the new lattice creation and annihilation operators

$$\hat{\rho}_\sigma(\mathbf{x}) = \frac{\hat{n}_{\delta\mathbf{i},\sigma}}{\delta^3} \quad (5.76)$$

$$\hat{\psi}_\sigma^\dagger(\mathbf{x}) = \frac{\hat{c}_{\delta\mathbf{i},\sigma}^\dagger}{\sqrt{\delta^3}} \quad (5.77)$$

$$\hat{\psi}_\sigma(\mathbf{x}) = \frac{\hat{c}_{\delta\mathbf{i},\sigma}}{\sqrt{\delta^3}}. \quad (5.78)$$

The position on the lattice is measured in integer multiples of the lattice spacing  $\mathbf{x} = \delta\mathbf{i}$  ( $\mathbf{i} \in \mathbb{Z}^3$ ). The  $\delta$  in the subscript of the lattice occupation number, creation and annihilation operators will be dropped in the following. The creation and annihilation operators on the lattice obey the anti-commutation relations

$$\{\hat{c}_{\mathbf{i}\sigma}^\dagger, \hat{c}_{\mathbf{j}\sigma'}^\dagger\} = 0 \quad (5.79)$$

$$\{\hat{c}_{\mathbf{i}\sigma}, \hat{c}_{\mathbf{j}\sigma'}\} = 0 \quad (5.80)$$

$$\{\hat{c}_{\mathbf{i}\sigma}, \hat{c}_{\mathbf{j}\sigma'}^\dagger\} = \delta_{\sigma\sigma'} \delta_{\mathbf{i}\mathbf{j}}. \quad (5.81)$$

The discrete version of the kinetic energy operator then reads

$$\begin{aligned} \hat{T} &= \sum_\sigma \int d^3x \hat{\psi}_\sigma^\dagger(\mathbf{x}) \frac{-1}{2} \Delta \hat{\psi}_\sigma(\mathbf{x}) \quad (5.82) \\ &= \sum_{\mathbf{i}\sigma} \frac{-1}{2\delta^2} \left( \hat{c}_{\mathbf{i}_x\mathbf{i}_y\mathbf{i}_z,\sigma}^\dagger \hat{c}_{\mathbf{i}_x+1\mathbf{i}_y\mathbf{i}_z,\sigma} + \hat{c}_{\mathbf{i}_x\mathbf{i}_y\mathbf{i}_z,\sigma}^\dagger \hat{c}_{\mathbf{i}_x\mathbf{i}_y+1\mathbf{i}_z,\sigma} + \hat{c}_{\mathbf{i}_x\mathbf{i}_y\mathbf{i}_z,\sigma}^\dagger \hat{c}_{\mathbf{i}_x\mathbf{i}_y\mathbf{i}_z+1,\sigma} + \text{h. c.} \right) \\ &\quad + \sum_{\mathbf{i}\sigma} \frac{3}{\delta^2} \hat{n}_{\mathbf{i}_x\mathbf{i}_y\mathbf{i}_z,\sigma} \end{aligned} \quad (5.83)$$

or in short

$$\hat{T} = \sum_{\mathbf{i}\mathbf{j}\sigma} t_{\mathbf{i}\mathbf{j}} \hat{c}_{\mathbf{i}\sigma}^\dagger \hat{c}_{\mathbf{j}\sigma}, \quad (5.84)$$



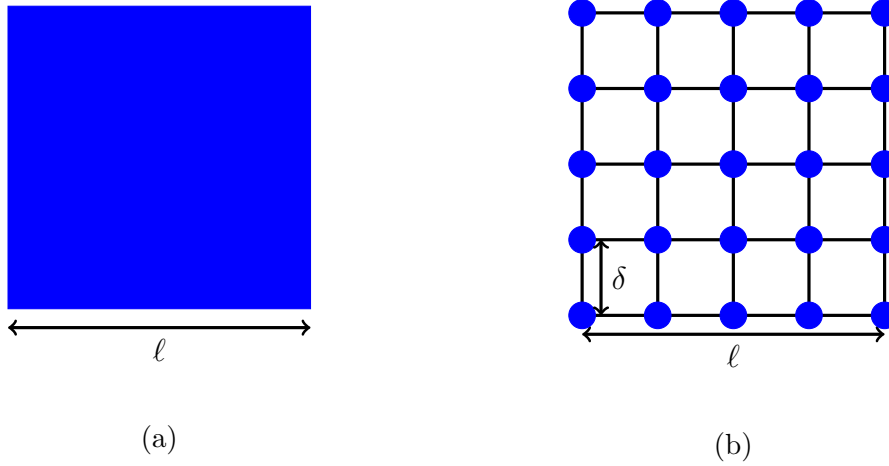


Figure 5.1: Schematic visualization of the position space discretization. (a) Continuous position space with edge length  $\ell$ . (b) Discrete lattice representation of the continuous position space with edge length  $\ell$ . The smallest characteristic length scale is the lattice spacing  $\delta$ . In the limit of infinitely many lattice sites and  $\delta \rightarrow 0$ , (a) and (b) are assumed to be equivalent.

where

$$t_{ij} = \begin{cases} \frac{-1}{2\delta^2} \delta_{|i-j|,1}, & \mathbf{i} \neq \mathbf{j} \\ \frac{3}{\delta^2}, & \mathbf{i} = \mathbf{j}. \end{cases} \quad (5.85)$$

The off-diagonal elements  $t_{i \neq j}$  describe the hopping of an electron on a lattice site with lattice vector  $\mathbf{i}$  to sites with positions  $\mathbf{j}$  within a sphere of radius 1.

### External potential

The external potential is quite simple to discretize. With all the definitions above, it reads

$$\hat{V} = \sum_{\sigma} \int d^3x \sum_A \frac{-Z_A}{|\mathbf{x} - \mathbf{R}_A|} \hat{\rho}_{\sigma}(\mathbf{x}) \quad (5.86)$$

$$= \sum_{i\sigma} v_i \hat{n}_{i\sigma}, \quad (5.87)$$

where it was defined

$$v_i = \sum_A \frac{-Z_A}{\delta |\mathbf{i} - \mathbf{i}_A|}. \quad (5.88)$$

If it happens that an electron on the lattice hits a nucleus at position  $\mathbf{R}_A = \delta \mathbf{i}_A$ , one has to account for the divergent potential by setting its value to

$$v_{\mathbf{i}_A} = \sum_A \frac{-Z_A}{\delta}. \quad (5.89)$$

### Electron-electron interaction

The electron-electron interaction on a real-space grid is

$$\hat{U} = \frac{1}{2} \sum_{\sigma\sigma'} \int d^3x d^3x' \frac{1}{|\mathbf{x} - \mathbf{x}'|} \left( \hat{\rho}_\sigma(\mathbf{x}) \hat{\rho}_{\sigma'}(\mathbf{x}') - \delta_{\sigma\sigma'} \delta(\mathbf{x} - \mathbf{x}') \hat{\psi}_\sigma^\dagger(\mathbf{x}) \hat{\psi}_{\sigma'}(\mathbf{x}') \right) \quad (5.90)$$

$$= \frac{1}{2} \sum_{i\sigma j\sigma'} u_{ij} \left( \hat{n}_{i\sigma} \hat{n}_{j\sigma'} - \delta_{\sigma\sigma'} \delta_{ij} \hat{c}_{i\sigma}^\dagger \hat{c}_{j\sigma'} \right), \quad (5.91)$$

where

$$u_{ij} = \begin{cases} \frac{1}{\delta|i-j|}, & i \neq j \\ \frac{1}{\delta}, & i = j. \end{cases} \quad (5.92)$$

Eq. (5.91) can be simplified further

$$\hat{U} = \frac{1}{2} \sum_{i\sigma j\sigma'} u_{ij} \hat{n}_{i\sigma} \hat{n}_{j\sigma'} - \frac{1}{2} \sum_{i\sigma} u_{ii} \hat{n}_{i\sigma} \quad (5.93)$$

$$\begin{aligned} &= \frac{1}{2} \sum_{i\sigma} u_{ii} \hat{n}_{i\sigma} + \frac{1}{2} \sum_{i \neq j, \sigma} u_{ij} \hat{n}_{i\sigma} \hat{n}_{j\sigma} + \frac{1}{2} \sum_{i, \sigma \neq \sigma'} u_{ii} \hat{n}_{i\sigma} \hat{n}_{i\sigma'} + \frac{1}{2} \sum_{i \neq j, \sigma \neq \sigma'} u_{ij} \hat{n}_{i\sigma} \hat{n}_{j\sigma'} \\ &\quad - \frac{1}{2} \sum_{i\sigma} u_{ii} \hat{n}_{i\sigma} \end{aligned} \quad (5.94)$$

$$= \frac{1}{2} \sum_{i \neq j, \sigma\sigma'} u_{ij} \hat{n}_{i\sigma} \hat{n}_{j\sigma'} + \sum_i u_{ii} \hat{n}_{i\uparrow} \hat{n}_{i\downarrow}. \quad (5.95)$$

The operator in the second sum of the last equation  $\hat{n}_{i\uparrow} \hat{n}_{i\downarrow}$  measures the double-occupancy of a lattice site. Hence, its matrix action on an orbital associated with a particular lattice site, which is needed for the MPO-construction of the electron-electron interaction, is

$$\boldsymbol{\eta}_\uparrow \boldsymbol{\eta}_\downarrow = \begin{pmatrix} 0 & 0 & 0 & 0 \\ 0 & 0 & 0 & 0 \\ 0 & 0 & 0 & 0 \\ 0 & 0 & 0 & 1 \end{pmatrix} \quad (5.96)$$

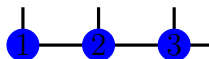
for all sites.

### The total quantum-chemical Hamiltonian

Putting everything together, one obtains the total electronic quantum-chemical Hamiltonian

$$\hat{H} = \sum_{i\sigma} t_{ii} \hat{n}_{i\sigma} + \sum_{i \neq j, \sigma} t_{ij} \hat{c}_{i\sigma}^\dagger \hat{c}_{j\sigma} + \sum_{i\sigma} v_i \hat{n}_{i\sigma} + \sum_i u_{ii} \hat{n}_{i\uparrow} \hat{n}_{i\downarrow} + \frac{1}{2} \sum_{i \neq j, \sigma\sigma'} u_{ij} \hat{n}_{i\sigma} \hat{n}_{j\sigma'}. \quad (5.97)$$

To construct the MPO-representation of this Hamiltonian, the graph making up the lattice in Fig. 5.1 (b) has to be labeled



## 5.2 The quantum-chemical Hamiltonian in different basis types

so that the lattice is mathematically represented by an ordered set  $\mathbb{L} = \{\mathbf{i}_1; \mathbf{i}_2; \mathbf{i}_3; \dots\}$  containing all lattice vectors. By labeling the lattice vectors, the Hamiltonian becomes

$$\begin{aligned} \hat{H} = & \sum_{k\sigma} t_{kk} \hat{n}_{k\sigma} + \sum_{k<l,\sigma} \left( t_{kl} \hat{c}_{k\sigma}^\dagger \hat{c}_{l\sigma} + \text{h. c.} \right) + \sum_{k\sigma} v_k \hat{n}_{k\sigma} + \sum_k u_{kk} \hat{n}_{k\uparrow} \hat{n}_{k\downarrow} \\ & + \sum_{k<l,\sigma\sigma'} u_{kl} \hat{n}_{k\sigma} \hat{n}_{l\sigma'} \end{aligned} \quad (5.98)$$

with

$$t_{kl} = \begin{cases} \frac{-1}{2\delta^2} \delta_{|\mathbf{i}_k - \mathbf{i}_l|, 1}, & k \neq l \\ \frac{3}{\delta^2}, & k = l \end{cases} \quad (5.99)$$

$$v_k = \begin{cases} \sum_A \frac{-Z_A}{\delta_{|\mathbf{i}_k - \mathbf{i}_A|}}, & \mathbf{i}_k \neq \mathbf{i}_A \\ \sum_A \frac{-Z_A}{\delta}, & \mathbf{i}_k = \mathbf{i}_A \end{cases} \quad (5.100)$$

$$u_{kl} = \begin{cases} \frac{1}{\delta_{|\mathbf{i}_k - \mathbf{i}_l|}}, & k \neq l \\ \frac{1}{\delta}, & k = l. \end{cases} \quad (5.101)$$

All the one-body operators can immediately be constructed as MPOs including the kinetic energy, external potential and the on-site Coulomb interaction of two electrons resulting from Pauli's principle. What is more, the two-body operator of the pure electrostatic electron-electron interaction can readily be brought into MPO-form. Making use of a matrix factorization technique and summing up spin, one can write

$$\sum_{k<l} u_{kl} \hat{n}_k \hat{n}_l = \sum_{s,k<l} q_{ks} r_{sl} \hat{n}_k \hat{n}_l \quad (5.102)$$

$$= \sum_s \begin{pmatrix} \hat{1}_1 & q_{1s} \hat{\eta}_1 & 0 \end{pmatrix} \odot \begin{pmatrix} \hat{1}_2 & q_{2s} \hat{\eta}_2 & 0 \\ 0 & \hat{1}_2 & r_{s2} \hat{\eta}_2 \\ 0 & 0 & \hat{1}_2 \end{pmatrix} \odot \dots \odot \begin{pmatrix} 0 \\ r_{sL} \hat{\eta}_L \\ \hat{1}_L \end{pmatrix}. \quad (5.103)$$

Here, it was again assumed that the lattice consists of a finite but large number of lattice sites  $\mathbb{L} = \{\mathbf{i}_1; \mathbf{i}_2; \dots; \mathbf{i}_L\}$ . It can directly be seen in the last equation that the size scaling of the operator matrices in the discrete position space formulation is much better than in any other basis. The size of an operator matrix scales linearly with the total number of lattice sites  $L$  compared to  $O(L^4)$ . Unfortunately, the amount of lattice sites needed for obtaining sufficiently accurate results must be huge. That is why it is a priori not clear which of the presented basis types is the best for DMRG calculations in terms of MPOs and MPSs.

It has been shown so far that the construction of the quantum-chemical electronic Hamiltonian as MPO formulated on a position space lattice scales linearly with the total number of lattice sites  $L$  taken into account, that means each of the  $L$  operator matrices forming the Hamiltonian MPO has a matrix dimension or size which grows linearly with  $L$ . Although discrete position space seems to be a promising starting point, there are complications which will be pointed out in the following.

It should be noted that, in practical applications, one can only treat systems embedded in a finite volume  $\mathcal{V} = \ell^3$  on a lattice of a finite number of sites limited

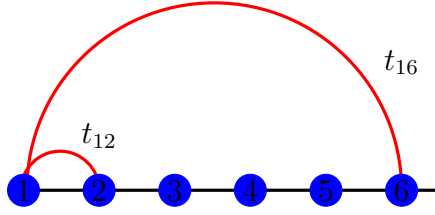


Figure 5.2: This sketch shows how labeling the lattice sites results in a chain-like picture and the nearest-neighbor hopping in the kinetic energy becomes an effective long-range hopping (red lines). Here, it was assumed that the actual lattice has  $3 \times 3$  sites. An electron on the square-lattice starting on the first site in the bottom left corner of the lattice can hop by one site to the right or upwards. That is the first and the second site are coupled by the hopping element  $t_{12}$  and the first and the sixth site in this sketch are coupled by  $t_{16}$  because the sites are separated by a distance of 1 from the first one.

by the computer resources. That already sets the accuracy for all the calculations because the exact quantum-chemical system in vacuum is theoretically obtained in the limit of infinitely many lattice sites  $L \rightarrow \infty$  and infinitesimally small lattice spacing  $\delta \rightarrow 0$ . For good accuracy, one thus needs a large number of lattice sites with a relatively small lattice spacing. This makes the construction of the Hamiltonian more extensive. Consider for instance the kinetic energy term. Even though electrons can just hop from one site to the next one, the labeling of the sites and the resulting chain-like picture leads to an effective long-range hopping because all the sites are coupled which are separated by a distance of 1 (see Fig. 5.2). The kinetic energy matrix with elements  $t_{kl}$  turns out to be sparse. But its large matrix dimension is a problem since one must decompose the kinetic energy matrix into a product of matrices to construct the MPO of the kinetic energy operator. Currently, this can only be done approximately by a sparse matrix factorization like the sparse singular value decomposition where one can only choose to get a certain number of the largest or smallest singular values and corresponding left- and right-singular vectors

$$t_{kl} \approx \sum_{s=1}^{L'} a_{ks} \lambda_{ss} b_{sl} \quad (L' < L). \quad (5.104)$$

$\mathbf{a}$  and  $\mathbf{b}$  denote the matrices of left- and right-singular vectors and  $\boldsymbol{\lambda}$  is the matrix containing the singular values

$$\mathbf{t} \approx \mathbf{a} \boldsymbol{\lambda} \mathbf{b}. \quad (5.105)$$

So far, there seems to be no better solution to account for the effective long-range hopping in the kinetic energy. In comparison to that, the external potential is not a problem as its MPO has a constant size for every site which does not grow by increasing the lattice size. The Coulomb interaction between electrons on different sites is the most tedious part in constructing the MPO-representation of the quantum-chemical Hamiltonian. Due to the long-range nature of the Coulomb potential the matrix  $\mathbf{u}$  with elements  $u_{kl}$  is not even sparse. It is completely dense making it hardly possible to build the matrix  $\mathbf{u}$  for large lattice sizes and decompos-

ing it via a sparse matrix decomposition method. What is more, as it will become clear from the DMRG algorithm in the next chapter and sections, one has to iterate over all the lattice sites again and again until convergence of the energy is reached, which can take quite some long time on a suitably large real-space lattice.

### 5.3 MPO-construction in the different basis types

It has been shown that, regarding the formal mathematical scaling, a discrete position space formulation may be more favorable for quantum-chemical problems than the other basis formulations since the MPO-construction of the Hamiltonian despite the long-range behavior of the Coulomb potential has asymptotically linear scaling with the number of lattice sites  $L$  with respect to its size per lattice site. The advantage of a position space formulation is furthermore that quantum-chemical systems can be studied directly on a, quantum-chemically speaking, post-Hartree-Fock level by variational renormalization methods like the density matrix renormalization group (DMRG) method without having to perform an a priori mean-field calculation. A further point is, having expressed the quantum-chemical system on a real-space lattice once, all the entities which are calculated ranging from the electronic density itself to correlation functions are defined on this lattice and can thus be visualized pictorially.

Unfortunately, even though a discrete real-space representation of quantum chemistry seems to be a good choice for MPO-based simulations, the huge lattice sizes are still a problem. The accuracy of calculations is directly connected to the number of lattice sites  $L$  and the smallness of the lattice spacing  $\delta$ . The exact solution of the quantum-chemical problem is obtained in the limit  $L \rightarrow \infty$  and  $\delta \rightarrow 0$ .

From all the other basis spaces, the orthonormalized atomic orbital formulation is also promising because it makes direct DMRG calculations (without Hartree-Fock) possible as well, which is especially useful in situations where the Hartree-Fock method is physically wrong and hard to converge. The asymptotic scaling of the MPO-construction is  $O(L^4)$ , but the number of states or sites is much smaller than in the discrete position space formulation. As it will be shown in the next chapter, an advantage of atomic orbitals over all the other basis types is that these orbitals are less entangled due to their local nature. This results in more efficient DMRG calculations, in particular for systems with linear spatial topology and systems in the regime between localized and delocalized electrons.

In the next chapter, the DMRG algorithm for quantum-chemical systems, which has been implemented for this dissertation, is presented and practical simulations are discussed both in the discrete position space and atomic orbital basis formulation.



# 6 Electronic structure studies with matrix product operators and states

The following chapter is devoted to the main research part of this dissertation. It is presented how electronic structure calculations for many-electron systems ranging from atoms to small molecules can be achieved with a state-of-the-art variational renormalization method like the density matrix renormalization group method. A pilot reference implementation of the DMRG algorithm for the ground-state search of quantum-chemical systems, which has been done in the programming language Python 3 [Pilgrim, 2010] using the SciPy library [Jones et al., 2001] and has been completely formulated in terms of matrix product operators and matrix product states, is presented. Moreover, results for example simulations on specific systems (e.g., He, H<sub>2</sub>, ionization energies of Be, H-chains, stretched C<sub>2</sub>H<sub>2</sub>, and small stretched C-chains) are shown and discussed to explain the behavior of the implemented search for ground-state energies and wave functions with the DMRG method due to the chosen parameters in the discrete real-space and atomic orbital formulation as it can also be found in Snajberk and Ochsenfeld [2017a] and Snajberk and Ochsenfeld [2017b], respectively. A comparison of the convergence behavior of the DMRG method in terms of molecular and atomic orbitals is presented and, at the end, a small detour to molecules with three-dimensional extents using the example of cubic hydrogen H<sub>8</sub> is done. Overall, the presented DMRG implementation turns out to be a direct correlation method which can directly (without pre-HF calculation) obtain numerically exact results for quantum-chemical many-body problems, especially for systems in the non-dynamical or static correlated regime where electrons are in a critical state between being localized and delocalized, and where other post-HF methods fail. For the above-mentioned test systems with linear topology, the atomic orbital based DMRG approach performs better than the real-space lattice and HF-orbital based approaches.

## 6.1 Ground-state search with the DMRG algorithm

### 6.1.1 Minimizing the Lagrangian

The density matrix renormalization group method belongs to the class of so-called variational renormalization methods. Its basic equations can be derived in a variational manner as shown by Schollwöck [2011]. For this purpose, let us assume that the Hamiltonian of the system to investigate has MPO-form and the many-body wave function is in MPS-shape. Now, the expression for the normalized energy expectation value is minimized with respect to the state matrices  $\Psi$  building the matrix product state  $|\psi\rangle$  under certain constraints. This results in the Lagrangian

function

$$\mathcal{L}(\{\Psi\}, \{\Psi^*\}) = \langle \psi | \hat{H} | \psi \rangle - \lambda (\langle \psi | \psi \rangle - 1), \quad (6.1)$$

where  $\lambda$  is a Lagrangian multiplier for the constraint

$$\langle \psi | \psi \rangle - 1 = 0 \quad (6.2)$$

making sure that the wave function  $|\psi\rangle$  is normalized. The Lagrangian function is minimized with respect to  $\Psi^{m_k^*}$  (the derivative with respect to  $\Psi^{m_k}$  yields an analogous set of equations)

$$\frac{\partial}{\partial \Psi^{m_k^*}} \mathcal{L}(\{\Psi\}, \{\Psi^*\}) = 0 \quad (k = 1, 2, \dots, L). \quad (6.3)$$

The derivative with respect to  $\Psi^{m_k^*}$  means the derivative with respect to all the elements of  $\Psi^{m_k^*}$ . For simplicity, it is assumed that all matrices in the MPS  $|\psi\rangle$  and in the MPO  $\hat{H}$  have been contracted up to the site or single-particle state  $k$ , that is the expectation value and the overlap become

$$\langle \psi | \hat{H} | \psi \rangle = \sum_{m_k n_k l l' \alpha \alpha' r r'} \Psi_{lr}^{m_k^*} \mathcal{P}_{l\alpha l'} H_{\alpha \alpha'}^{m_k n_k} \mathcal{Q}_{r\alpha' r'} \Psi_{l'r'}^{n_k} \quad (6.4)$$

$$\langle \psi | \psi \rangle = \sum_{m_k l l' r r'} \Psi_{lr}^{m_k^*} \mathcal{S}_{lr, l'r'} \Psi_{l'r'}^{m_k}. \quad (6.5)$$

The minimization of  $\mathcal{L}(\{\Psi\}, \{\Psi^*\})$  with respect to all the matrix elements of one state matrix, say  $\Psi^{m_k^*}$ , then results in the following set of equations

$$0 = \frac{\partial}{\partial \Psi_{lr}^{m_k^*}} \mathcal{L}(\{\Psi\}, \{\Psi^*\}) = \frac{\partial}{\partial \Psi_{lr}^{m_k^*}} \left( \sum_{m_k n_k l l' \alpha \alpha' r r'} \Psi_{lr}^{m_k^*} \mathcal{P}_{l\alpha l'} H_{\alpha \alpha'}^{m_k n_k} \mathcal{Q}_{r\alpha' r'} \Psi_{l'r'}^{n_k} - \lambda \sum_{m_k l l' r r'} \Psi_{lr}^{m_k^*} \mathcal{S}_{lr, l'r'} \Psi_{l'r'}^{m_k} \right) \quad (6.6)$$

$$= \sum_{n_k l' r' \alpha \alpha'} \mathcal{P}_{l\alpha l'} H_{\alpha \alpha'}^{m_k n_k} \mathcal{Q}_{r\alpha' r'} \Psi_{l'r'}^{n_k} - \lambda \sum_{l' r'} \mathcal{S}_{lr, l'r'} \Psi_{l'r'}^{m_k} \quad (6.7)$$

$$= \sum_{n_k l' r'} \tilde{H}_{lr, l'r'}^{m_k n_k} \Psi_{l'r'}^{n_k} - \lambda \sum_{l' r'} \mathcal{S}_{lr, l'r'} \Psi_{l'r'}^{m_k}, \quad (6.8)$$

or written as matrix vector equation

$$\tilde{H}_k \vec{\Psi}_k = \lambda \mathcal{S} \vec{\Psi}_k. \quad (6.9)$$

The search for the ground state turns out to be the iterative solution of  $L$  generalized eigenvalue problems. The Lagrangian multiplier  $\lambda$  here serves as the total ground-state energy. By a transformation making all state matrices orthogonal and leaving the energy and the total wave function unchanged

$$\Psi'^{m_k} = \mathbf{X}_{k-1}^{-1} \Psi^{m_k} \mathbf{X}_k, \quad (6.10)$$



Eq. (6.9) can be turned into an ordinary eigenvalue problem

$$\tilde{\mathbf{H}}'_k \vec{\Psi}'_k = \lambda \vec{\Psi}'_k \quad (6.11)$$

because  $\mathbf{S}$  becomes the identity matrix. This is numerically much easier to handle. The DMRG algorithm in terms of matrix product states and operators is based on Eq. (6.11). This last equation demonstrates what the concept of basis renormalization implies. Instead of having to solve a problem in an exponentially large basis space, the matrix product states and their operator analogues enable us just to solve a set of polynomially large problems. If the lattice contains  $L$  sites and the MPS-matrices are of the size  $M \times M$ , the size of the renormalized basis space is truncated to a growth of the order  $O(M^2L)$ .

### 6.1.2 Implementational details on the single-site DMRG algorithm

In the following, the so-called single-site DMRG algorithm implemented for this dissertation to study quantum-chemical systems is presented. It is called one-site DMRG because only one site matrix of the MPS wave function is optimized at a time. The used programming language is Python 3 ([www.python.org](http://www.python.org) and for a good introductory book, see [Pilgrim, 2010]). For all the mathematical routines (e.g., matrix multiplication, tensor manipulation, sparse matrices, sparse diagonalization etc.), the NumPy and SciPy libraries are used ([www.scipy.org](http://www.scipy.org) [Jones et al., 2001]). It is clear that Python 3 is not the most efficient programming language, but to test algorithmic ideas in a pilot implementation in a fast and readable way, it is outstanding. The pilot implementation here is based on two formulations of quantum-chemical systems: a discrete real-space lattice and a Cholesky-orthonormalized atomic orbital formulation.

#### Lattice creation

The first step is to initialize the lattice to use for the DMRG simulation.

- **Real-space lattice:** A box volume in which the quantum-chemical system is embedded is chosen and filled with lattice sites. The accuracy of the calculations is now set by the amount of lattice sites and the smallness of the lattice spacing. Including the origin of the coordinate system, the total number of lattice sites is odd.
- **Atomic orbitals:** The atomic orbitals are considered as sites in an abstract lattice which can be occupied by electrons. The ordering of these orbitals is naturally dictated by the geometry of the system.

#### MPO construction of the Hamiltonian

Next, the Hamiltonian of the system to investigate must be constructed as a matrix product operator. Concerning the initial steps, this is the most time-consuming part because the Hamiltonian incorporates long-range interactions such as the electron-electron interaction. The operator matrices  $\mathbf{H}^{mn}$  can become quite large. Therefore,

it is convenient to try to compress their sizes. For this purpose, a MPO-compression scheme has been implemented according to Fröwis et al. [2010]. This compression scheme is based on a least-square fit of the Hamiltonian in MPO-form

$$\min_{\hat{O}} \|\hat{H} - \hat{O}\|^2. \quad (6.12)$$

The norm  $\|\cdot\|$  is the operator analogue of the Euclidean 2-norm, the so-called Frobenius norm defined as

$$\|\hat{O}\| = \sqrt{\text{Tr}(\hat{O}^\dagger \hat{O})}. \quad (6.13)$$

The idea of the compression scheme is to guess a matrix product operator  $\hat{O}$  whose operator-valued matrices have a smaller size than the MPO of  $\hat{H}$ . By minimizing then the squared distance between  $\hat{H}$  and  $\hat{O}$  under the operator 2-norm with respect to the operator matrices of  $\hat{O}$ , one obtains an approximation of the original Hamiltonian MPO, but with a smaller size, which makes further steps faster. The original Hamiltonian  $\hat{H}$  is very sparse due to its construction. Therefore, it can be compressed tremendously. Unfortunately, the dimension of quantum-chemical MPOs normally gets so large that this compression scheme is not feasible any more. That is why other compression schemes are suggested in section 6.2.

### Initialization of a starting guess-state

Since DMRG is an iterative procedure—Eq. (6.11) is solved for each state matrix  $\Psi$ —one has to start with a guess-MPS. This MPS can be randomly chosen, that is one fixes the size of the involved state matrices. However, there are some numerical subtleties one must pay attention at. If the number of lattice sites is large, say around 1000 sites, it is good to bring some information about the occupation numbers into the guess-MPS because otherwise the long MPS cannot be normalized and its state matrices cannot be orthogonalized. What is more, the effective Hamiltonian matrix in Eq. (6.11)  $\tilde{H}$  will contain numerical infinities or “NaNs”.

### Initialization of pre-contractions

In this step, all the state and operator matrices are contracted up to the first site beginning from the right end with site  $L$

$$\mathcal{Q}_{i_L \alpha_L j_L}^{(L)} = \sum_{m_L n_L} \Psi_{i_L}^{m_L*} H_{\alpha_L}^{m_L n_L} \Psi_{j_L}^{n_L}. \quad (6.14)$$

For site  $L - 1$ , we then have

$$\mathcal{Q}_{i_{L-1} \alpha_{L-1} j_{L-1}}^{(L-1)} = \sum_{\substack{m_{L-1} n_{L-1} \\ i_L \alpha_L j_L}} \Psi_{i_{L-1}}^{m_{L-1}*} \mathcal{Q}_{i_L \alpha_L j_L}^{(L)} H_{\alpha_{L-1} \alpha_L}^{m_{L-1} n_{L-1}} \Psi_{j_{L-1} j_L}^{n_{L-1}} \quad (6.15)$$

and so on.  $i, j$  and  $\alpha$  are the indices of the state and operator matrices respectively. On a single site, the contractions form some kind of site-expectation value. One should note here that the state matrices have not been orthogonalized. In fact, it is not necessary at the beginning as long as one orthogonalizes the matrices during the iterations after each iteration step. One can even guess the pre-contractions

from the right and rely on the fact that the DMRG method figures out the correct contractions—when starting from the left—during the iterations step by step.

### Sweeping

Now, the actual DMRG iterations begin. Having sorted the lattice in a chain-like fashion, Eq. (6.11) is formed for the first site and solved for the wave function state matrix  $\Psi^{m_1}$ , i.e., the effective Hamilton matrix is constructed using the pre-contractions and it is diagonalized (Lanczos or Davidson method). In order to orthogonalize the state matrices and thus normalize the total wave function gradually during the sweeping procedure, a QR decomposition of the just obtained state matrix is performed

$$\Psi_{i_1}^{m_1} \longrightarrow \Psi_{m_1 i_1} = \sum_{a_1} Q_{m_1 a_1} R_{a_1 i_1}. \quad (6.16)$$

It should be noted here that the size of the  $Q$  matrix must be truncated to the original size of the guess state matrices, otherwise the size of the obtained state matrices will grow exponentially. In this case, the truncation is no approximation because the exponential growth is just a consequence of the QR-orthogonalization steps. The  $R$  matrix is then formally multiplied into the state matrix of the second site, but this multiplication is actually unnecessary since the state matrix for the second site will be calculated in the next iteration step and its explicit shape does not matter.  $\Psi^{m_1}$  is now updated by  $Q^{m_1}$

$$Q_{m_1 a_1} \longrightarrow Q_{a_1}^{m_1}. \quad (6.17)$$

Additionally, one has to carry out the contractions of the new state matrix and the operator matrix like in the pre-contraction step

$$\mathcal{P}_{a_1 \alpha_1 b_1}^{(1)} = \sum_{m_1 n_1} Q_{a_1}^{m_1*} H_{\alpha_1}^{m_1 n_1} Q_{b_1}^{n_1}. \quad (6.18)$$

After that, all the same sub-steps are performed for the second site and so on

$$\Psi_{a_1 i_2}^{m_2} \longrightarrow \Psi_{m_1 a_1, i_2} = \sum_{a_2} Q_{m_1 a_1, a_2} R_{a_2 i_2} \quad (6.19)$$

$$\mathcal{P}_{a_2 \alpha_2 b_2}^{(2)} = \sum_{m_2 n_2} Q_{a_1 a_2}^{m_2*} \mathcal{P}_{a_1 \alpha_1 b_1}^{(1)} H_{\alpha_1 \alpha_2}^{m_2 n_2} Q_{b_1 b_2}^{n_2} \quad (6.20)$$

and the state matrix on site 2 is of course updated by the newly obtained  $Q^{m_2}$ . One continues with these steps until the right end of the chain is reached. Now, the chain is reverted and the iterations mentioned above are repeated till the end of the chain is reached again. Finally, a so-called sweep is done. A sweep consists of micro-iterations including the solution of Eq. (6.11) for each lattice site. A full sweep is done when the micro-iteration steps have returned to the site where the sweep started. Fig. 6.1 shows the sweeping procedure pictorially. This sweeping procedure is now continued over and over again, thus finding the correct weights of the ground-state wave function with respect to the chosen size of its state matrices, until the ground-state energy has been converged.

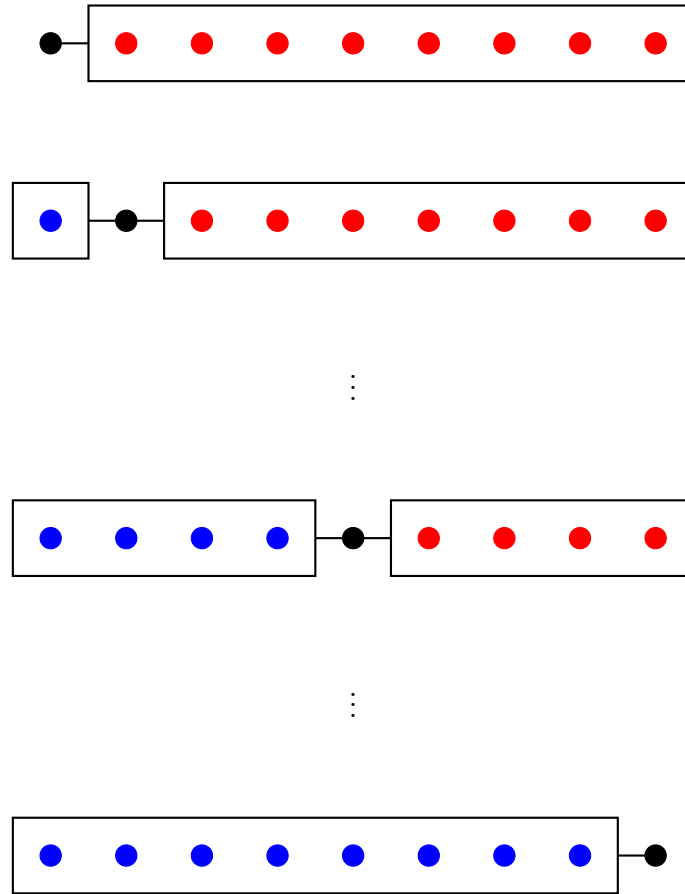


Figure 6.1: One half of a sweeping cycle is shown from the top to the bottom. The search for the ground-state wave function coefficients and thus the state matrices of the corresponding MPS starts at the first site of the lattice reordered in a chain-like fashion. In the first step (top), all the sites have been contracted from the right (red dots in a rectangle) forming the  $\mathcal{Q}$  contraction expressions. The black dot represents the site where Eq. (6.11) is solved and the black line denotes the site's coupling to the rest. When going to the next site, the state matrix at the site before is orthogonalized and all the site matrices are contracted, which forms the  $\mathcal{P}$  expressions (blue dots in a rectangle). In this manner, one goes from the left to the right end of the chain determining all the state matrices and contracting all the sites gradually. When the last site is reached (bottom), the chain is reverted and one continues to determine the state matrices until the end of the chain is reached again.

### Quality of convergence

When the energy is converged, the quality of the found ground-state can be estimated by looking at the variance of the Hamiltonian

$$\text{var}(\hat{H}) = \langle \psi | \hat{H}^2 | \psi \rangle - \lambda^2, \quad (6.21)$$

which has to go to zero since  $|\psi\rangle$  ought to be an eigenstate of  $\hat{H}$ . Unfortunately, calculating the variance is only possible for Hamiltonians with a small MPO-size because it incorporates the square of the Hamiltonian and thus formally the multiplication of two MPOs, which is numerically demanding.

Another convergence criterion can therefore be the expectation value of the particle number operator

$$N = \langle \psi | \hat{N} | \psi \rangle. \quad (6.22)$$

$N$  must converge towards an integer number representing the total number of particles in the system when the total energy is close to its exact value.

### Parallelization

Though there are some ideas to parallelize the DMRG algorithm [Stoudenmire and White, 2013], it is not clear at the current stage of this thesis how to parallelize the central sweeping procedure of the DMRG algorithm, which is serial by design. However, at least some parts can be parallelized: the MPO-construction per site can be parallelized because—as it has been shown in the previous chapter—the total Hamiltonian-MPO can be written as sum of MPOs

$$\hat{H} = \sum_{\alpha \geq 0} \hat{H}_{\text{MPO}}^{(\alpha)}, \quad (6.23)$$

where  $\hat{h} = \hat{H}_{\text{MPO}}^{(0)}$  corresponds to the MPO of the one-electron Hamiltonian and  $\hat{U} = \sum_{\alpha > 0} \hat{H}_{\text{MPO}}^{(\alpha)}$  is the electron-electron interaction. The sum in Eq. (6.23) can be parallelized. As a consequence, all the micro-iteration steps using the total Hamiltonian (e.g., the left and right contractions and the construction of the effective Hamilton matrix at a specific site) can also be parallelized. Fig. 6.2 shows how CPU-parallelization affects the MPO-construction times using the example of increasing hydrogen chains in the atomic orbital STO-3G basis [Hehre et al., 1969]. Using 8 CPU cores leads to a speed-up in construction time, but for more cores the gained speed-up gradually saturates. To save RAM-memory, the Hamiltonian MPO is written to disk. Fig. 6.3 depicts the disk usage of the MPO-construction with increasing number of electrons and orbitals.

### 6.1.3 Particle number conservation

In performing ground-state searches for quantum-chemical systems with the DMRG method in MPS/MPO-formulation, it is sometimes important to include symmetries like the conservation of the particle number explicitly. This is especially important when calculating the lowest-lying energy and corresponding wave function of an ion in chemistry (ions are not the subject of this thesis). Otherwise the ground-state search will end up with a state and an energy corresponding to the lowest

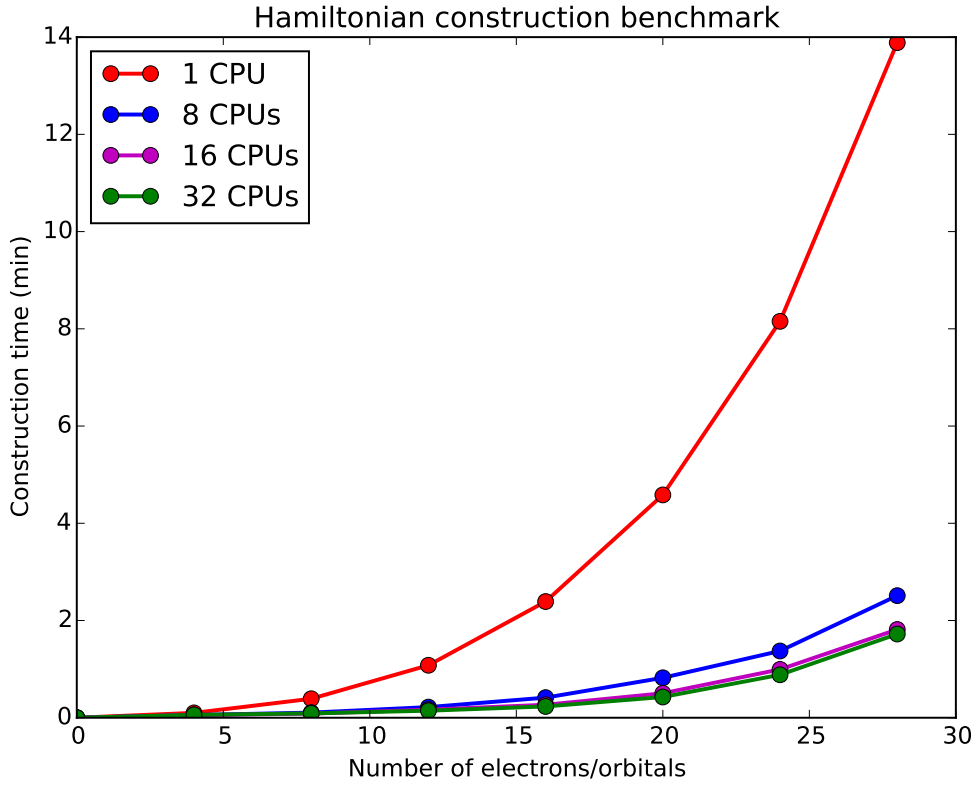


Figure 6.2: MPO-construction times with increasing number of electrons and orbitals using the example of a hydrogen chain in the atomic orbital STO-3G basis [Hehre et al., 1969].

possible eigenvalue of the quantum-chemical Hamiltonian, which is charge-neutral. Therefore, one must include particle number conservation in the guess-state or in the Hamiltonian. In the following, it is shown how to include the symmetry of particle number conservation in the Hamiltonian. There are two known ways which will be presented in the following [McCulloch, 2007, Peotta and Di Ventura, 2013, Singh et al., 2010, 2011, Li et al., 1993].

### Particle number conservation by projection

In group theory, particle number conservation belongs to the Abelian symmetry group  $U(1)$ . If particle number is conserved in the Hamiltonian, one says that the Hamiltonian is  $U(1)$ -symmetric. This means the Hamiltonian is invariant with respect to a change in the single-particle states or, phrased in terms of second quantization, in the creation and annihilation operators by a phase factor

$$\hat{a}_{i\sigma}^\dagger = e^{i\theta} \hat{c}_{i\sigma}^\dagger \quad (6.24)$$

$$\hat{a}_{i\sigma} = e^{-i\theta} \hat{c}_{i\sigma}. \quad (6.25)$$

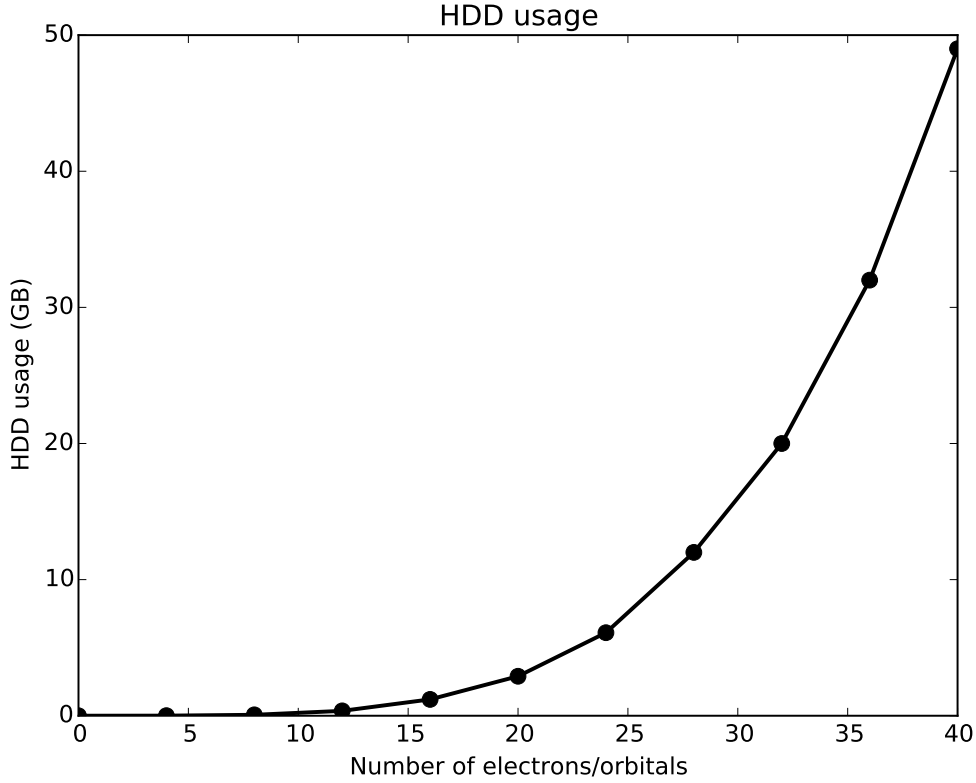


Figure 6.3: Disk usage of the MPO-construction of increasing hydrogen chains formulated in the atomic orbital STO-3G basis [Hehre et al., 1969].

Consider a quantum-chemical Hamiltonian in an unspecified basis in second quantization which consists of sums and products of creation and annihilation pairs

$$\hat{H}(\{\hat{c}^\dagger, \hat{c}\}) = \sum_{ij,\sigma} h_{ij} \hat{c}_{i\sigma}^\dagger \hat{c}_{j\sigma} + \frac{1}{2} \sum_{ijkl,\sigma\sigma'} u_{ijkl} \hat{c}_{i\sigma}^\dagger \hat{c}_{j\sigma'}^\dagger \hat{c}_{l\sigma'} \hat{c}_{k\sigma} \quad (6.26)$$

$$= \sum_{ij,\sigma} h_{ij} e^{-i\theta} \hat{a}_{i\sigma}^\dagger e^{i\theta} \hat{a}_{j\sigma} + \frac{1}{2} \sum_{ijkl,\sigma\sigma'} u_{ijkl} e^{-i\theta} \hat{a}_{i\sigma}^\dagger e^{-i\theta} \hat{a}_{j\sigma'}^\dagger e^{i\theta} \hat{a}_{l\sigma'} e^{i\theta} \hat{a}_{k\sigma} \quad (6.27)$$

$$= \sum_{ij,\sigma} h_{ij} \hat{a}_{i\sigma}^\dagger \hat{a}_{j\sigma} + \frac{1}{2} \sum_{ijkl,\sigma\sigma'} u_{ijkl} \hat{a}_{i\sigma}^\dagger \hat{a}_{j\sigma'}^\dagger \hat{a}_{l\sigma'} \hat{a}_{k\sigma} \quad (6.28)$$

$$= \hat{H}(\{\hat{a}^\dagger, \hat{a}\}) . \quad (6.29)$$

This invariance immediately implies that the Hamiltonian commutes with the particle number operator

$$[\hat{H}, \hat{N}] = \hat{H}\hat{N} - \hat{N}\hat{H} = 0 . \quad (6.30)$$

As a consequence, the Hamiltonian can be expanded in a set of many-particle states which are eigenstates of the particle number operator

$$\hat{N} |N\rangle = N |N\rangle \quad (6.31)$$

$$\hat{H} = \sum_{MN} H_{MN} |M\rangle \langle N| , \quad (6.32)$$

where  $M$  and  $N$  are the possible numbers of particles including also the case of zero particles. The goal is now to project the Hamiltonian onto the space of many-particle states (Slater determinants) with the correct predefined particle number. This can be achieved by the projection operator

$$\hat{P}_N |M\rangle = \delta_{\hat{N},N} |M\rangle = \begin{cases} |M\rangle, & M = N \\ 0, & M \neq N. \end{cases} \quad (6.33)$$

This is an operator whose eigenvalues are either 1 if  $M = N$  or 0 otherwise. Expanded in terms of occupation number states, the operator has the form

$$\hat{P}_N = \sum_{\mathbf{mn}} P_{\mathbf{mn}} |\mathbf{m}\rangle \langle \mathbf{n}| \quad (6.34)$$

$$= \sum_{\mathbf{mn}} \delta_{\sum_i n_i, N} \delta_{\mathbf{mn}} |\mathbf{m}\rangle \langle \mathbf{n}|. \quad (6.35)$$

It would now be possible theoretically to project the Hamiltonian onto the space of many-particle states with correct predefined particle number  $N$

$$\hat{H}_N = \hat{P}_N^\dagger \hat{H} \hat{P}_N, \quad (6.36)$$

but this is quite inefficient in practice due to the exponentially large basis space. Therefore, the goal must be to find a MPO-representation of  $\hat{P}_N$ . To find a suitable MPO-representation is part of this dissertation. The condition of particle number conservation  $\delta_{\sum_i n_i, N}$  is equivalent to the equation

$$n_1 + n_2 + \dots + n_L = N. \quad (6.37)$$

$L$  is as usual the total number of lattice sites or single-particle states. We now introduce auxiliary particle numbers  $N_i$  without changing the last equation

$$n_1 + n_2 + \dots + n_L = N_1 - N_1 + N_2 - N_2 + \dots + N_{L-1} - N_{L-1} + N. \quad (6.38)$$

This leads to a set of equations

$$n_1 = N_1 \quad (6.39)$$

$$n_2 = N_2 - N_1 \quad (6.40)$$

$$\vdots$$

$$n_L = N - N_{L-1}. \quad (6.41)$$

Thus, one can write

$$\delta_{\sum_i n_i, N} = \sum_{N_1 N_2 \dots N_{L-1}} \delta_{n_1+0, N_1} \delta_{n_2+N_1, N_2} \dots \delta_{n_L+N_{L-1}, N}, \quad (6.42)$$

where it is necessary to sum over all auxiliary particle numbers. With that, the projection operator reads

$$\hat{P}_N = \sum_{\mathbf{mnN}} \delta_{n_1+0, N_1} \delta_{m_1 n_1} \delta_{n_2+N_1, N_2} \delta_{m_2 n_2} \dots \delta_{n_L+N_{L-1}, N} \delta_{m_L n_L} |\mathbf{m}\rangle \langle \mathbf{n}|. \quad (6.43)$$



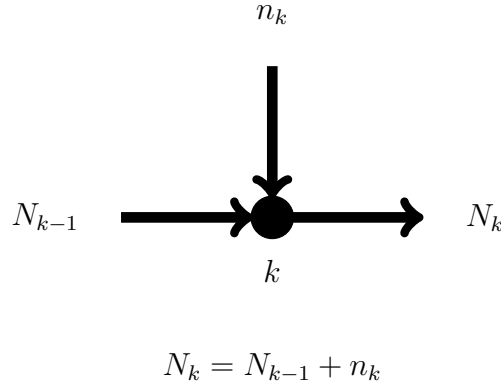


Figure 6.4: It is shown how particle number conservation is implemented locally on a specific lattice site. During the sweeping procedure particles accumulate on the lattice sites such that there are  $N$  particles in total. One must thus keep track of the local portion of particles moving through the lattice. The sum of particles going into a site must equal the number of particles going out. This makes it possible to ensure that one starts with a zero-particle occupation of the lattice and eventually reaches a  $N$ -particle occupation of the whole lattice. In this way, all possible particle number combinations on the lattice can be established.

Its MPO-representation can then be deduced as

$$\hat{P}_N = \sum_{\mathbf{m}\mathbf{n}N} P_{N_1}^{m_1 n_1} P_{N_1 N_2}^{m_2 n_2} \cdots P_{N_{L-1}}^{m_L n_L} |\mathbf{m}\rangle \langle \mathbf{n}| \quad (6.44)$$

$$= \sum_{\mathbf{m}\mathbf{n}} \mathbf{P}^{m_1 n_1} \mathbf{P}^{m_2 n_2} \cdots \mathbf{P}^{m_L n_L} |\mathbf{m}\rangle \langle \mathbf{n}| \quad (6.45)$$

$$= \hat{\mathbf{P}}_1 \odot \hat{\mathbf{P}}_2 \odot \cdots \odot \hat{\mathbf{P}}_L \quad (6.46)$$

with

$$\left( \hat{\mathbf{P}}_k \right)_{N_{k-1} N_k} = \sum_{m_k n_k} P_{N_{k-1} N_k}^{m_k n_k} |m_k\rangle \langle n_k| \quad (6.47)$$

$$= \sum_{m_k n_k} \delta_{n_k + N_{k-1}, N_k} \delta_{m_k n_k} |m_k\rangle \langle n_k|. \quad (6.48)$$

Fig. 6.4 visualizes how the particle number projection operator  $\hat{P}_N$  can be constructed as a matrix product operator. The lattice is directed indicating the direction of the sweeping procedure. The projection operator is constructed such that it keeps track of the particle number “moving” through the lattice starting with 0 particles at the first site and finishing with  $N$  particles at the last site. Going from site to site, particles may be added by the occupation number indices  $m$  and  $n$ . However, the particle number is conserved only if the sum of all particles moving towards a site equals the number of particles leaving a site. The auxiliary particle numbers  $N_k$  range from 0 to the maximally possible number of particles moving through the lattice. All possible particle number combinations on the lattice can be established in this manner.

Projecting the Hamiltonian into the correct particle number sector works quite well for small particle numbers. But for growing numbers of particles, it is impractical because the size of the site matrices of the particle-number-projected Hamiltonian  $\hat{H}_N$  increases quadratically with the number of auxiliary particle numbers

$$(H_N)^{m_k n_k}_{N_{k-1} \alpha_{k-1} N'_{k-1}, N_k \alpha_k N'_k} = \sum_{m'_k, n'_k} P_{N_{k-1} N_k}^{m_k m'_k} H_{\alpha_{k-1} \alpha_k}^{m'_k n'_k} P_{N'_{k-1} N'_k}^{n'_k n_k}. \quad (6.49)$$

That is why another way to conserve the particle number is useful.

### Particle number conservation by introducing a chemical potential

Recall the derivation of the DMRG equations by considering the Lagrangian function Eq. (6.1). Particle number conservation can also be enforced by introducing an additional constraint

$$\langle \psi | \hat{N}_\uparrow | \psi \rangle - N_\uparrow = 0 \quad (6.50)$$

and

$$\langle \psi | \hat{N}_\downarrow | \psi \rangle - N_\downarrow = 0 \quad (6.51)$$

with Lagrangian multipliers  $\mu_\uparrow$  and  $\mu_\downarrow$ . The latter Lagrangian multipliers are called chemical potential. This results in a modified Lagrangian function

$$\mathcal{L}(\{\Psi\}, \{\Psi^*\}) = \langle \psi | \hat{H} | \psi \rangle - \mu_\uparrow (\langle \psi | \hat{N}_\uparrow | \psi \rangle - N_\uparrow) - \mu_\downarrow (\langle \psi | \hat{N}_\downarrow | \psi \rangle - N_\downarrow) - \lambda (\langle \psi | \psi \rangle - 1) \quad (6.52)$$

$$= \langle \psi | \hat{H}(\mu_\uparrow, \mu_\downarrow) | \psi \rangle - \lambda (\langle \psi | \psi \rangle - 1), \quad (6.53)$$

where

$$\hat{H}(\mu_\uparrow, \mu_\downarrow) = \hat{H} - \sum_{i\sigma} \mu_\sigma \hat{n}_{i\sigma}. \quad (6.54)$$

By tuning the chemical potentials, one can fix the number of particles with different spin-projections along the  $z$ -axis. One therefore has to consider  $\hat{H}(\mu_\uparrow, \mu_\downarrow)$  in the DMRG equations instead of the standard Hamiltonian  $\hat{H}$ . The advantage of conserving the particle number in this way is that the size of the Hamiltonian MPO does not increase. The energy of the  $N$ -particle system then reads

$$E_N = E(\mu_\uparrow, \mu_\downarrow) + \mu_\uparrow N_\uparrow + \mu_\downarrow N_\downarrow. \quad (6.55)$$

## 6.2 MPO compression schemes

As mentioned in section 6.1.2, the mathematical compression scheme by Fröwis et al. [2010] for Hamiltonian MPOs gets unfeasible for growing numbers of electrons and sites. For this reason, two physical compression schemes either for DMRG on a real-space lattice or on an orbital lattice such as atomic orbitals are suggested in the following.

### 6.2.1 Reduction of the lattice size and momentum space expansion of the electron-electron interaction on a real-space lattice

Because of the sweeping procedure, it is unfortunately of no use at the current stage of technology and theory to consider a discrete real-space lattice as a single-particle basis for DMRG calculations though the formal scaling of the construction of the Hamiltonian MPO at a given site is linear. One must consider a huge number of lattice sites to achieve accurate results. Nevertheless highly approximative DMRG calculations are possible using a real-space lattice. The one-electron Hamiltonian  $\hat{h}$  can be constructed and expressed on a real-space lattice. Its matrix elements are given on an ordered grid with lattice spacing  $\delta$  and  $L$  points as

$$h_{kl} = \begin{cases} \frac{-1}{2\delta^2} \delta_{|\mathbf{i}_k - \mathbf{i}_l|, 1}, & k \neq l \\ \frac{3}{\delta^2} + \sum_A \frac{-Z_A}{\delta |\mathbf{i}_k - \mathbf{i}_A|}, & k = l, \end{cases} \quad (6.56)$$

where  $\mathbf{i}_k \in \mathbb{Z}^3$  are the discrete lattice vectors. One has to regularize the external potential when an electron hits the lattice site of one of the nuclei  $\mathbf{i}_A$  such that

$$v_{kl} = \sum_A \frac{-Z_A}{\delta} \quad (k = l, \mathbf{i}_k = \mathbf{i}_A). \quad (6.57)$$

The matrix  $\mathbf{h}$  is very sparse and can thus be diagonalized by a sparse matrix eigensolver like the Lanczos method. The kept orthonormal eigenvectors  $C_{kp}$  of  $\mathbf{h}$  are to form the single-particle basis states (expressed on a real-space grid) for the MPO-construction of the total Hamiltonian  $\hat{H}$  and subsequent DMRG calculations.

Having obtained the eigenstates  $C_{kp}$  of the non-interacting electron system  $\mathbf{h}$  defined on a position space lattice, the total Hamiltonian of the interacting system on a position space lattice

$$\hat{H} = \sum_{kl, \sigma} h_{kl} \hat{c}_{k\sigma}^\dagger \hat{c}_{l\sigma} + \frac{1}{2} \sum_{kl, \sigma\sigma'} u_{kl} \hat{c}_{k\sigma}^\dagger \hat{c}_{l\sigma'}^\dagger \hat{c}_{l\sigma'} \hat{c}_{k\sigma} \quad (6.58)$$

with

$$u_{kl} = \frac{1}{\delta |\mathbf{i}_k - \mathbf{i}_l|} \quad (6.59)$$

is transformed into the eigenbasis of  $\hat{h}$

$$\hat{c}_{k\sigma}^\dagger = \sum_p C_{pk}^\dagger \hat{c}_{p\sigma}^\dagger \quad (6.60)$$

$$\hat{c}_{k\sigma} = \sum_\mu C_{k\mu} \hat{c}_{\mu\sigma}. \quad (6.61)$$

Thus, the lattice size is reduced while the formal scaling of the MPO-construction changes.

The challenge now is how to transform the electron-electron interaction because its matrix  $\mathbf{u}$  is completely dense in discrete real space such that it cannot be stored in memory. Formally, the electron-electron interaction is transformed by the one-

electron density on a single lattice site

$$P_{k,pq} = C_{pk}^\dagger C_{kq}. \quad (6.62)$$

And, the electron-electron interaction in the eigenbasis of the non-interacting one-electron part  $\hat{h}$  is obtained by

$$u_{prqs} = \sum_{kl} P_{pr,k}^T u_{kl} P_{l,qs}. \quad (6.63)$$

Due to the large lattice size, the electron-electron interaction term  $u_{prqs}$  must be calculated on the fly. This is possible, but takes very long. That is why it is suggested to expand the electron-electron interaction in momentum space

$$u_{kl} = \sum_{n=1}^Q \tilde{u}_n e^{i\frac{\pi}{\ell} \mathbf{q}_n \delta(\mathbf{i}_k - \mathbf{i}_l)} \quad (6.64)$$

where it can be truncated systematically. The last equation can be seen as a truncated Fourier series of the electron-electron interaction where  $Q$  denotes the number of Fourier components or lattice sites in momentum space. The  $\mathbf{q}_n \in \mathbb{Z}^3$  are the discrete lattice vectors of a lattice in momentum space. The  $\tilde{u}_n$  are the expansion coefficients or Fourier components which are obtained as follows:

$$\tilde{u}_n = \int_{\mathcal{V}} \frac{d^3x}{\mathcal{V}} \frac{e^{-i\frac{\pi}{\ell} \mathbf{q}_n \mathbf{x}}}{|\mathbf{x}|}. \quad (6.65)$$

$\mathcal{V} = (2\ell)^3$  is the integration volume because one has to take into account that the maximal distance along one coordinate direction electrons can interact over is  $2\ell$ , which is twice the edge length of the box the system is embedded in. Using the identity

$$\frac{1}{|\mathbf{x}|} = \frac{2}{\sqrt{\pi}} \int_0^\infty dt e^{-t^2(x^2+y^2+z^2)}. \quad (6.66)$$

one can write

$$\tilde{u}_n = \frac{2}{\sqrt{\pi}} \int_0^\infty dt \int_{\mathcal{V}} \frac{d^3x}{\mathcal{V}} e^{-i\frac{\pi}{\ell} \mathbf{q}_n \mathbf{x}} e^{-t^2(x^2+y^2+z^2)}. \quad (6.67)$$

The last equation can now be integrated for every space coordinate separately. As an example, it is done here for the  $x$ -coordinate. All the other coordinates are integrated out analogously. The integral with respect to the  $x$ -direction is indicated by  $\tilde{u}_n^{(x)}$ . One obtains

$$\tilde{u}_n^{(x)}(t) = \int_{-\ell}^{\ell} \frac{dx}{2\ell} e^{-i\frac{\pi}{\ell} q_{n,x} x} e^{-t^2 x^2} \quad (6.68)$$

$$= \frac{\sqrt{\pi}}{4\ell t} e^{-\frac{\pi^2 q_{n,x}^2}{4\ell^2 t^2}} \left( \text{Erf} \left( \ell t + \frac{i\pi q_{n,x}}{2\ell t} \right) - \text{Erf} \left( -\ell t + \frac{i\pi q_{n,x}}{2\ell t} \right) \right). \quad (6.69)$$

$\text{Erf}(\cdot)$  denotes the so-called error function [Abramowitz and Stegun, 2012]. The Fourier or momentum space components  $\tilde{u}_n$  can now be calculated by numerically

integrating the expression

$$\tilde{u}_n = \frac{2}{\sqrt{\pi}} \int_0^\infty dt \tilde{u}_n^{(x)}(t) \tilde{u}_n^{(y)}(t) \tilde{u}_n^{(z)}(t). \quad (6.70)$$

Having the series expansion of the electron-electron interaction  $u_{kl}$ , the transformation into the eigenbasis of  $\hat{h}$  reads

$$u_{prqs} = \sum_{kl} P_{pr,k}^T u_{kl} P_{l,qs} \quad (6.71)$$

$$= \sum_{kln} P_{pr,k}^T \tilde{u}_n e^{i\frac{\pi}{L} \mathbf{q}_n \delta(\mathbf{i}_k - \mathbf{i}_l)} P_{l,qs} \quad (6.72)$$

$$= \sum_{n=1}^Q \tilde{P}_{pr,n}^\dagger \tilde{P}_{n,qs}, \quad (6.73)$$

where it was defined

$$\tilde{P}_{n,pr} = \sum_k \sqrt{\tilde{u}_n} e^{-i\frac{\pi}{L} \mathbf{q}_n \delta \mathbf{i}_k} P_{k,pr}. \quad (6.74)$$

With this systematic truncation of the Fourier series of the electron-electron interaction, the construction of the electron interaction in position space and its transformation to the one-particle eigenbasis of  $\hat{h}$  is speeded up and memory-efficient. The Hamiltonian to use for DMRG calculations is then

$$\hat{H} = \sum_{pq,\sigma} h_{pq} \hat{c}_{p\sigma}^\dagger \hat{c}_{q\sigma} + \frac{1}{2} \sum_{pqrs,\sigma\sigma'} u_{prqs} \hat{c}_{p\sigma}^\dagger \hat{c}_{q\sigma'}^\dagger \hat{c}_{s\sigma'} \hat{c}_{r\sigma} \quad (6.75)$$

with

$$h_{pq} = \varepsilon_p \delta_{pq} \quad (6.76)$$

because the Hamiltonian is expressed in terms of the eigenbasis of  $\hat{h}$  and  $\varepsilon_p$  are the eigenenergies of the one-electron Hamiltonian.

### 6.2.2 Singular value compression of the electron-electron interaction on an orbital lattice

Another physical compression scheme presented here uses the singular value decomposition of the two-electron integral matrix. Consider the electron-electron interaction in the orthonormalized atomic orbital basis  $u_{\mu\nu\kappa\lambda}^{\text{ON}} = u_{\mu\kappa\nu\lambda}^{\text{ON}}$  and reshape it into a matrix

$$u_{\mu\kappa\nu\lambda}^{\text{ON}} \longrightarrow u_{\mu\kappa,\nu\lambda}^{\text{ON}}. \quad (6.77)$$

By performing a singular value decomposition of this matrix and keeping only the largest singular values  $\lambda_\alpha$  up to a certain threshold  $\lambda_{\text{thresh}}$ , one can compress the MPO-construction

$$u_{\mu\kappa,\nu\lambda}^{\text{ON}} = \sum_{\alpha=1}^{N_{\text{thresh}}} x_{\mu\kappa,\alpha} \lambda_\alpha y_{\alpha,\nu\lambda} \quad (6.78)$$

$$= \sum_{\alpha=1}^{N_{\text{thresh}}} x'_{\mu\kappa,\alpha} y'_{\alpha,\nu\lambda}. \quad (6.79)$$

$N_{\text{thresh}} \in \mathbb{N}$  is chosen such that  $\lambda_{\alpha} \geq \lambda_{N_{\text{thresh}}}$ . In practice, a threshold of  $\lambda_{N_{\text{thresh}}} = 10^{-6}$  Hartree turned out to be reasonable for quantum-chemical Hamiltonians. Using a singular value instead of a QR decomposition (see section 5.2.2) makes it possible to construct the MPO of the electron-electron interaction and compress the dimension of its MPO at the same time.

## 6.3 DMRG applications

In this section, results for DMRG calculations of certain quantum-chemical systems formulated both on a discrete position space lattice and on an orthonormalized atomic orbital lattice are presented. First, we start with the DMRG method formulated on a three-dimensional discrete position space lattice, which has been developed for this dissertation, and then, results for the atomic orbital based DMRG version, also developed for this dissertation, are presented.

### 6.3.1 The He-atom and the H<sub>2</sub>-molecule on a real-space lattice

#### He-atom

Let us begin with energy calculations of the He-atom and how the energy converges with shrinking lattice spacing. The helium atom is embedded in a box with 10 Bohr edge length. To avoid finite volume boundary effects, the box must be chosen as large as possible. The one-particle Hamiltonian  $\hat{h}$  is diagonalized on a real-space lattice in this box. The lowest-lying eigenstates of  $\hat{h}$  form the single-particle basis states for the DMRG lattice. First, the electron-electron interaction is considered to be exact. The dimension of the MPS-matrices is set to 16. In table 6.1, it is shown how the helium ground-state energy calculated with the real-space lattice DMRG approach for 5 orbitals expressed on a real-space lattice converges towards the reference value with shrinking lattice spacing and growing number of lattice points in position space. The reference CCSD (cc-pVQZ) value of  $-2.902410$  Hartree has been obtained with the program package Psi4 [Turney et al., 2012] using the coupled-cluster method [Crawford and Schaefer, 2000] and the quantum-chemical basis set cc-pVQZ [Dunning Jr, 1989]. Unfortunately, because of the enormous increase of calculation times when shrinking the lattice spacing, it was not possible to go below 0.2 Bohr as lattice spacing. To go further down with the lattice spacing, it is necessary to use the momentum space truncation or compression of the electron-electron interaction. Table 6.2 demonstrates for a given set of DMRG orbitals (5 orbitals), corresponding energy ( $-2.222093$  Hartree), and lattice spacing (0.5 Bohr) how the presented truncation using the momentum space expansion of the electron-electron interaction behaves and how it converges towards the exact electron-electron interaction limit when including higher numbers of momentum space points into the momentum space expansion. Table 6.3 shows the continuation of table 6.1 further down to a lattice spacing of 0.1 Bohr using the momentum space expansion ( $21^3$  momentum space points) for the electron-electron interaction term. It can be seen

how the DMRG energy further approaches the reference energy value by decreasing the lattice spacing.

Lattice spacing $\delta$	Number of orbitals
	5
0.5	-2.222093
0.3	-2.462735
0.2	-2.661304
$\vdots$	$\vdots$
CCSD (cc-pVQZ):	-2.902410

Table 6.1: Energy convergence of the helium ground-state energy with respect to the smallness of the lattice spacing  $\delta$ . The helium atom is embedded in the center of a box with edge length 10 Bohr. The 5 lowest-lying eigenstates of the one-electron Hamiltonian are used as the DMRG sites. As numerically exact reference, the CCSD (cc-pVQZ) energy of the helium atom is used.

Momentum space points	Energy
$3^3$	-2.602687
$5^3$	-2.452617
$9^3$	-2.285077
$13^3$	-2.235321
$17^3$	-2.226094
$21^3$	-2.223312
$25^3$	-2.222659
$31^3$	-2.222483
$\vdots$	$\vdots$
exact expansion	-2.222093

Table 6.2: Energy convergence of the obtainable helium ground-state energy taken from table 6.1 (5 orbitals,  $\delta = 0.5$  Bohr) with varying momentum space expansions of the electron-electron interaction. With increasing numbers of momentum space points, the energy converges to the exact electron-electron interaction limit.

Lattice spacing $\delta$	Number of orbitals
	5
0.5	-2.222093
0.3	-2.462735
0.2	-2.661304
0.1 (mom. exp.)	-2.806292
$\vdots$	$\vdots$
CCSD (cc-pVQZ):	-2.902410

Table 6.3: Continuation of table 6.1 with an electron-electron interaction expanded in momentum space.  $21^3$  points in momentum space have been used.

### H<sub>2</sub>-molecule

Next, the potential energy curve of the hydrogen molecule is calculated for different lattice spacings and it is compared with the quantum-chemical coupled-cluster method for different basis sets (see figure 6.5). For this purpose, the H<sub>2</sub>-molecule is put into a box of edge length 10 Bohr. For the DMRG calculations, the 5 lowest-lying orbitals of the one-electron Hamiltonian are chosen as DMRG sites and the MPS-matrices have a size of 16 throughout all the calculations. The reference energy curve has been obtained with the CCSD (cc-pVQZ) method. Fig. 6.5 shows the interpolated potential energy curves of H<sub>2</sub> obtained with the discrete real-space lattice DMRG approach for the lattice spacings 0.2 and 0.1 Bohr. In both cases, the electron-electron interaction has been expanded in momentum space using  $21^3$  momentum space points. Moreover, the zero-lattice-spacing limit has been provided by extrapolation. The comparison with the CCSD methods shows that the extrapolated curve nearly coincides with the CCSD (cc-pVDZ) curve. In particular, it can be seen that DMRG qualitatively gives physically correct results even for the largest lattice spacing in this set because all curves calculated with DMRG are similar regarding their shapes to the CCSD (cc-pVQZ) reference curve. Above all, the comparison with the CCSD (STO-3G) potential energy curve indicates that DMRG tends to find the exact ground-state solution of the quantum-chemical Schrödinger equation in its position space representation—of course depending on the lattice spacing—and that it captures correlation effects which go under the name “static” or “non-dynamic” correlation in quantum chemistry quite well. Physically speaking, this is the part of electron correlation which occurs when bonds in molecules for instance are stretched and the one-Slater-determinant ansatz from mean-field theory breaks down. There, the electrons are so-to-say in a critical state between being localized or delocalized on the set of possible one-electron states. Unfortunately, 0.1 was the smallest possible lattice spacing at the stage of this dissertation.

### 6.3.2 Atomic orbital DMRG

This section is now about results obtained with the developed atomic orbital based DMRG method (AO-DMRG). The AO-DMRG program developed for this thesis is interfaced to the quantum-chemical program package PyQuante (<http://pyquante.sourceforge.net>) to calculate the one- and two-electron integrals in



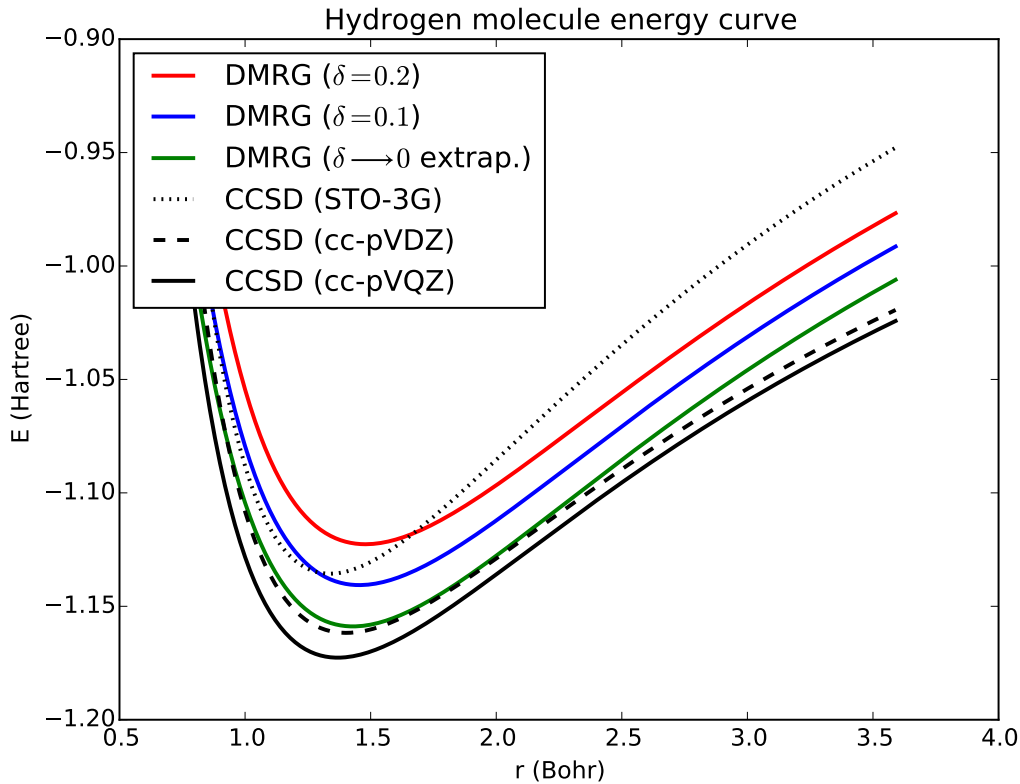


Figure 6.5: Comparison of discrete real-space lattice DMRG calculations for varying lattice spacings and coupled-cluster calculations of the  $\text{H}_2$  ground-state potential energy curve.  $r$  is the distance of the nuclei and  $E$  the corresponding energy. The reference energy curve has been obtained with the CCSD (cc-pVQZ) method. The zero-lattice spacing curve ( $\delta \rightarrow 0$ ) is also provided by extrapolation of the 0.2 and 0.1 lattice spacing curves.

the atomic orbital basis. Throughout this section, the electron-electron interaction is compressed according to the scheme presented in section 6.2.2 using the threshold of  $10^{-6}$  Hartree.

### Ionization energies of the Be-atom

As an introductory example, calculations of the first and second ionization energies (IE)

$$\text{IE}_n = E_{-n}^{(0)} - E^{(0)} \quad (6.80)$$

of the Be-atom in an orthonormalized STO-3G atomic orbital basis are shown both using the particle number conserving projection and the chemical potential technique.  $\text{IE}_n$  is the  $n$ th ionization energy meaning the amount of energy needed to ionize the system  $n$  times



Starting point is the Hamiltonian expressed in terms of orthonormalized atomic orbitals

$$\hat{H} = \sum_{\mu\nu,\sigma} h_{\mu\nu}^{\text{ON}} \hat{a}_{\mu\sigma}^\dagger \hat{a}_{\nu\sigma} + \frac{1}{2} \sum_{\mu\nu\kappa\lambda,\sigma\sigma'} u_{\mu\nu\kappa\lambda}^{\text{ON}} \hat{a}_{\mu\sigma}^\dagger \hat{a}_{\nu\sigma'}^\dagger \hat{a}_{\lambda\sigma'} \hat{a}_{\kappa\sigma}. \quad (6.82)$$

This Hamiltonian is brought into MPO-form and one applies the particle number projection operator as MPO

$$\hat{H}_N = \hat{P}_N^\dagger \hat{H} \hat{P}_N. \quad (6.83)$$

Using the MPO-form of  $\hat{H}_N$  as input operator and the orthonormalized atomic orbitals sorted from small to high angular momentum as DMRG sites, one obtains for the first ionization energy

$$\text{IE}_1 = -14.098200 + 14.403655 \text{ Hartree} \quad (6.84)$$

$$= 0.305455 \text{ Hartree} \quad (6.85)$$

and for the second ionization energy

$$\text{IE}_2 = -13.440000 + 14.403655 \text{ Hartree} \quad (6.86)$$

$$= 0.963655 \text{ Hartree}. \quad (6.87)$$

These values were obtained within 2 sweeps using MPS-matrix sizes of 4 and a convergence criterion of  $10^{-6}$  Hartree. The charge-neutral ground-state energy of beryllium is  $E^{(0)} = -14.403655$  Hartree. They coincide with the values from full-CI calculations with the program Psi4.

The same values for the ionization energies  $\text{IE}_1$  and  $\text{IE}_2$  are also obtained by introducing a chemical potential term

$$\hat{V}_{\text{chempot}} = - \sum_{\mu\sigma} \mu_\sigma \hat{n}_{\mu\sigma} \quad (6.88)$$

to the Hamiltonian Eq. (6.82) with the chemical potentials  $\mu_\uparrow$  and  $\mu_\downarrow$ . The chemical potentials must be chosen such that, in the case of  $\text{Be}^+$  and  $\text{Be}^{2+}$ , the system may only contain 3 and 2 electrons respectively. This is achieved by setting the chemical potentials equal to the highest ‘‘occupied’’ eigenenergy of the one-electron Hamiltonian in Eq. (6.82). For  $\text{Be}^+$  for example, to make sure that only one  $\uparrow$ -electron is in the system, the corresponding chemical potential has to be

$$\mu_\uparrow = -1.744638 \text{ Hartree}. \quad (6.89)$$

With  $\mu_\downarrow = 0$ , this results in a 4-electron triplet state ( $N_\uparrow = 1$  and  $N_\downarrow = 3$ ). Raising now  $\mu_\downarrow$  to

$$\mu_\downarrow = -0.2 \text{ Hartree} \quad (6.90)$$

leads to 3-electron  $\text{Be}^+$  with an energy

$$E(\text{Be}^+) = E(\mu_\uparrow, \mu_\downarrow) + \mu_\uparrow N_\uparrow + \mu_\downarrow N_\downarrow \quad (6.91)$$

$$= -14.098200 \text{ Hartree}. \quad (6.92)$$

For  $\text{Be}^{2+}$ , both chemical potentials must be equal to the highest occupied eigenen-

ergy of the one-electron Hamiltonian

$$\mu_{\uparrow} = -1.744638 \text{ Hartree} \quad (6.93)$$

$$\mu_{\downarrow} = -1.744638 \text{ Hartree}. \quad (6.94)$$

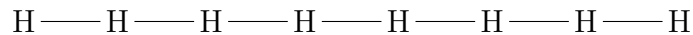
This then results in the total energy

$$E(\text{Be}^{2+}) = -13.440000 \text{ Hartree} \quad (6.95)$$

and a singlet 2-electron system.

### Hydrogen chain

The next example calculated to demonstrate the benefit of using atomic orbitals as DMRG sites is a chain of 8 hydrogen atoms



all separated by 2 Bohr. As atomic orbitals, the STO-3G basis is used meaning that in this case the DMRG sites and the locations of the hydrogen atoms coincide. Remember that the DMRG wave function in terms of a MPS is written as

$$|\psi_{\text{DMRG}}\rangle = \sum_{l_i r} \Psi_{lr}^{n_i} |l n_i r\rangle \quad (6.96)$$

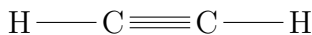
when the MPS-matrix of the wave function at the  $i$ th DMRG site is determined.  $|l n_i r\rangle$  is called “renormalized determinant”. If there are  $M$   $|l\rangle$  and  $|r\rangle$  states respectively and 4  $|n_i\rangle$  states, then the wave function is expanded in terms of  $4M^2$  renormalized determinants. Table 6.4 shows how the energy of the  $\text{H}_8$ -molecule approaches the exact (FCI) result with an increasing number of renormalized determinants and increasing sizes of the involved MPS-matrices. It highlights a significant property of the DMRG algorithm in terms of MPSs: it is variational in  $M$ . Moreover, timings are provided for each energy calculation. The calculations were run with 16 CPUs. The deviation of the energy obtained with a restricted Hartree-Fock calculation and the exact energy indicates that this system is strongly correlated and DMRG gives physically correct (within the chosen atomic orbital basis) results which are quite close to the FCI result, even for moderately large input parameters  $M$ . As it is shown in the next paragraph, the good performance concerning the ground-state energy description of DMRG is due to the use of orthonormal atomic orbitals as sites. It is not because they have little overlap—they are orthonormal and thus their overlap is always zero. It is rather because they reduce the entanglement of the sites. As a consequence, the MPS-matrix size  $M$  or the amount of needed renormalized determinants can be kept low and one is nevertheless close to the exact result.

MPS size $M$	Renorm. det.	Energy (Hartree)	Time (min)
4	64	-4.217049	1
8	256	-4.257578	8
12	576	-4.283668	10
16	1024	-4.285468	11
20	1600	-4.285694	53
24	2304	-4.285810	143
28	3136	-4.285892	250
32	4096	-4.285952	196
40	6400	-4.286002	504
50	10000	-4.286009	814
60	14400	-4.286010	1402
FCI		-4.286011	

Table 6.4: DMRG ground-state energies for a  $H_8$ -molecule with strongly correlated electrons using the Cholesky orthonormalized STO-3G basis as sites are shown regarding various input parameters  $M$ . Furthermore, timings are provided for the different DMRG calculations. With increasing MPS-matrix size  $M$ , the DMRG energies converge towards the exact (FCI) result. The Hartree-Fock energy is  $E_{\text{HF}} = -4.138573$  Hartree.

### Elongated ethine $C_2H_2$

Ethine is a molecule of linear geometry



and thus the atomic orbital based DMRG approach (AO-DMRG) is expected to perform well too. To create a highly non-dynamically correlated case, the bonds of ethine are stretched to 4 Bohr. For the AO-DMRG calculations of the ground-state energy of the elongated ethine molecule (triplet state) in table 6.5, the atomic orbital sites (STO-3G) are sorted with respect to the atom positions and angular momenta of the basis functions from left to right (see figure 6.6). Table 6.5 shows a comparison of the AO-DMRG approach and the standard quantum-chemical MO-DMRG approach for different MPS-matrix sizes  $M$ . For the MO-DMRG approach, the DMRG sites are formed by the molecular orbitals obtained from a restricted open-shell Hartree-Fock calculation with the program package PyQuante and sorted with respect to the corresponding orbital energies in increasing order from left to right. What can be seen is that, for the same value of  $M$ , the naturally ordered AO approach gives results which are closer and converge faster to the exact energy (FCI program in Psi4) than the canonically ordered MO approach. This is an immediate result of entanglement reduction between the site in the AO basis which makes it possible to keep the MPS-matrix sizes smaller and to be still closer to the exact energy. The CCSD(T) energy (routine in Psi4) is also provided in table 6.5 to point out that we investigate a highly statically correlated case which has immense multi-reference character and where standard quantum-chemical methods fail. Due to its

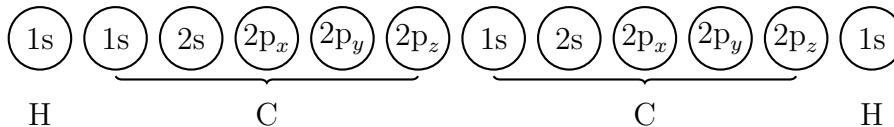


Figure 6.6: Natural ordering of the atomic orbitals as DMRG sites with respect to atom position and angular momentum of the basis functions. The use of atomic orbitals leads to a reduction of entanglement between the DMRG sites. Thus, the MPS-matrix size  $M$  can be kept smaller than in the case of canonically ordered (orbital energy ordering) HF-orbitals.

intrinsic multi-configurational or multi-determinantal ansatz, DMRG—especially in the AO-formulation—can handle such multi-reference cases quite well.

$M$	AO-DMRG( $M$ )	MO-DMRG( $M$ )
4	-75.351739	-75.272006
16	-75.418983	-75.372264
28	-75.424161	-75.392286
40	-75.425521	-75.421537
ROHF	-74.941021	
CCSD(T)	-75.412935	
FCI	-75.431742	

Table 6.5: Comparison of the AO-DMRG and MO-DMRG approach for various MPS-matrix sizes  $M$  with respect to the exact (FCI) energy. The restricted open-shell Hartree-Fock (ROHF) energy and the CCSD(T) energy are also provided for comparison and to highlight that the elongated  $C_2H_2$ -molecule is of strong non-dynamical correlation. The ROHF, CCSD(T), and FCI results are obtained with the program package Psi4.

### Small stretched $C_2$ -chains

The biggest systems investigated with the AO-DMRG approach in this dissertation are small stretched  $C_2$ -chains ( $(C_2)_1$ ,  $(C_2)_2$ , and  $(C_2)_3$  with an inter-atomic distance of 5 Bohr respectively) in the STO-3G atomic orbital basis. These systems are strong representatives of the static electron correlation and have highly non-trivial spin states. This highlights an advantage of DMRG compared to other quantum-chemical methods: DMRG is able to determine the absolute spin state and thus the spin multiplicity automatically whereas, for standard quantum-chemical methods like CCSD(T), one must give the spin state to be searched as input for the calculation. Table 6.6 shows a comparison of ground-state calculations for the different  $C_2$  chain lengths with the AO-DMRG method and various quantum-chemical methods including ROHF and CCSD(T). The longest AO-DMRG calculation for  $(C_2)_3$  took 14 days. FCI calculations are unfortunately not possible at least for the  $(C_2)_3$ -molecule because of RAM requirement issues. CISD already needs around 250 GB RAM in the case of  $(C_2)_3$ . For the ROHF and CCSD(T) method, the program package CFOUR [Stanton et al.] has been used this time.

The data indicate the advantage and use of the AO-DMRG method since the calculations need less than 10 GB of RAM with a relatively small MPS-matrix size

parameter  $M = 16$  for such highly non-dynamically correlated systems. The AO-ordering according to the scheme presented in figure 6.6 may not be optimal, but it is a good and natural starting point to sort the DMRG sites in order to reduce the entanglement between the sites and thus to lower the computational effort. Eventually, since DMRG is variational in  $M$  the energies obtained with the atomic orbital implementation of the DMRG method can be considered to be closer to the numerically exact results than all the other methods tested in this thesis.

Method	Energy (Hartree)		
	$(C_2)_1$	$(C_2)_2$	$(C_2)_3$
ROHF	-74.3947582538	-148.6803701902	-222.7650689991
CCSD(T)	-74.4344676250	-148.8686854431	-223.2968979819
AO-DMRG(16)	-74.4452513113	-148.8896971930	-223.3276834310

Table 6.6: Comparison of ground-state energy calculations with the AO-DMRG method and other quantum-chemical methods for various  $C_2$ -chain lengths.

### Comparison of the AO-DMRG implementation with other quantum-chemical DMRG programs

In this section, the AO-DMRG implementation of this thesis is compared with other quantum-chemical DMRG programs including CheMPS2 and BLOCK using the  $C_2H_2$  molecule in the STO-3G basis from above as test system.

Comparative calculations (see table 6.7) with the DMRG program CheMPS2 [Wouters et al., 2014a,b, 2016, Wouters and Van Neck, 2014] interfaced to the program package Psi4 and the program BLOCK developed within the Chan group with contributions by Chan and Head-Gordon [2002], Chan [2004], Ghosh et al. [2008], Sharma and Chan [2012], and Olivares-Amaya et al. [2015] show that the AO-DMRG approach completely formulated in terms of matrix product states and operators outperforms the standard quantum-chemical DMRG ansatz based on a sorted chain of Hartree-Fock orbitals as DMRG sites and implemented in the BLOCK program with respect to the size parameter  $M$  of the MPS-matrices for elongated, linear molecules at least.

CheMPS2 is a spin-adapted, symmetry using quantum-chemical DMRG program. It implements the two-site DMRG algorithm. For calculations, it uses the MPS-representation of the many-particle wave function, but no MPO-formulation of the Hamiltonian. Instead, it uses complementary operators as shown in the article by Wouters et al. [2014b]. It is interfaced to the program package Psi4, which makes it easy to perform DMRG calculations on top of a HF-calculation. The orbital ordering is the canonical one according to the HF-orbital energies.

The BLOCK program is also a spin-adapted, symmetry using quantum-chemical DMRG program which implements the single- as well as the two-site DMRG algorithm. It does not use a complete MPO-representation of the Hamiltonian, but it also uses a MPS-representation of the wave function. As orbital ordering measure, it uses the Fiedler vector [Fiedler, 1973] by default. In the field of spectral graph partitioning, the Fiedler vector is the eigenvector of the Laplacian matrix of a graph corresponding to its second smallest eigenvalue called the algebraic connectivity.

From table 6.7, it can be seen that DMRG converges much faster to the exact energy of the system regarding the MPS-matrix size  $M$  using the local representation by atomic orbitals than the other tested programs implementing the standard quantum-chemical DMRG approach using molecular orbitals.

$M$	CheMPS2( $M$ )	AO-DMRG( $M$ )	BLOCK( $M$ )	BLOCK <sub>fv</sub> ( $M$ )
4	-75.277071	-75.351739		
16	-75.368982	-75.418983		
28	-75.392609	-75.424161		
40	-75.414218	-75.425521		
250			-75.431732	-75.431723
FCI	-75.431742			

Table 6.7: Performance comparison of the AO-DMRG and the quantum-chemical DMRG programs CheMPS2 and BLOCK with respect to the MPS-matrix size parameter  $M$ . By default, the smallest  $M$ -value in the BLOCK program is 250. The subscript “fv” means that the calculation has been carried out with an orbital ordering using the Fiedler vector. Without “fv” means that the MOs in the BLOCK program are ordered canonically according to increasing orbital energy. The smallest possible  $M$ -value for the BLOCK program is 250. Energies are given in Hartree.

### Increasing the basis set

A remaining question to be answered is whether the AO-approach still performs better than the MO-approach when the underlying Gaussian basis set is increased and thus the amount of DMRG sites grows. Table 6.8 shows the result of the analysis referring to the example of  $C_2H_2$  from above. The energies shown are converged within a maximum of 100 sweeps. The used basis sets are the STO-3G [Hehre et al., 1969], the 6-31G [Hehre et al., 1972], and the cc-pVDZ [Dunning Jr, 1989] basis sets. The computational effort increases with an increasing number of basis functions because the electron-electron interaction consists of a growing number of terms. A peculiarity happens using molecular orbitals when increasing the basis set: MO-DMRG seems to converge to a state where an electron has been added to the total number of electrons  $N = 14$ . So, the ground-state search ends up in the wrong many-electron state of the molecule unless adding an artificial chemical potential to the external potential or increasing the MPS-matrix size  $M$ . Compared to the MO-DMRG approach with canonically ordered sites, the AO-DMRG approach converges to the correct neutral many-electron state when the number of basis functions and thus the number of DMRG sites grows. The recommendation is to use atomic orbitals instead of molecular orbitals when the investigated system is in the strongly correlated regime.

The future goal should of course be to do quantum-chemical simulations with the AO-DMRG method using large basis sets. For this dissertation however, the focus has been put on increasing the number of electrons. Therefore, the use of the STO-3G basis set throughout this application section has been necessary at the current stage of research in order to be able to increase the MPS-parameter  $M$  beyond the value of 4.

Method	Basis set	$N$	Energy (Hartree)
AO-DMRG(4)	STO-3G	14.0	-75.351739
	6-31G	14.0	-75.842861
	cc-pVDZ	14.000039*	-76.207292
MO-DMRG(4)	STO-3G	14.0	-75.272006
	6-31G	15.0*	-76.363516
	cc-pVDZ	15.0*	-76.383164

Table 6.8: Comparison of the MO-DMRG and AO-DMRG approach, implemented in the program written for this thesis, for increasing atomic orbital basis sets. The parentheses behind the method show the MPS-matrix size  $M$ .  $N$  is the expectation value of the particle number operator with respect to the calculated DMRG wave function.

\*When increasing the basis set,  $M$  must be increased to avoid the DMRG wave function converge to the wrong particle number state. For MOs, DMRG ends up in the wrong particle number state when increasing the atomic orbital basis.

### A small detour to cubic hydrogen

It is not immediately clear if the naturally ordered AO-DMRG approach also performs better than its MO-implementation for molecules which have extents in three dimensions with strongly correlated electrons since the atomic orbitals which are not linearly aligned have to be ordered in a chain-like fashion for DMRG. The simplest model system investigated for this thesis is cubic  $H_8$  with a primitive cubic lattice structure (4 Bohr edge length). Table 6.9 nicely shows that the local representation by atomic orbitals also outperforms the molecular orbital ansatz even if the chain-like ordering of the atomic orbitals for the DMRG algorithm is not perfect. The reference RHF-FCI calculation in table 6.9 has been carried out with the program package Psi4. The AO-description of molecules in principle allows a geometrical ordering of the DMRG sites in space as opposed to molecular orbitals, which could make the use of tensor network states—the generalization of matrix product states—as representation of the many-body wave function possible in future projects. The use of tensor network states will certainly enhance the convergence of AO-DMRG further. DMRG in terms of tensor network states is however not the subject of this dissertation.

$M$	AO-DMRG( $M$ )	MO-DMRG( $M$ )
4	-3.740883	-3.692207
16	-3.769260	-3.713874
28	-3.773209	-3.713874
RHF	-3.120556	
FCI	-3.780244	

Table 6.9: Investigation of the convergence performance of the AO-DMRG and MO-DMRG approach for a non-linear, cubic system  $H_8$ . The shown ground-state energies are in Hartree.



## 7 Conclusion

The main research goal of this dissertation has been the development of a state-of-the-art density matrix renormalization group (DMRG) approach, which is suitable for quantum-chemical applications especially in the regime of strong or static electron correlation, where exact calculations may not be feasible any more and where standard quantum-chemical methods like Hartree-Fock and methods on top of it like the coupled-cluster singles doubles with perturbative triples CCSD(T) method or the configuration interaction CI method are qualitatively wrong. During the research process, it has turned out that DMRG as a method to find the lowest-lying many-particle eigenstates of a certain Hamiltonian can be applied directly to quantum-chemical problems as an eigensolver and is not a mere post-HF method. DMRG can actually be used to diagonalize a quantum-chemical problem directly without any pre-simulations. It is a matter of the right single-particle basis states to make a direct DMRG method. For this purpose, a discretized real-space lattice formulation of quantum-chemical Hamiltonians and a formulation in terms of the quantum-chemical Gaussian atomic orbital basis sets as single-particle states for DMRG have been investigated.

The first project of this dissertation has then been to develop a formalism how to construct the quantum-chemical Hamiltonian as a matrix product operator (MPO)—the operator analogue of matrix product states (MPS)—in either of the basis formulations and how to incorporate fixed particle numbers in order to be able to calculate energies of charged systems. This construction formalism has emerged to be parallelizable locally, i.e., the construction of the MPO at a specific site in the DMRG chain can be parallelized. Fixing the particle number is achieved by either a MPO-projection operator projecting the Hamiltonian on the subspace bearing the desired number of particles or by adding a chemical potential term to the Hamiltonian. There are pros and cons concerning both approaches: the projection operator approach has the advantage that one can fix the particle number without any further information about the system, but the disadvantage is that the application of the MPO-projection to the Hamiltonian in MPO-form increases the size of the matrices representing the new projected Hamiltonian MPO, which directly results from how MPOs are multiplied, and thus increases the computational cost of DMRG. The disadvantage of introducing a chemical potential to the Hamiltonian to fix the particle number is that one does not know at the beginning how to choose the chemical potential. A good starting point is however to diagonalize the non-interacting one-electron problem and use its eigenenergies to choose the correct value for the chemical potential. Unfortunately, finding the right value of the chemical potential is a little connected to trial and error, but the advantage of adding a chemical potential is that the computational cost regarding the Hamiltonian as MPO stays the same. The found MPO-constructions of the quantum-chemical Hamiltonian are efficient because their MPO-matrix sizes can be systematically compressed speeding-up construction times as well as making it possible to treat systems in a bigger basis

space.

The generic formalism to construct any Hamiltonian in a second-quantized, quantum lattice model form as MPO has led to the second project of this dissertation: the development of a basis set free, direct DMRG approach for quantum-chemical systems on a real-space grid coming from the discretization of the Hamiltonian formulated in continuous real space and expressed in terms of quantum field operators instead of the standard fermionic creation and annihilation operators. The MPO-representation of the quantum-chemical Hamiltonian formulated on a discretized position space lattice has the best formal asymptotic scaling properties with respect to the growth of the MPO-matrix sizes of the Hamiltonian MPO in all the presented single-particle basis spaces ranging from discrete position space and discrete momentum space to the Hartree-Fock orbital and atomic orbital basis spaces. The MPO-matrix size asymptotically scales as  $O(L)$  where  $L$  denotes the amount of lattice sites. Unfortunately, the amount of lattice sites must be enormously large for sufficiently accurate results. In the test calculations for this thesis, it had not been possible to go beyond 132651 lattice points. The problem stems from the electron-electron interaction matrix which is completely dense in real space. Therefore, a compression scheme based on an expansion of the electron-electron interaction in momentum space or in terms of a Fourier series has been presented. This momentum space expansion made it possible to go down to accuracies determined by a lattice size of 1030301 lattice sites. The applications of the discrete position space lattice DMRG approach for the helium atom and the hydrogen molecule have shown that, even if the lattice sizes and thus the results are limited by today's computer resources, the developed basis set free approach captures the qualitative physical behavior of the exact solution of the investigated quantum-chemical Hamiltonian correctly. This is not the case for the basis set dependent quantum-chemical methods like truncated coupled-cluster and configuration interaction in small basis sets particularly in the non-dynamically correlated regime.

The third major project has directly resulted from the study of the discrete position space DMRG approach. To keep the idea of a direct ab initio DMRG method for quantum-chemical applications and to circumvent the difficulty of needing huge amounts of lattice sites for sufficiently accurate results, the quantum-chemical Gaussian basis sets have been discussed as DMRG sites. Using these atomic orbitals, a Hartree-Fock calculation in preparation of DMRG calculations is not needed. What is needed is just the one- and two-electron integrals in the atomic orbital basis. Thus, approximative, Hartree-Fock outnumbering and exact energy calculations within the quantum-chemical basis set are possible immediately. The matrix product operator size of the Hamiltonian formally scales as  $O(L^4)$ , but it can be compressed according to the presented singular value compression scheme of the electron-electron interaction. It can be brought down to a size scaling of  $O(L^2 N_{\text{trunc}})$  where  $N_{\text{trunc}}$  is the number of kept singular values regarding a certain truncation threshold. Test simulations of linear, elongated molecules ranging from a H<sub>8</sub>-chain, C<sub>2</sub>H<sub>2</sub> to small C<sub>2</sub>-chains, which are designed to have strong orbital interactions and thus highly multi-determinantal character where a mean-field description completely leads to wrong results, have shown that one can not only skip a Hartree-Fock calculation as needed in standard quantum-chemical DMRG implementations, DMRG in terms of an atomic orbital basis like the STO-3G basis even outperforms its common implementation in terms of molecular orbitals. This is because the entanglement between

the interacting orbitals—in the context of DMRG, sites—is reduced due to the local nature of the atomic orbitals. In standard quantum-chemical DMRG implementations based on a Hartree-Fock pre-calculation, the energy convergence with respect to the matrix size of the involved matrix product state is influenced by the ordering of the molecular orbitals. The natural ordering of the atomic orbitals according to atom position and angular momentum of the basis function however leads to an immediate entanglement reduction of the DMRG chain, a matrix product state with smaller matrix size, and a resulting convergence boost. A detour to a small cubic hydrogen system where the atomic orbitals are not centered on a line through the nuclei has also shown that atomic orbitals do a good job in describing the physical situation as far as the case of static electron correlation is concerned. Compared to molecular orbitals, the AO-DMRG many-body energy is closer to the numerically exact energy with the same computational cost. Even though the non-linearly distributed atomic orbitals of a molecule with three-dimensional extents have to be numbered and ordered in a chain-like fashion when using a matrix product state ansatz for the many-electron wave function, DMRG in terms of AOs performs better than in terms of MOs in the case of strong electron correlation.

As far as the ordering of the atomic orbitals is concerned, a geometrical ordering appears to be the most natural choice to improve the performance of DMRG. For linear molecules, matrix product state wave functions sufficiently capture the correlation between the atom-centered atomic orbitals. A further improvement, which has not been a research part of this dissertation, could be the use of the generalization of matrix product states: tensor network states. Increasing the tensor rank (a matrix is a tensor of rank 2) gives more flexibility in capturing the leading orbital correlations, i.e., only electrons occupying the highest angular momentum orbitals are really correlated, which coincides with chemical intuition of active valence electrons. Besides that, tensor network state wave functions could be designed to reflect the geometry of a generic, non-linear molecule and its thus resulting electron-orbital correlations.



# List of publications

Below, the publications which have been produced during the preparation of this dissertation are listed. The chapters 4, 5, and 6 of this dissertation cover the contents of the listed publications in more detail.

- Philipp B. Snajberk and Christian Ochsenfeld, *Matrix product operator based density matrix renormalization group approach in the atomic orbital basis for describing static electron correlation*, submitted.
- Philipp B. Snajberk and Christian Ochsenfeld, *Density matrix renormalization group treatment of the electronic structure of small atoms and molecules on a position space lattice*, submitted.



# Bibliography

- M. Abramowitz and I. Stegun. *Handbook of Mathematical Functions: With Formulas, Graphs, and Mathematical Tables*. Dover Books on Mathematics. Dover Publications, 2012. ISBN 9780486158242.
- A. Altland and B. D. Simons. *Condensed Matter Field Theory*. Cambridge University Press, 2010. ISBN 9781139485135.
- A. Banerjee and J. Simons. The coupled-cluster method with a multiconfiguration reference state. *International Journal of Quantum Chemistry*, 19(2):207–216, 1981.
- C. W. Bauschlicher Jr and S. R. Langhoff. Full CI benchmark calculations on N<sub>2</sub>, NO, and O<sub>2</sub>: A comparison of methods for describing multiple bonds. *The Journal of Chemical Physics*, 86(10):5595–5599, 1987.
- C. W. Bauschlicher Jr and P. R. Taylor. Benchmark full configuration-interaction calculations on H<sub>2</sub>O, F, and F<sup>-</sup>. *The Journal of Chemical Physics*, 85(5):2779–2783, 1986.
- C. W. Bauschlicher Jr, S. R. Langhoff, P. R. Taylor, N. C. Handy, and P. J. Knowles. Benchmark full configuration-interaction calculations on HF and NH<sub>2</sub>. *The Journal of Chemical Physics*, 85(3):1469–1474, 1986.
- M. Born and R. Oppenheimer. Zur Quantentheorie der Molekeln. *Annalen der Physik*, 389(20):457–484, 1927.
- H. Bruus and K. Flensberg. *Many-Body Quantum Theory in Condensed Matter Physics: An Introduction*. Oxford Graduate Texts. OUP Oxford, 2004. ISBN 9780198566335.
- R. Bulla, T. A. Costi, and T. Pruschke. Numerical renormalization group method for quantum impurity systems. *Reviews of Modern Physics*, 80:395–450, Apr 2008. doi: 10.1103/RevModPhys.80.395. URL <http://link.aps.org/doi/10.1103/RevModPhys.80.395>.
- G. K.-L. Chan. An algorithm for large scale density matrix renormalization group calculations. *The Journal of Chemical Physics*, 120(7):3172–3178, 2004.
- G. K.-L. Chan and M. Head-Gordon. Highly correlated calculations with a polynomial cost algorithm: A study of the density matrix renormalization group. *The Journal of Chemical Physics*, 116(11):4462–4476, 2002.
- G. K.-L. Chan and S. Sharma. The density matrix renormalization group in quantum chemistry. *Annual Review of Physical Chemistry*, 62(1):465–481, 2011. doi: 10.1146/annurev-physchem-032210-103338. URL <http://dx.doi.org/10.1146/annurev-physchem-032210-103338>. PMID: 21219144.

## Bibliography

- G. K.-L. Chan and T. Van Voorhis. Density-matrix renormalization-group algorithms with nonorthogonal orbitals and non-Hermitian operators, and applications to polyenes. *The Journal of Chemical Physics*, 122(20):204101, 2005.
- J. Čížek. On the correlation problem in atomic and molecular systems. Calculation of wavefunction components in Ursell-type expansion using quantum-field theoretical methods. *The Journal of Chemical Physics*, 45(11):4256–4266, 1966.
- T. D. Crawford and H. F. Schaefer. An introduction to coupled cluster theory for computational chemists. *Reviews in computational chemistry*, 14:33–136, 2000.
- S. Das, D. Mukherjee, and M. Kállay. Full implementation and benchmark studies of mukherjee’s state-specific multireference coupled-cluster ansatz. *The Journal of Chemical Physics*, 132(7):074103, 2010.
- S. Daul, I. Ciofini, C. Daul, and S. R. White. Full-CI quantum chemistry using the density-matrix renormalization group. *eprint arXiv:cond-mat/9912348*, 1999. URL <http://arxiv.org/abs/cond-mat/9912348v1>.
- T. H. Dunning Jr. Gaussian basis sets for use in correlated molecular calculations. I. The atoms boron through neon and hydrogen. *The Journal of Chemical Physics*, 90(2):1007–1023, 1989.
- M. Fiedler. Algebraic connectivity of graphs. *Czechoslovak mathematical journal*, 23(2):298–305, 1973.
- V. Fock. Näherungsmethode zur Lösung des quantenmechanischen Mehrkörperproblems. *Zeitschrift für Physik*, 61(1-2):126–148, 1930.
- F. Fröwis, V. Nebendahl, and W. Dür. Tensor operators: Constructions and applications for long-range interaction systems. *Physical Review A*, 81:062337, Jun 2010. doi: 10.1103/PhysRevA.81.062337. URL <http://link.aps.org/doi/10.1103/PhysRevA.81.062337>.
- J. E. Gentle. *Numerical Linear Algebra for Applications in Statistics*. Statistics and Computing. Springer New York, 2012. ISBN 9781461206231.
- D. Ghosh, J. Hachmann, T. Yanai, and G. K.-L. Chan. Orbital optimization in the density matrix renormalization group, with applications to polyenes and  $\beta$ -carotene. *The Journal of Chemical Physics*, 128(14):144117, 2008.
- G. Giuliani and G. Vignale. *Quantum Theory of the Electron Liquid*. Masters Series in Physics and Astronomy. Cambridge University Press, 2005. ISBN 9780521821124.
- D. J. Griffiths. *Introduction to Quantum Mechanics*. Always learning. Pearson, 2013. ISBN 9781292024080.
- K. A. Hallberg. New trends in density matrix renormalization. *Advances in Physics*, 55(5-6):477–526, 2006. doi: 10.1080/00018730600766432. URL <http://dx.doi.org/10.1080/00018730600766432>.



- D. R. Hartree. The wave mechanics of an atom with a non-Coulomb central field. Part I. Theory and methods. 24(01):89–110, 1928.
- D. R. Hartree and W. Hartree. Self-consistent field, with exchange, for beryllium. *Proceedings of the Royal Society of London. Series A, Mathematical and Physical Sciences*, 150(869):9–33, 1935.
- W. J. Hehre, R. F. Stewart, and J. A. Pople. Self-consistent molecular-orbital methods. I. Use of Gaussian expansions of Slater-type atomic orbitals. *The Journal of Chemical Physics*, 51(6):2657–2664, 1969. doi: <http://dx.doi.org/10.1063/1.1672392>. URL <http://scitation.aip.org/content/aip/journal/jcp/51/6/10.1063/1.1672392>.
- W. J. Hehre, R. Ditchfield, and J. A. Pople. Self-consistent molecular orbital methods. XII. Further extensions of Gaussian-type basis sets for use in molecular orbital studies of organic molecules. *The Journal of Chemical Physics*, 56(5):2257–2261, 1972.
- T. Helgaker, P. Jorgensen, and J. Olsen. *Molecular Electronic-Structure Theory*. Wiley, 2014. ISBN 9781119019558.
- J. Hubbard. Electron correlations in narrow energy bands. *Proceedings of the Royal Society of London A: Mathematical, Physical and Engineering Sciences*, 276(1365):238–257, 1963. ISSN 0080-4630. doi: 10.1098/rspa.1963.0204. URL <http://rspa.royalsocietypublishing.org/content/276/1365/238>.
- C. Hubig, I. McCulloch, and U. Schollwöck. Generic construction of efficient matrix product operators. *arXiv preprint arXiv:1611.02498*, 2016. URL <https://arxiv.org/abs/1611.02498>.
- M. Imada, A. Fujimori, and Y. Tokura. Metal-insulator transitions. *Reviews of Modern Physics*, 70:1039–1263, Oct 1998. doi: 10.1103/RevModPhys.70.1039. URL <http://link.aps.org/doi/10.1103/RevModPhys.70.1039>.
- E. Ising. Beitrag zur Theorie des Ferromagnetismus. *Zeitschrift für Physik*, 31(1):253–258, 1925. ISSN 0044-3328. doi: 10.1007/BF02980577. URL <http://dx.doi.org/10.1007/BF02980577>.
- E. Jones, T. Oliphant, P. Peterson, et al. SciPy: Open source scientific tools for Python, 2001. URL <http://www.scipy.org/>.
- S. Keller and M. Reiher. Spin-adapted matrix product states and operators. *The Journal of Chemical Physics*, 144(13):134101, 2016.
- S. Keller, M. Dolfi, M. Troyer, and M. Reiher. An efficient matrix product operator representation of the quantum chemical Hamiltonian. *The Journal of Chemical Physics*, 143(24):244118, 2015.
- P. J. Knowles and N. C. Handy. A new determinant-based full configuration interaction method. *Chemical physics letters*, 111(4):315–321, 1984.

## Bibliography

- J. Kondo. Resistance minimum in dilute magnetic alloys. *Progress of Theoretical Physics*, 32(1):37–49, 1964. doi: 10.1143/PTP.32.37. URL <http://ptp.oxfordjournals.org/content/32/1/37.abstract>.
- J. Kussmann, M. Beer, and C. Ochsenfeld. Linear-scaling self-consistent field methods for large molecules. *Wiley Interdisciplinary Reviews: Computational Molecular Science*, 3(6):614–636, 2013.
- M. S. Lee and M. Head-Gordon. Polarized atomic orbitals for self-consistent field electronic structure calculations. *The Journal of Chemical Physics*, 107(21):9085–9095, 1997.
- X.-P. Li, R. W. Nunes, and D. Vanderbilt. Density-matrix electronic-structure method with linear system-size scaling. *Physical Review B*, 47:10891–10894, Apr 1993. doi: 10.1103/PhysRevB.47.10891. URL <http://link.aps.org/doi/10.1103/PhysRevB.47.10891>.
- K. H. Marti, B. Bauer, M. Reiher, M. Troyer, and F. Verstraete. Complete-graph tensor network states: A new fermionic wave function ansatz for molecules. *New Journal of Physics*, 12(10):103008, 2010.
- I. P. McCulloch. From density-matrix renormalization group to matrix product states. *Journal of Statistical Mechanics: Theory and Experiment*, 2007(10):P10014, 2007. URL <http://stacks.iop.org/1742-5468/2007/i=10/a=P10014>.
- A. Messiah. *Quantum Mechanics*. Dover Books on Physics. Dover Publications, 2014. ISBN 9780486784557.
- V. Murg, F. Verstraete, Ö. Legeza, and R. Noack. Simulating strongly correlated quantum systems with tree tensor networks. *Physical Review B*, 82(20):205105, 2010.
- N. Nakatani and G. K.-L. Chan. Efficient tree tensor network states (TTNS) for quantum chemistry: Generalizations of the density matrix renormalization group algorithm. *The Journal of Chemical Physics*, 138(13):134113, 2013.
- R. Olivares-Amaya, W. Hu, N. Nakatani, S. Sharma, J. Yang, and G. K.-L. Chan. The ab-initio density matrix renormalization group in practice. *The Journal of Chemical Physics*, 142(3):034102, 2015.
- S. Östlund and S. Rommer. Thermodynamic limit of density matrix renormalization. *Physical Review Letters*, 75:3537–3540, Nov 1995. doi: 10.1103/PhysRevLett.75.3537. URL <http://link.aps.org/doi/10.1103/PhysRevLett.75.3537>.
- S. Peotta and M. Di Ventra. Improving the Gutzwiller ansatz with matrix product states. *eprint arXiv:1307.8416*, 2013. URL <http://arxiv.org/abs/1307.8416>.
- M. Pilgrim. *Dive Into Python 3*. Books for professionals by professionals. Apress, 2010. ISBN 9781430224167.
- S. Rommer and S. Östlund. Class of ansatz wave functions for one-dimensional spin systems and their relation to the density matrix renormalization group. *Physical Review B*, 55:2164–2181, Jan 1997. doi: 10.1103/PhysRevB.55.2164. URL <http://link.aps.org/doi/10.1103/PhysRevB.55.2164>.

- U. Schollwöck. The density-matrix renormalization group. *Reviews of Modern Physics*, 77:259–315, Apr 2005. doi: 10.1103/RevModPhys.77.259. URL <http://link.aps.org/doi/10.1103/RevModPhys.77.259>.
- U. Schollwöck. The density-matrix renormalization group in the age of matrix product states. *Annals of Physics*, 326(1):96–192, 2011. ISSN 0003-4916. doi: <http://dx.doi.org/10.1016/j.aop.2010.09.012>. URL <http://www.sciencedirect.com/science/article/pii/S0003491610001752>. January 2011 Special Issue.
- E. Schrödinger. Quantisierung als Eigenwertproblem. *Annalen der Physik*, 385(13): 437–490, 1926. ISSN 1521-3889. doi: 10.1002/andp.19263851302. URL <http://dx.doi.org/10.1002/andp.19263851302>.
- S. Sharma and G. K.-L. Chan. Spin-adapted density matrix renormalization group algorithms for quantum chemistry. *The Journal of Chemical Physics*, 136(12): 124121, 2012.
- C. D. Sherrill. An introduction to configuration interaction theory. *School of Chemistry and Biochemistry, Georgia Institute of Technology, Atlanta*, 1995.
- C. D. Sherrill and H. F. Schaefer III. The configuration interaction method: Advances in highly correlated approaches. volume 34 of *Advances in Quantum Chemistry*, pages 143–269. Academic Press, 1999. doi: [http://dx.doi.org/10.1016/S0065-3276\(08\)60532-8](http://dx.doi.org/10.1016/S0065-3276(08)60532-8). URL <http://www.sciencedirect.com/science/article/pii/S0065327608605328>.
- S. Singh, R. N. C. Pfeifer, and G. Vidal. Tensor network decompositions in the presence of a global symmetry. *Physical Review A*, 82:050301, Nov 2010. doi: 10.1103/PhysRevA.82.050301. URL <http://link.aps.org/doi/10.1103/PhysRevA.82.050301>.
- S. Singh, R. N. C. Pfeifer, and G. Vidal. Tensor network states and algorithms in the presence of a global U(1) symmetry. *Physical Review B*, 83:115125, Mar 2011. doi: 10.1103/PhysRevB.83.115125. URL <http://link.aps.org/doi/10.1103/PhysRevB.83.115125>.
- J. C. Slater. The theory of complex spectra. *Physical Review*, 34:1293–1322, Nov 1929. doi: 10.1103/PhysRev.34.1293. URL <http://link.aps.org/doi/10.1103/PhysRev.34.1293>.
- P. B. Snajberk and C. Ochsenfeld. Density matrix renormalization group treatment of the electronic structure of small atoms and molecules on a position space lattice. *submitted*, 2017a.
- P. B. Snajberk and C. Ochsenfeld. Matrix product operator based density matrix renormalization group approach in the atomic orbital basis for describing static electron correlation. *submitted*, 2017b.
- J. F. Stanton, J. Gauss, M. E. Harding, P. G. Szalay, et al. CFOUR, coupled-cluster techniques for computational chemistry, a quantum-chemical program package. URL <http://www.cfour.de>.

## Bibliography

- E. M. Stoudenmire and S. R. White. Real-space parallel density matrix renormalization group. *Physical Review B*, 87:155137, Apr 2013. doi: 10.1103/PhysRevB.87.155137. URL <http://link.aps.org/doi/10.1103/PhysRevB.87.155137>.
- E. M. Stoudenmire, L. O. Wagner, S. R. White, and K. Burke. One-dimensional continuum electronic structure with the density-matrix renormalization group and its implications for density-functional theory. *Physical Review Letters*, 109:056402, Aug 2012. doi: 10.1103/PhysRevLett.109.056402. URL <http://link.aps.org/doi/10.1103/PhysRevLett.109.056402>.
- A. Szabo and N. S. Ostlund. *Modern quantum chemistry: Introduction to advanced electronic structure theory*. Dover Publications, Mineola, New York, 1996.
- P. G. Szalay, T. Müller, G. Gidofalvi, H. Lischka, and R. Shepard. Multiconfiguration self-consistent field and multireference configuration interaction methods and applications. *Chemical reviews*, 112(1):108–181, 2011.
- J. M. Turney, A. C. Simmonett, R. M. Parrish, E. G. Hohenstein, F. A. Evangelista, J. T. Fermann, B. J. Mintz, L. A. Burns, J. J. Wilke, M. L. Abrams, N. J. Russ, M. L. Leininger, C. L. Janssen, E. T. Seidl, W. D. Allen, H. F. Schaefer, R. A. King, E. F. Valeev, C. D. Sherrill, and T. D. Crawford. Psi4: an open-source ab initio electronic structure program. *Wiley Interdisciplinary Reviews: Computational Molecular Science*, 2(4):556–565, 2012. ISSN 1759-0884. doi: 10.1002/wcms.93. URL <http://dx.doi.org/10.1002/wcms.93>.
- T. van Mourik and J. H. van Lenthe. Benchmark full configuration interaction calculations on the helium dimer. *The Journal of Chemical Physics*, 102(19):7479–7483, 1995.
- F. Verstraete and I. Cirac. Matrix product states represent ground states faithfully. *Physical Review B*, 73(9):094423, 2006.
- M. Vojta. Quantum phase transitions. *Reports on Progress in Physics*, 66(12):2069, 2003. URL <http://stacks.iop.org/0034-4885/66/i=12/a=R01>.
- H.-J. Werner, M. Kállay, and J. Gauss. The barrier height of the  $F + H_2$  reaction revisited: Coupled-cluster and multireference configuration-interaction benchmark calculations. *The Journal of Chemical Physics*, 128(3):034305, 2008.
- S. R. White. Density matrix formulation for quantum renormalization groups. *Physical Review Letters*, 69:2863–2866, Nov 1992. doi: 10.1103/PhysRevLett.69.2863. URL <http://link.aps.org/doi/10.1103/PhysRevLett.69.2863>.
- S. R. White. Density-matrix algorithms for quantum renormalization groups. *Physical Review B*, 48:10345–10356, Oct 1993. doi: 10.1103/PhysRevB.48.10345. URL <http://link.aps.org/doi/10.1103/PhysRevB.48.10345>.
- S. R. White and R. L. Martin. Ab initio quantum chemistry using the density matrix renormalization group. *The Journal of Chemical Physics*, 110(9):4127–4130, 1999. doi: <http://dx.doi.org/10.1063/1.478295>. URL <http://scitation.aip.org/content/aip/journal/jcp/110/9/10.1063/1.478295>.

- K. G. Wilson. The renormalization group: Critical phenomena and the Kondo problem. *Reviews of Modern Physics*, 47:773–840, Oct 1975. doi: 10.1103/RevModPhys.47.773. URL <http://link.aps.org/doi/10.1103/RevModPhys.47.773>.
- K. G. Wilson. Ab initio quantum chemistry: A source of ideas for lattice gauge theorists. *Nuclear Physics B-Proceedings Supplements*, 17:82–92, 1990.
- S. Wouters and D. Van Neck. The density matrix renormalization group for ab initio quantum chemistry. *European Physical Journal D*, 68(9):272, 2014. doi: 10.1140/epjd/e2014-50500-1.
- S. Wouters, T. Bogaerts, P. Van Der Voort, V. Van Speybroeck, and D. Van Neck. Communication: DMRG-SCF study of the singlet, triplet, and quintet states of oxo-Mn(Salen). *The Journal of Chemical Physics*, 140(24):241103, 2014a. doi: 10.1063/1.4885815.
- S. Wouters, W. Poelmans, P. W. Ayers, and D. Van Neck. CheMPS2: a free open-source spin-adapted implementation of the density matrix renormalization group for ab initio quantum chemistry. *Computer Physics Communications*, 185(6): 1501–1514, 2014b. doi: 10.1016/j.cpc.2014.01.019.
- S. Wouters, V. Van Speybroeck, and D. Van Neck. DMRG-CASPT2 study of the longitudinal static second hyperpolarizability of all-trans polyenes. *The Journal of Chemical Physics*, 145(5):054120, 2016. doi: 10.1063/1.4959817.



# Curriculum vitae

## Personal details

Name	Philipp Bertone Snajberk
Date of birth	July 24, 1985
Place of birth	Starnberg, Germany
Citizenship	German

## Education

March 7, 2017	Oral thesis defense
June 2012	Starting to be a PhD student at the faculty of chemistry and pharmacy (LMU Munich) in the group of Prof. Dr. Ochsenfeld (Chair of theoretical chemistry)
August 2011	Diploma of physics with focus on solid state physics (LMU, Munich)
July 2010	Starting the diploma thesis at the faculty of physics (LMU, Munich) in the group of Prof. Dr. von Delft (Chair of theoretical solid state physics) Thesis title: <i>Supersymmetric Virial Expansion for Propagation Probabilities and Response Functions of Gaussian Ensembles of the Almost Diagonal RMTs</i>
October 2005	Beginning of studies at the faculty of physics (LMU, Munich)
June 2005	University entrance diploma (Munich)